Quantifying Temperature's Effect on the Cardiovascular System

by

Anna Colleen Crouch

A dissertation submitted in partial fulfillment
of the requirements for the degree of
Doctor of Philosophy
(Mechanical Engineering)
in the University of Michigan
2019

Doctoral Committee:

Assistant Professor Joan M. Greve, Co-Chair
Associate Professor Eric Johnsen, Co-Chair
Assistant Professor of Research, Jose A. Diaz
Professor Albert J. Shih

Anna Colleen Crouch

accrouch@umich.edu

ORCID iD: 0000-0002-1194-4897

Dedication

This dissertation is dedicated to all my family, friends, and colleagues that have made this journey possible. Without this incredible support system, I would not have been able to finish my PhD and more importantly would not have been able to have such a wonderful life these past five years. As my momma always says, “This time is your life. Don’t wait for your life to start after some accomplishment.”

To my parents, for the incredible love and support regardless of what career path I choose. For the wonderful adventures and quality time, and listening to me talk at least twice a day when I called. Without you both, I never would have made it in to a PhD program nonetheless finished one.

To my brothers, thanks for keeping me humble all these years. No one can make me laugh (or cry) like you two can. Without you two and your wonderful partners, my life would not be as fulfilling.

To my Winchester friends, you all are like family. Thanks for loving me through those awkward middle school years. To my Tullahoma friends, thank you for challenging me throughout high school and for accepting the Franklin County girl into your hearts. To my Tech friends, I will always think of Atlanta as home. To my Ann Arbor friends, this journey would not have been worth it without all of you.

Acknowledgements

This dissertation work would not have been possible without my committee, lab members, and the ME and BME departments. I would first like to thank Joan Greve for allowing me to bring my own research idea to the lab and supporting my ideas to try new research projects. Thank you to all my committee members, Eric Johnsen and Albert Shih, for their insight and suggestions. It is especially important for me to thank Jose Diaz for his support both as a researcher and as a friend.

I would like to thank both the ME department and the BME department: faculty, staff, and students. I have had the benefit of having two departments treat me as their own. I would also like to thank the cardiovascular center and specifically Dr. Jose Jalife and Dr. Daniel Michele for their leadership and training as part of the NIH T32 (grant number: T32-HL 125242). The two years on the training grant helped me become a better researcher. To CRLT-Engin and to Dr. Rhima Coleman, thank you for helping me become a better teacher. To Rackham Student Government, thank you for helping me become a better leader.

I would like to thank the Greve lab members (past and present) who have made this work possible and made coming into lab enjoyable. To my mentees, Lauryn Fitzgerald, Adam Manders, and Aditi Batra, it has been an absolute pleasure to work with you and watch you all grow into amazing scientist. I would like to thank Amos Cao for his wonderful coding skills. A special thanks to Paige Castle for her contribution to this work as well as her friendship. Finally, a huge thank you goes to my amazing friend and lab partner Olivia Palmer. We did it!

Funding for this work was provided by the University of Michigan Rackham Merit Fellowship (RMF), Rackham Summer Awards, Rackham Research Grants, the National Institutes of Health Training Grant, and the Biomedical Engineering Department startup funds.

Preface

This dissertation summarizes research that I have conducted over the past four and a half years while working in Dr. Joan Greve's laboratory. Sections of this thesis have been previously published and are presented here with some modifications as outlined below.

Chapter two contains portions of work, with modifications, that have been previously published as follows: Crouch, A.C., Manders, A., Cao, A., Scheven, U.M., Greve, J., Cross-sectional area of the murine aorta linearly increases with increasing core body temperature. International Journal of Hyperthermia. 2018;34:1121–1133. https://www.tandfonline.com/eprint/ZfBt8yyxBuduYZjxcdKY/full

Chapter three contains portions of work, with modifications, that have been previously published as follows: Crouch, A.C., Scheven, U.M., Greve, J.M., Cross-sectional areas of deep/core veins are smaller at lower core body temperatures. Physiological Reports. 2018;6:e13839. https://physoc.onlinelibrary.wiley.com/doi/10.14814/phy2.13839

Chapter four contains portions of work, with modifications, will be submitted as a thematic series: Crouch, A.C., Cao, A., Scheven, U., Greve, J.M. In vivo MRI assessment of blood flow in arteries and veins from head-to-toe across age and sex in C57BL/6 mice and Crouch, A.C., Batra, A., Scheven, U., Greve, J.M. *Redistribution of Blood Volume in Arteries and Veins Due to Changes in Core Body Temperature: a sex and age comparison.*

Chapter five contains portions of work, with modifications, that have been submitted as follows: Crouch, A.C., Castle, P.E., FitzGerald, L.N., Scheven, U.M., Greve, J.M. Assessing

structural and functional response of murine vasculature to acute β-adrenergic stimulation in vivo during hypothermic and hyperthermic conditions.

For Chapter 2, contributors include A. Colleen Crouch (ACC), Adam Manders (AM), Amos Cao (AC), Ulrich M Scheven (UMS), and Joan M Greve (JMG). ACC and JMG conceived and designed the study; ACC and AM collected and analyzed data; AC and UMS developed the in-house image analysis method for infrarenal aorta; ACC performed statistical analysis; ACC and JMG interpreted the data; ACC and JMG wrote the paper; ACC and JMG critically revised the paper; all authors gave final approval of the paper. For Chapter 3, ACC and JMG conceived and designed the study; ACC collected and analyzed data; UMS developed the in-house image analysis method; ACC performed statistical analysis and interpreted the data; ACC and JMG wrote the paper; ACC, UMS, and JMG critically revised the paper. For Chapter 4, ACC conceived and designed the study; ACC and AB collected and analyzed data; ACC, AAC, UMS developed the in-house image analysis method; ACC performed statistical analysis and interpreted the data; ACC wrote the paper; ACC and JMG critically revised the paper; all authors gave final approval of the paper. For Chapter 5, contributors ACC, Paige E. Castle (PEC), Lauryn N. FitzGerald (LNF), UMS, and JMG. ACC and PEC conceived and designed the study; ACC, PEC, LNF collected and analyzed data; ACC and PEC performed statistical analysis and interpreted the data; ACC and JMG wrote the paper; ACC, PEC, UMS, and JMG critically revised the paper; all authors gave final approval of the paper. For Chapter 6, the ideas were developed by ACC with collaboration from Jose Diaz and Connie Lee for the temperature probe work.

Table of Contents

List of Tables

List of Figures

Abstract

Those diseases that **medicines** do not cure are cured by the **knife**. Those that the **knife** does not cure are cured by **fire**. Those that **fire** does not cure, must be considered **incurable**.

—Hippocrates

Hippocrates in 370 BC made the first recorded mention of the use of heat as a therapeutic. To this day, the effect of temperature on the body is of interest to clinicians, athletes, researchers, and perhaps anyone that has lived through Georgia summers or Michigan winters. The body maintains temperature homeostasis by the process of thermoregulation. The body's ability to thermoregulate is an important coping mechanism to withstand various physiological states, such as fever, and environmental exposures such as the weather. The cardiovascular (CV) system plays a vital role in thermoregulation because of its influence on heat transfer via forced convection and conduction by changes in blood distribution, blood velocity, and proximity of tissues. It remains unclear how the allocation of blood in various compartments (such as the innermost core, fat, muscle, and skin) changes with temperature. Challenges in measuring core vasculature have resulted in a lack of empirical information regarding how it might change with core temperature. Therefore, to fully understand the CV system's role in thermoregulation, this thesis focuses on using murine models to study the effect of temperature on core vasculature. The overall purpose is to provide a novel and physiologically accurate approach to studying thermoregulation by incorporating structural and functional changes in the CV system occurring in the core.

Using murine models and MRI, we noninvasively quantified structural and functional vascular response in core arteries and veins to increasing core body temperature. We also studied the effects of sex and age on the CV response to increasing temperature. Using a PID-controlled heater to blow hot air across the animals, core temperature was increased from mild hypothermia (35 °C) to mild hyperthermia (38 °C). At each temperature, we imaged three to four locations of the body from head-to-toe, and quantified blood flow and velocity, vessel area, and measured circumferential cyclic strain of the core vessels. Our most significant quantitative results include: cross-sectional area of the aorta increased significantly and linearly with temperature for all groups, but at a diminished rate for aged animals ($p < 0.01$; male and female: adult, 0.019 and 0.024 $mm^2/°C$; aged, 0.017 and 0.011 $mm^2/°C$); jugular, aorta, femoral artery and vein linearly increased with temperature (0.10, 0.017, 0.017, and 0.027 $mm^2/°C$, respectively; $p<0.05$); and, flow in the infrarenal IVC linearly increased with temperature for all groups ($p = 0.002$; adjusted means: male vs. female, 0.37 and 0.28 mL/(min • °C); adult vs. aged, 0.22 and 0.43 mL/(min • °C)). Overall, we have shown: 1) that increases in flow occur in most arteries and veins, which is opposite to current hypotheses regarding the venous response; 2) that the magnitude of increased flow varies based on anatomical location; and, 3) that the increase in flow sometimes involves cross-sectional area and velocity and other times involves only one or the other. These vascular responses are also influenced by sex and age.

It is important to incorporate the cardiovascular changes occurring in the core into future bioheat or computational fluid dynamics modeling because blood flow is critical in heat generation and transfer in vivo. This research can help researchers, clinicians, and others interested in temperature's effect to better model and predict cardiovascular outcomes.

Chapter 1
Introduction

1.1 Temperature Matters

"Those diseases that medicines do not cure are cured by the knife. Those that the knife does not cure are cured by fire. Those that fire does not cure, must be considered incurable." This quote, attributed to Hippocrates in 370 BC, is often used to represent a thermal medicine approach to treating modern disease with 'medicines' representing pharmaceuticals, 'knife' for surgery, and 'fire' for thermal interventions. Thermal therapies have been used for thousands of years for treatment of disease, but thermal conditions can also have detrimental effects.

Temperature variations and thus heat transfer, known as hot and cold or thermal conditions, (referred to simply as 'temperature' in this thesis) can have therapeutic applications, be detrimental to overall human health, and affect performance and comfort. For therapeutic uses of temperature, both high and low temperatures are utilized; for example, higher temperature (hot) uses included, but are not limited to, thermal ablation for tumors [1], bacterial infection treatment with nanoparticles [2], and mild-hyperthermia combination treatments with immunotherapy for cancer [3]. Lower temperature (cold) uses include, but are not limited to, neural protection in brain ischemia [4], hypoxic-ischemic encephalopathy [5], pain management, and cardiac arrest [6].

The detrimental health effects of temperatures are caused by either external factors, such as weather, internal factors, such as fever, or a combination of the two. The work presented in this thesis is mainly focused on external factors; however, future work includes combination studies. Injury and illness due to heat is not only present in athletes [7], people in the military [8],

and those at high risk including the elderly [9] as illustrated in data from the CDC in Figure 1.1 [10], but heat injury is increasingly becoming a public health issue [11] that may escalate with climate change [12]. Exposure to cold temperatures can lead to frostbite and hypothermia not only in the elderly [9] but for anyone exposed to extreme temperatures [13].

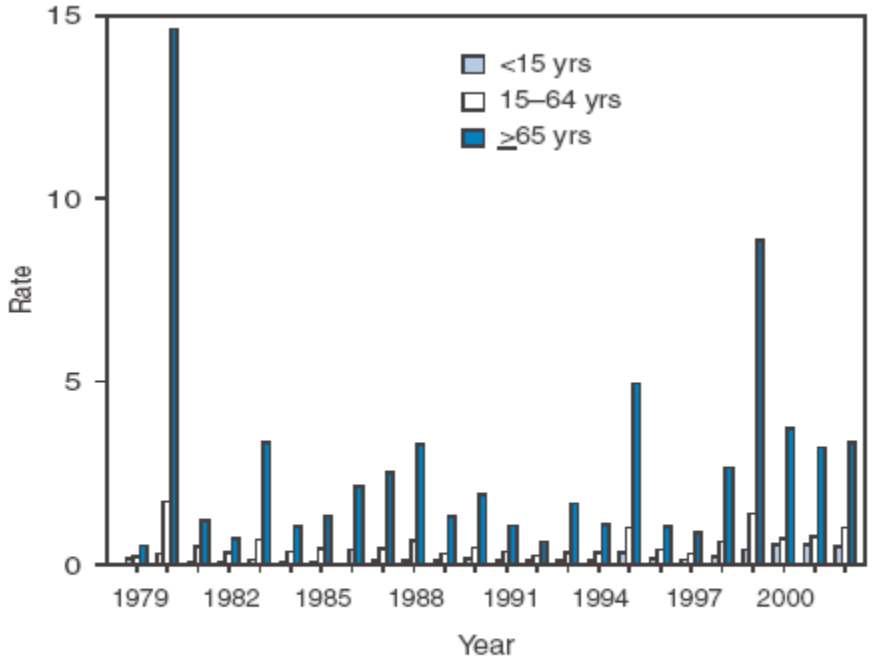

* Per 1,000,000 population.
† *International Classification of Diseases, Ninth Revision* (ICD-9), code E900.0.
§ ICD-10, code X30.

Figure 1.1 "Annual rate* of heat-related deaths attributed to weather conditions or exposure to excessive natural heat, by age group and year- US 1979-2002" [10]

Even without extreme temperatures, temperature variations can affect performance and comfort level. Performance deficits due to temperature are seen during exercise [15-17] and while performing mentally taxing tasks while wearing thermally insulating suits such as during explosive ordinance disposal [18]. Whether affecting comfort, performance, or overall human health, temperature matters, and the effect of temperature on the body should continue to be investigated.

1.2 Thermoregulation and bioheat transfer: the basics

Exposure to external temperatures, as well as changes in internal metabolic heat generation (e.g. exercise and fever), alters the temperature gradients in the body, and the body must respond to prevent or lessen fluctuations in core body temperature. Animals, including humans, maintain core temperature via the process of thermoregulation [19]. For humans, homeostatic temperature conditions average at 37 °C or 98.6 °F with deviations occurring due to circadian rhythm, menstrual cycle, and animal variability [20,21]. Researchers continue to investigate how the body, including at the molecular and cellular scale, sense temperature and how this impacts thermoregulation. In brief, Vriens et al, in Nature Reviews 2014, showed how temperature is perceived at the skin and peripheral locations as shown in Figure 1.2 [22]. Once the body senses the temperature, the body begins to thermoregulate. For most animals whether ectotherms or endotherms ('cold-' or 'warm-blooded'), behavioral changes are the first mechanism to regulate body temperature. For example, humans may turn on a fan, put on more clothes, or other behaviors once they perceive a change in temperature. Other endothermic animals, such as mice, huddle together when cold [23]. In addition to behavioral changes, the body has numerous mechanisms to maintain body temperature.

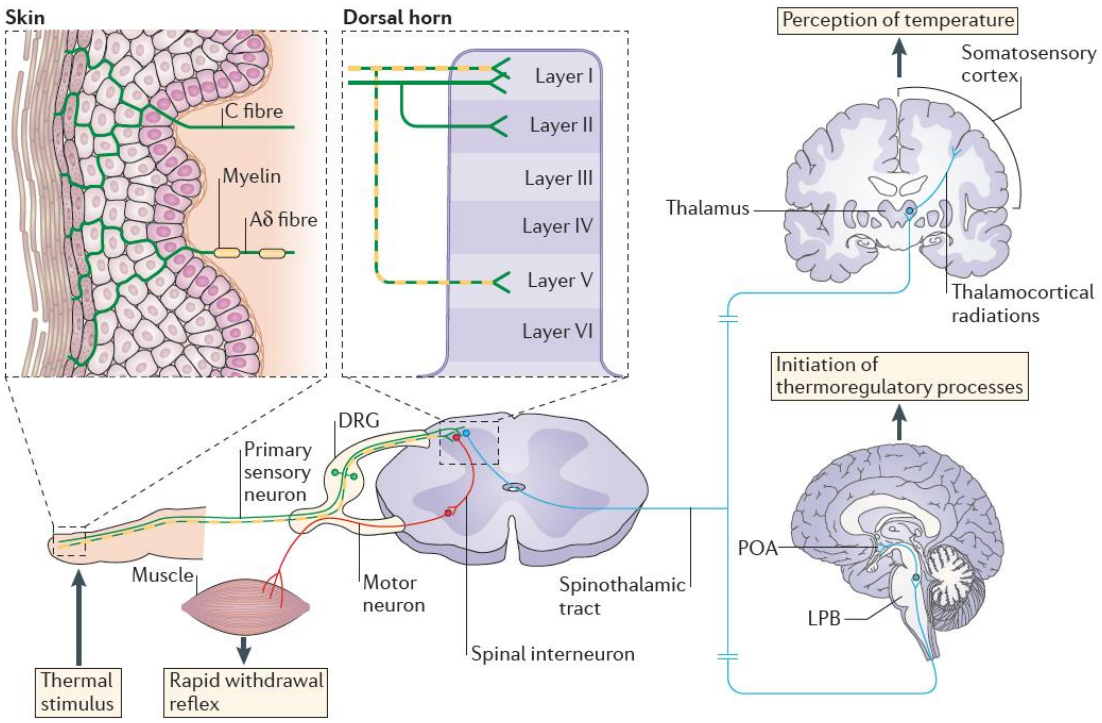

Figure 1.2 "Neurons involved in thermosensation." [from 22, page 574]

Temperature varies throughout the body, and researchers use bioheat equations to calculate heat transfer, and thus to quantify the temperatures in the body for various applications, including the above therapeutic applications.

Heat transfer is defined as thermal energy in transit due to a spatial temperature difference [25]. The three modes of heat transfer are conduction, convection, and radiation and each have their respective rate equations that quantify the amount of energy being transferred per unit time. Conduction occurs between two stationary mediums of different temperatures, and Fourier's law, in one-dimension, is given in Equation 1 with heat flux q''_x (W/m^2) and thermal conductivity k (W/m • K).

Equation 1

$$q''_x = -k\frac{dT}{dx}$$

Convection occurs between a surface and a moving fluid when they are at different temperatures, and Netwon's law of cooling, is given in Equation 2 with convection heat transfer coefficient h ($W/m^2 \bullet K$) and temperatures for the surface T_s and fluid T_∞.

Equation 2

$$q'' = h(T_s - T_\infty)$$

Thermal radiation is unique in that all surfaces of finite temperature emit energy via electromagnetic waves. The equation for the difference between thermal energy that is released by radiation emission and that which is gained from radiation absorption is given in Equation 3 with emissivity ε, Boltzmann constant σ ($\sigma=5.67\times10^{-8}$ $W/m^2 \bullet K^4$), and temperature for the surrounding $T_{sur.}$

Equation 3

$$q''_{rad} = \varepsilon\sigma(T_s^4 - T_{sur}^4)$$

These three modes of heat transfer are also occurring in the body and from the body to the environment. In 1948, Pennes bioheat equation [26] was published which describe the heat transport occurring in the living tissues of the body as given by Equation 4 with the first two-terms describing conduction with radius r (m), geometry factor ω (ω = 1 for polar, ω = 2 for spherical coordinates), the second term describing metabolic heat generation q_m (W/m^3), and the third term describing convection with density of blood ρ_{bl} (kg/m^3), blood perfusion rate w_{bl} (s^{-1}), heat capacitance of blood c_{bl} ($J \bullet kg^{-1} \bullet K^{-1}$), and arterial blood temperature $T_{bl,a}$ assumed to be constant. Radiation is neglected in this equation due to the limited contribution in the body.

Equation 4

$$k\left(\frac{\partial^2 T}{\partial r^2} + \frac{\omega}{r}\frac{\partial T}{\partial r}\right) + q_m + \rho_{bl} w_{bl} c_{bl}\left(T_{bl,a} - T\right) = \rho c \frac{\partial T}{\partial t}$$

Although the gold-standard for bioheat equations, the Pennes' pivotal bioheat equation has limitations [27], including overlooking contributions from large blood vessels in both the conductive and convection terms, and there is a lack of empirical values describing geometric or hemodynamic characteristics of core vasculature which could assist in model parameterization and validation [27,28] particularly in whole body modeling [29]. Researchers continue to develop models to accurately predict body temperatures. Not only are the physics of heat transfer and the appropriate mathematical models still being investigated, the physiology and the body's mechanisms for heat removal and generation are also areas of research. This thesis focuses primarily on the third term in the equation or the 'convection' term.

The body utilizes two pathways to achieve homeostasis. The passive system includes heat conduction through tissues and convective heat transfer via the CV system (forced) and from the skin's surface to the environment (natural). The active system includes changes in cardiac output (CO), vasodilation or constriction, sweating, and shivering and is depicted in Figure 1.3 [29].

Fiala et al. use computational modeling to determine temperature inputs and outputs for the body and incorporates both the passive and active systems [29]. For the active system, Fiala uses only two temperature inputs for the body (hypothalalum: T_h and skin: T_{sk}) and does not incorporate changes in core body temperature or changes in core blood flow. However, the cardiovascular system is composed of more than just the blood vessels in the skin, and to be able to fully model thermoregulation and bioheat, the entire body's response to temperature must be understood.

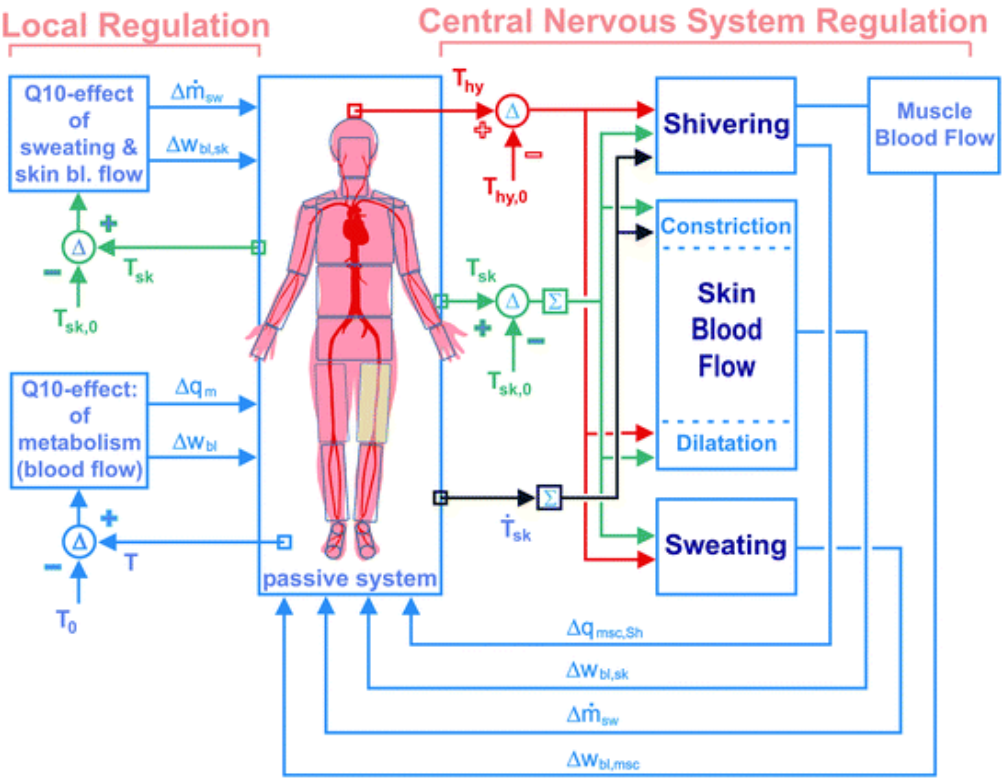

Figure 1.3 "Schematic diagram of the reference active system model." [29]

1.3 Cardiovascular System's Role in Thermoregulation

If the heat is not removed from the body to the environment, humans would heat up by an estimated 1 °C/ hour and a person would die within a few hours [19]. For the body to maintain a set core temperature (Tc), heat generated must be removed from the body, through the muscle (Tm), and finally through the skin (Ts), and the CV system plays an essential role in both the active and passive system to achieve this as depicted in Figure 1.4. However, it remains unclear how the allocation of blood in various compartments (e.g. core, fat, muscle, and skin) changes with temperature [16,30]. Early work suggested skin was the primary compartment in which increases in blood flow occurred when core temperature was increased [31], but it has also been demonstrated that there are increases to the muscle with increased temperature [32-36].

The body is actively thermoregulating even in the resting state, and this is the focus of this thesis: to study the effect of temperature on the CV system. However, the impact of

temperature on different physiological states is of interest to the author. To demonstrate, one example is the body during exercise illustrated in Figure 1.4. The active homeostasis system responds differently at rest (minimum muscle heat generation, Tc > Tm) compared to during a bout of exercise (maximum muscle heat generation, Tm > Tc). The result is that the pathway of overall heat dissipation is changed dramatically. Subsequently, the CV system responds by increasing blood flow to the skin (SkBF) to increase heat dissipation. However, this decreases the amount of blood flow to muscle (MBF), thereby decreasing muscle function during exercise [37].

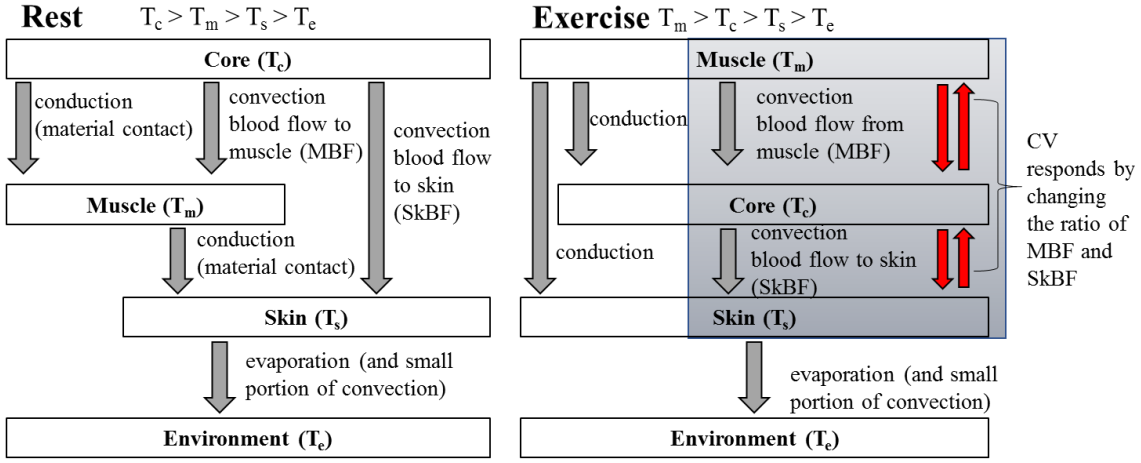

Figure 1.4 Representation of the heat transfer at rest and during exercise

Changes in metabolic demand during exercise are not the only influences on the role of the CV system in thermoregulation. Sex and age also affect the body's response to temperature [38]. The differences in sex can potentially be attributed to body composition (fat vs. muscle content), anthropometric characteristics (mass and surface area), physiological differences (water regulation, sex hormones, and exercise capacity), and social behaviors (daily physical activity and clothing choices) [39]. Aging affects thermoperception, heat loss and thermogenesis, and central nervous system regulation [9,40]. Sex and age not only influence the body's ability to

perceive and respond to changes in temperature [9,38,39,41-43], they also affect the function of the CV system [44-47].

Challenges in measuring core vasculature have resulted in a lack of empirical information regarding how it might change with core temperature. Magnetic Resonance Imaging (MRI) can be used to non-invasively measure the core vasculature due to high spatial and temporal resolution. Therefore, to fully understand the CV system's role in thermoregulation, this thesis focuses on using murine models and MRI to study the effect of temperature on core vasculature. The overall purpose is to provide a novel and physiologically accurate approach to studying thermoregulation by incorporating structural and functional changes in the CV system occurring in the core.

1.4 Magnetic Resonance Imaging (MRI)

Compared to other imaging modalities, MRI is one of the most flexible imaging platforms because it combines high resolution anatomical imaging with functional and metabolic analyses [55]. MRI is currently used to guide thermal therapies [56] and to investigate the brain's role in thermoregulation [57]. However, to our knowledge, preclinical MRI has not been used to study the cardiovascular system in regards to thermoregulation. Historically, preclinical MRI studies of the cardiovascular system have been focused on pathological disease such as deep vein thrombosis which is also studied in our lab [58,59]. With this work, we have been the first to use an ultrahigh field 7 Tesla MRI to conduct thermoregulation studies.

1.5 Murine Models and Limitations

Murine models are widely used as a preclinical model due to their similar biology to humans, the ability for researchers to conduct experiments in a highly controlled manner, and the ability for researchers to create transgenics. The current gold standard for thermoregulation

studies are using non-anesthetized rodents to study biomarkers such as core and skin temperature [48,49]. In this work, we studied anesthetized healthy wildtype C57BL/6 mice, one of the most common backgrounds used in research, to acquire baseline data in the core to compare future measurements from disease models and gene knockout animals with limited thermoregulation ability [50].

Murine models have limitations. Mice only have sweat glands on their paws and use their tails to regulate temperature. Murine studies also often require anesthesia. Anesthesia has been shown to reduce the core temperature at which physiological responses such as vasoconstriction occur; however, the intensity of the vascular response is maintained [51]. In addition, although isoflurane has vasodilatory effects which can be dose and step-size dependent, [52,53] our attentive control and monitoring of our animals' physiology allows us to minimize these effects by using low doses and making small adjustments throughout an imaging session. Studies also show a slight reduction in cardiac output under anesthesia, but heart rates are closer to those recorded in conscious mice using isoflurane [54].

1.6 Thesis Structure

This thesis describes the development of a novel and physiologically accurate approach to studying thermoregulation by incorporating structural and functional changes in the CV system occurring in the core. We hypothesized that a relationship between vessel size/deformation, blood flow, and temperature exists in the core, and these changes should be incorporated into modeling. Not only does this thesis describe a new approach to studying the effect of temperature on the cardiovascular system, the effect of age and sex on vascular response was also investigated. The chapters to follow are broken down in the following manner: Chapter 2 describes the geometric and functional arterial response across sex and age, Chapter 3

describes and compares the geometric and functional arterial and venous response, Chapter 4 describes the blood distribution, quantifying blood velocity and flow across sex and age, with increases in core body temperature, Chapter 5 describes a collaboration study combining two cardiovascular stressors: thermal stress and dobutamine, and Chapter 6 includes the conclusion and describes future work.

1.7 References

[1] Chu KF, Dupuy DE. Thermal ablation of tumours: biological mechanisms and advances in therapy. Nat. Rev. Cancer 2014;14:199–208.

[2] Meeker DG, Wang T, Harrington WN, et al. Versatility of targeted antibiotic-loaded gold nanoconstructs for the treatment of biofilm-associated bacterial infections. Int. J. Hyperth. 2018;34:209–219.

[3] Saga T, Sakahara H, Nakamoto Y, et al. Enhancement of the therapeutic outcome of radio-immunotherapy by combination with whole-body mild hyperthermia. Eur. J. Cancer 2001;37:1429–1434.

[4] Yenari MA, Han HS. Neuroprotective mechanisms of hypothermia in brain ischaemia. Nat. Rev. Neurosci. 2012;13:267–278.

[5] Shankaran S, Laptook AR, Ehrenkranz RA, et al. Whole-Body Hypothermia for Neonates with Hypoxic–Ischemic Encephalopathy. N. Engl. J. Med. 2005;353:1574–1584.

[6] Holzer M, Bernard SA, Hachimi-Idrissi S, et al. Hypothermia for neuroprotection after cardiac arrest: Systematic review and individual patient data meta-analysis. Crit. Care Med. 2005;33:414–418.

[7] Bailes JE, Cantu RC, Day AL. The Neurosurgeon in Sport: Awareness of the Risks of Heatstroke and Dietary Supplements. Neurosurgery. 2002;51:283–288.

[8] Bricknell MCM. Heat illness--a review of military experience (Part 2). 1996;

[9] Brody GM. Hyperthermia and hypothermia in the elderly. Clin. Geriatr. Med. 1994;10:213–229.

[10] Morbidity and Mortality Weekly Report (MMWR). Heat-Related Mortality--Arizona, 1993-2002, and United States, 1979-2002. 2005.

[11] Centers for Disease Control (CDC). Picture of America Heat-Related Illness Fact Sheet

[12] Martens WJM. Climate change, thermal stress and mortality changes. Soc. Sci. Med. 1998;46:331–344.

[13] Fritz RL, Perrin DH. Cold exposure injuries: prevention and treatment. Clin. Sports Med. 1989;8:111–128.

[14] Morbidity and Mortality Weekly Report (MMWR). Heat-Related Mortality--Arizona, 1993-2002, and United States, 1979-2002. 2005.

[15] Tucker R, Rauch L, Harley YR, et al. Impaired exercise performance in the heat is associated with an anticipatory reduction in skeletal muscle recruitment. Pflugers Arch. - Eur. J. Physiol. 2004;448:422–430.

[16] Rowell LB. Human Cardiovascular Adjustments to Exercise and Thermal Stress. Physiol. Rev. 1974;54:75–159.

[17] Lim L, Byrne C, Lee JK. Human Thermoregulation and Measurement of Body Temperature in Exercise and Clinical Settings. 2008;37.

[18] Stewart IB, Rojek AM, Hunt AP. Heat Strain During Explosive Ordnance Disposal. Mil. Med. 2011;176:959–963.

[19] Parsons KC. Human thermal environments: the effects of hot, moderate, and cold environments on human health, comfort, and performance. 3rd ed. CRC Press/Taylor & Francis; 1993.

[20] Werner J, Buse M. Temperature profiles with respect to inhomogeneity and geometry of the human body. J. Appl. Physiol. 1988;65:1110–1118.

[21] Hinson JM, Laprairie KN, Cundiff JM. One Size Does NOT Fit ALL. J Appl Physiol. 2005;32:26–30.

[22] Vriens J, Nilius B, Voets T. Peripheral thermosensation in mammals. Nature Reviews Neuroscience 2014;15 (9): 573-589.

[23] Gordon CJ. Behavioral and autonomic thermoregulation in mice exposed to microwave radiation. J. Appl. Physiol. 1983;55:1242–1248.

[24] Vriens J, Nilius B, Voets T. Peripheral thermosensation in mammals. Nat. Publ. Gr. 2014;15(9):573-89.

[25] Incropera FP, Dewitt DP, Bergman TL, et al. Fundamentals of Heat and Mass Transfer. 6th ed. Hoboken, NJ, USA: Wiley & Sons, Inc.; 2007.

[26] Pennes HH. Analysis of tissue and arterial blood temperatures in the resting human forearm. J. Appl. Physiol. 1948;1:93–121.

[27] Wissler EH. Pennes' 1948 paper revisited. J. Appl. Physiol. 1998;85:35–41.

[28] Bhowmik A, Singh R, Repaka R, et al. Conventional and newly developed bioheat transport models in vascularized tissues: A review. J. Therm. Biol. 2013;38:107–125.

[29] Fiala D, Havenith G. Modelling Human Heat Transfer and Temperature Regulation. Springer International Publishing; 2015. p. 265–302.

[30] González-Alonso J. Human thermoregulation and the cardiovascular system. Exp. Physiol. 2012;97:340–346.

[31] Dastre A, Morat J. Influence du sang asphyxique sur l'appareil nerveux de la circulation [Influence of asphyxial blood on the nervous system of circulation]. Arch. Physiol. Norm. Pathol. 1884;3:1–45.

[32] Akyürekli D, Gerig LH, Raaphorst GP. Changes in muscle blood flow distribution during hyperthermia. Int. J. Hyperth. 1997;13:481–496.

[33] Pearson J, Low DA, Stöhr E, et al. Hemodynamic responses to heat stress in the resting and exercising human leg: insight into the effect of temperature on skeletal muscle blood flow. Am. J. Physiol. - Regul. Integr. Comp. Physiol. 2011;300:663–673.

[34] Binzoni T, Tchernin D, Richiardi J, et al. Haemodynamic responses to temperature changes of human skeletal muscle studied by laser-Doppler flowmetry. Physiol. Meas. 2012;33:1181–1197.

[35] Chiesa ST, Trangmar SJ, González-Alonso J. Temperature and blood flow distribution in the human leg during passive heat stress. J. Appl. Physiol. 2016;120:1047–1058.

[36] González-Alonso J, Calbet JAL, Boushel R, et al. Blood temperature and perfusion to exercising and non-exercising human limbs. Exp. Physiol. 2015;100:1118–1131.

[37] Akyureklit D, Gerigt LH, Raaphorstt GP. Changes in muscle blood flow distribution during hyperthermia. INT. J. Hyperth. 1997;13:481–496.

[38] McDonald RB, Day C, Carlson K, et al. Effect of age and gender on thermoregulation. Am. J. Physiol. 1989;257:R700-4.

[39] Kaciuba-Uscilko H, Grucza R. Gender differences in thermoregulation. Curr. Opin. Clin. Nutr. Metab. Care. 2001;4:533–536.

[40] Rida M, Ghaddar N, Ghali K, et al. Elderly bioheat modeling: changes in physiology, thermoregulation, and blood flow circulation. Int. J. Biometeorol. 2014;58:1825–1843.

[41] Centers for Disease Control and Prevention U. Hypothermia-related deaths--United States, 1999-2002 and 2005. MMWR Morb. Mortal. Wkly. Rep. 2006;55:282–284.

[42] Collins KJ, Exton-Smith AN. 1983 Henderson Award Lecture. Thermal homeostasis in old age. J. Am. Geriatr. Soc. 1983;31:519–524.

[43] Noe RS, Jin JO, Wolkin AF. Exposure to Natural Cold and Heat: Hypothermia and Hyperthermia Medicare Claims, United States, 2004–2005. Am. J. Public Health. 2012;102:e11–e18.

[44] Van Someren EJW. Chapter 22 – Age-Related Changes in Thermoreception and Thermoregulation. Handb. Biol. Aging. 2011. p. 463–478.

[45] Chen CH, Nakayama M, Nevo E, et al. Coupled systolic-ventricular and vascular stiffening with age: implications for pressure regulation and cardiac reserve in the elderly. J. Am. Coll. Cardiol. 1998;32:1221–1227.

[46] O'Toole ML. Gender differences in the cardiovascular response to exercise. Cardiovasc. Clin. 1989;19:17–33.

[47] Minson CT, Wladkowski SL, Cardell AF, et al. Age alters the cardiovascular response to direct passive heating. J. Appl. Physiol. 1998;84:1323–1332.

[48] Leon LR, DuBose DA, Mason CW. Heat stress induces a biphasic thermoregulatory response in mice. Am. J. Physiol. Regul. Integr. Comp. Physiol. 2005;288:R197-204.

[49] Quinn CM, Duran RM, Audet GN, et al. Cardiovascular and thermoregulatory biomarkers of heat stroke severity in a conscious rat model. J. Appl. Physiol. 2014;117:971–978.

[50] Leon LR. The use of gene knockout mice in thermoregulation studies. J. Therm. Biol. 2005;30:273–288.

[51] Støen R, Sessler DI. The Thermoregulatory Threshold is Inversely Proportional to Isoflurane Concentration. Anesthesiology. 1990;72:822–827.

[52] Matta BF, Heath KJ, Tipping K, et al. Direct cerebral vasodilatory effects of sevoflurane and isoflurane. Anesthesiology. 1999;91:677–680.

[53] Hartley CJ, Reddy AK, Madala S, et al. Effects of isoflurane on coronary blood flow velocity in young, old and ApoE(-/-) mice measured by Doppler ultrasound. Ultrasound Med. Biol. 2007;33:512–521.

[54] Constantinides C, Mean R, Janssen BJ. Effects of isoflurane anesthesia on the cardiovascular function of the C57BL/6 mouse. ILAR J. 2011;52:e21-31.

[55] Albanese C, Rodriguez OC, VanMeter J, et al. Preclinical magnetic resonance imaging and systems biology in cancer research: current applications and challenges. Am. J. Pathol. 2013;182:312–318.

[56] Carpentier A, McNichols RJ, Stafford RJ, et al. Laser thermal therapy: Real-time MRI-guided and computer-controlled procedures for metastatic brain tumors. Lasers Surg. Med. 2011;43:943–950.

[57] Muzik O, Diwadkar VA. In vivo correlates of thermoregulatory defense in humans: Temporal course of sub-cortical and cortical responses assessed with fMRI. Hum. Brain Mapp. 2016;37:3188–3202.

[58] Palmer OR, Chiu CB, Cao A, et al. In vivo characterization of the murine venous system before and during dobutamine stimulation: implications for preclinical models of venous disease. Ann. Anat. - Anat. Anzeiger. 2017;214:43–52.

[59] Palmer OR, Shaydakov ME, Rainey JP, et al. Update on the electrolytic IVC model for pre-clinical studies of venous thrombosis. Res. Pract. Thromb. Haemost. 2018;2:266–273.

Chapter 2
Geometric and functional arterial response due to increases in body temperature

2.1 Abstract

Purpose: To date, the response of core vasculature to increasing core temperature has not been adequately studied *in vivo*. Our objective was to non-invasively quantify the arterial response in murine models due to increases in body temperature, with a focus on core vessels of the torso, and investigate whether responses were dependent on sex or age.

Methods: Male and female, adult and aged mice were anesthetized and underwent magnetic resonance imaging. Data were acquired from the Circle of Willis (CoW), heart, infrarenal aorta, and peripheral arteries at core temperatures of 35, 36, 37, and 38°C (± 0.2°C).

Results: Vessels in the CoW did not change. Ejection fraction decreased and cardiac output increased with increasing temperature in adult female mice. Cross-sectional area of the aorta increased significantly and linearly with temperature for all groups, but at a diminished rate for aged animals ($p < 0.01$; male and female: adult, 0.019 and 0.024 mm^2/°C; aged, 0.017 and 0.011 mm^2/°C). Aged male mice had a diminished response in the periphery (% increase in femoral artery area from 35 to 38°C, male and female: adult, 67 and 65%; aged, 0.1 and 57%).

Conclusion: Previously unidentified increases in aortic area due to increasing core temperature are biologically important because they may affect conductive and convective heat transfer. Leveraging non-invasive methodology to quantify sex and age dependent vascular responses due to increasing core temperature could be combined with bioheat modeling in order to improve understanding of thermoregulation.

2.2 Introduction

Core temperature impacts human health and performance [1–5]. Humans maintain core temperature via the process of thermoregulation [6]. The body utilizes two pathways to achieve this homeostasis. The passive system includes heat conduction through tissues and convective heat transfer via the CV system (forced) and from the skin's surface to the environment (natural). The active system includes changes in cardiac output (CO), vasodilation or constriction, sweating, and shivering [7]. The CV system plays an essential role in both systems. However, it remains unclear how the allocation of blood in various compartments (e.g. core, fat, muscle, and skin) changes with temperature [8,9]. Early work suggested skin was the primary compartment in which increases in blood flow occurred when core temperature was increased [10],but it has also been demonstrated that there are increases to the muscle with increased temperature [11–15]. Sex and age not only influence the body's ability to perceive and respond to changes in temperature [3,16–20], they also affect the function of the CV system [21–24]. Therefore, to fully understand the CV system's role in the complex process of thermoregulation, blood distribution (influenced by cardiac output, vessel size, blood flow velocity, and pressure) must be quantified, ideally across sex and age.

Because it is easily accessible, changes in the skin due to temperature have been quantified using numerous methods [25–27]. It is more difficult to quantify changes in the other compartments, with the core perhaps being the most challenging to investigate due to the impact of invasive methods on core tissues. Observed CV changes in the core due to increasing core temperature include: regional increases and decreases in cerebral blood flow depending on the temperature range [28–30], increased cardiac output [31,32], and decreased total peripheral resistance [31,33]. Noticeably absent from this body of knowledge is data regarding if there are

geometric and functional changes in the core vessels of the torso, the primary large-caliber supply system that transports blood at higher temperatures to the small-caliber distribution system located throughout the body. Mathematical modeling has been used as an alternative approach. However, barriers remain to this methodology reaching its full potential. Even Pennes' pivotal bioheat equation has limitations [34], including overlooking contributions from large blood vessels, and there is a lack of empirical values describing geometric or hemodynamic characteristics of core vasculature which could assist in model parameterization and validation [34,35]. Consequently, there remains an inability to quantify or model the coalescing vascular changes in the CV system due to changes in core temperature.

Magnetic resonance imaging (MRI) can be used to non-invasively study core vasculature due to high spatial resolution and few limitations on tissue penetration depth. Temporal resolution can be leveraged to study processes that change across the cardiac cycle. Rodent models are often used to study thermoregulation because of the potential to manipulate relevant genes and to vary core temperature and/or environment while making the necessary measurements [36]. Previous *in vitro* studies do not include the influence of surrounding structures which affect vascular biomechanical forces and subsequent health of the CV system and which are important in modeling [37]. Surrounding structures and blood also act as heat sources/sinks [38], and thus, it is important that whole-body thermoregulation studies be conducted in vivo.

Using murine models and MRI, we noninvasively quantified cardiac indices of left ventricular function and changes in the cerebral, infrarenal, and peripheral arteries at four target core temperatures. The effects of sex and age on the CV response to increasing temperature from minimally hypothermic to minimally hyperthermic were measured. We hypothesized that as core

temperature was increased from 35 to 38 °C: 1) cerebral vasculature and the aorta would not change; 2) cardiac output would increase; 3) peripheral vasculature would dilate; and, 4) responses would differ based on sex and age. To our knowledge, these data are the first to empirically quantify the spatially and temporally resolved response of core vasculature to changes in core temperature *in vivo* from head-to-toe. This geometric and functional data could be used to couple bioheat modeling and computational fluid dynamics (CFD) in order to improve understanding of thermoregulation.

2.3 Methods

All experiments were approved by the local Institutional Animal Care and Use Committee. Animals were housed in a room with temperature (22 °C ± 2 °C) and humidity (~27%) control and an alternate 12-hour light/dark cycle.

Healthy adult (10- to 22-weeks-old, ~20-30 human years) and aged (50- to 60-weeks-old, ~45-50 human years [39]), male and female, C57BL/6 mice were studied (n = 5 each, total = 20). Mice were anesthetized with 1.25-2% isoflurane in 1 L/min of oxygen [40]. Animals were placed in the supine position and imaged at 7T (Agilent Technologies, Santa Clara, CA) using a 40 mm inner diameter transmit-receive volume coil (Morris Instruments, Ontario, Canada). Core temperatures were increased from being minimally hypothermic (35 °C) to minimally hyperthermic (38 °C), while avoiding pathological changes [41,42]. The target core temperature was controlled via forced convection within ± 0.2 ^{o}C using a custom-built proportional-integral-derivative (PID) controller (LabVIEW, National Instruments, Austin TX) interfaced with a commercially available system which includes a heater blowing warm air through the bore of the magnet and over the animal and a rectal temperature probe. PID controllers are used to

efficiently approach a desired setpoint, while managing overshoot and oscillations. Respiration and heart rate were monitored (SA Instruments, Stony Brook, NY).

Two MRI techniques (time-of-flight [TOF] MR angiography and CINE imaging) were used to investigate three anatomical regions of interest: the head, torso, and periphery (Figure 2.1). To acquire all locations for a given animal, with four core temperatures tested at each location, three imaging sessions (head, torso, and periphery) were required. The total imaging time for each session was approximately two hours. Each region was completed for all animal groups within two weeks before acquiring data from the next region; therefore, ages ranged 1-2 weeks within a region and 2-8 weeks between regions.

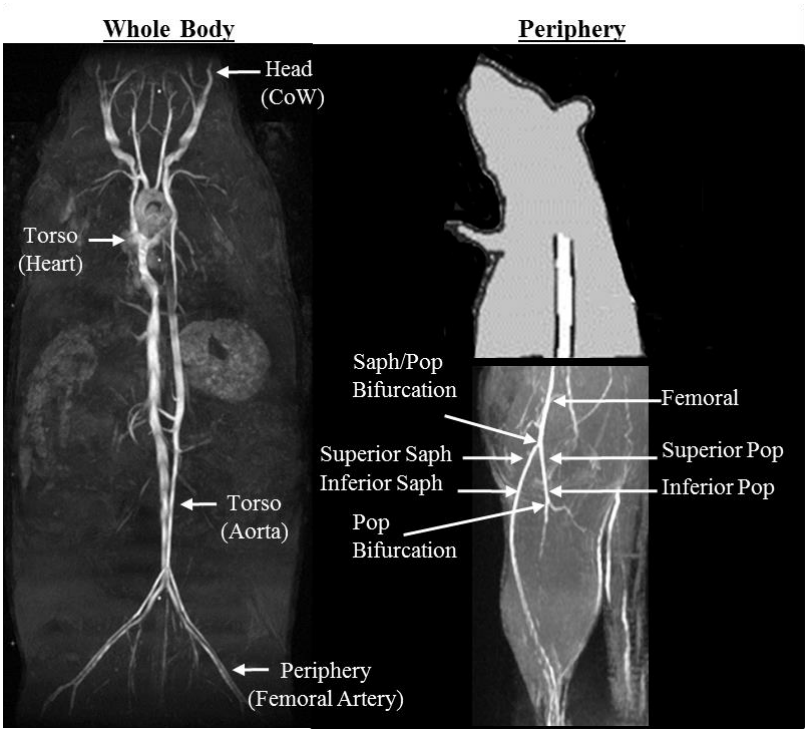

Figure 2.1 Maximum intensity projections (MIPs) illustrates where data were acquired and quantified from four anatomical locations along the body

Head: Circle of Willis (area)

Sagittal 2D gradient echo images were used to plan 3D TOF angiograms [repetition time/echo time (TR/TE) 50/3 ms, field of view (FOV) $(20\ mm)^3$, flip angle (α) 60^o, matrix 128^3

zero-filled to 256^3, slab thickness 20 mm, number of excitations (NEX) 2, resolution $(78\mu m)^3$, ~13 minutes]. The axial and sagittal 2D slices derived from the 3D TOF data were used to quantify the cross-sectional area of anterior cerebral arteries (ACA) and middle cerebral arteries (MCA), respectively, using a threshold value (Analyze, AnalyzeDirect, Stilwell, KS). Data acquired at 38 °C were used to establish a separate threshold value for each mouse that defined the area of the vessel based on user judgement. This threshold value was then used to analyze data for the other three temperatures. The location examined for both the ACA and MCA was 0.39 mm (5 slices) distal from the CoW ring (Figure 2.2).

Torso: Heart (heart rate, stroke volume, ejection fraction, cardiac output)

Heart rate was measured from a 2-lead ECG placed along axis II. Coronal 2D images were used to plan slices perpendicular to the long axis of the left ventricle (LV). Five to six 2D contiguous slices were planned through the LV, depending on the size of the organ. For each slice, a cardiac-gated and respiratory compensated 2D CINE acquisition with 12 frames was used to acquire data across the cardiac cycle [TR/TE 180/2 ms, FOV $(30\ mm)^2$, α 30^o, matrix 128^2 zero-filled to 256^2, slice thickness 1 mm, NEX 4, resolution $(117\ \mu m)^2$, ~20 minutes]. The endocardial area of each frame was defined manually (Analyze, AnalyzeDirect, Stilwell, KS). For each slice, the end-diastolic and end-systolic areas were determined by selecting the maximum and minimum areas, respectively. The end-diastolic volume (EDV) and end-systolic volume (ESV) were calculated:

Equation 5

$$EDV = \sum_{i=1}^{5-6} Slice\ area\ max_i * Slice\ thickness \quad ESV = \sum_{i=1}^{5-6} Slice\ area\ min_i * Slice\ thickness$$

Stroke volume (SV = EDV – ESV), ejection fraction (SV/EDV*100%), and cardiac output (SV*heart rate) were calculated from these values.

Torso: Infrarenal Aorta (area, circumferential cyclic strain)

Coronal maximum intensity projections (MIPs) from axial 3D acquisitions were used to plan slices perpendicular to the aorta. A cardiac-gated and velocity compensated 2D CINE acquisition with 12 frames was used to acquire data across the cardiac cycle [TR/TE ~120/4 ms depending on heart rate, FOV $(20\ mm)^2$, α 60^o, matrix 256^2 zero-filled to 512^2, slice thickness 1 mm, NEX 6, resolution $(39\ \mu m)^2$, ~18 voxels across the vessel, ~5 minutes]. The CINE images were analyzed for area and circumferential cyclic strain using an in-house semi-automated process. An automatic boundary of the vessel was defined by using a threshold value of 50% of the maximum signal intensity in a user-defined region selected across the 12 frames. This boundary could be modified by the user, if needed. Vessel area was calculated using polar integration. Green-Lagrange circumferential cyclic strain, to quantify vessel stiffness [43], was calculated using the following equation:

Equation 6

$$\varepsilon_i = \frac{1}{2}\left[\left(\frac{P_i}{P_{dias}}\right)^2 - 1\right] \times 100\%\ with\ i \to 1 - 12$$

where P_i is the perimeter at a given time frame and P_{dias} is the perimeter of the vessel at end diastole. This definition assumes uniform strain around the circumference and the *in vivo* diastolic perimeter is representative of the vessel's unloaded state. Green-Lagrange circumferential strain can reflect changes in area, provided the vessel's expansion preserves its shape. In this case, a strain value of 50% corresponds to a doubling of cross-sectional area during the cardiac cycle.

Periphery: Femoral, popliteal, and saphenous arteries (area, tracking length)

Coronal and axial 2D gradient echo images were used to plan 3D TOF angiograms [TR/TE 15/2 ms, FOV 25x35x35 mm^3, α 20^o, matrix 128^3 zero-filled to 256^3, slab thickness 30

mm, NEX 2, resolution 98x137x137 μm^3, ~13, 9, and 5 voxels across femoral, popliteal, and saphenous arteries, ~8 minutes]. Similar to the CoW, 2D slices from the 3D TOF acquisitions were used to quantify the cross-sectional area of the peripheral arteries using a threshold value defined from data acquired at 38 °C. Three locations of the peripheral arteries were examined (Figure 2.1)): femoral 0.68 mm (five slices) proximal to the saphenous-popliteal bifurcation, popliteal and saphenous 0.68 mm distal to the saphenous-popliteal bifurcation (superior), and popliteal and saphenous 0.68 mm proximal to popliteal bifurcation (inferior). The tracking length over which the saphenous artery could be visualized in the 3D acquisitions was determined by using the same threshold value as the area calculations and calculating the number of slices between the saphenous-popliteal bifurcation and the last slice for which the saphenous vessel could be seen.

Vessel conspicuity in 3D TOF angiograms is dependent on blood flow velocity as well as vessel size. While 2D acquisitions still rely on the movement of blood for contrast relative to stationary tissue, they are nearly independent of blood flow velocity. Therefore, to evaluate the contribution of blood flow velocity to visualization of peripheral vessels, a second group of adult male mice (14- to 15-weeks-old, n = 5) were imaged using 2D slices perpendicular to the femoral artery and the popliteal and saphenous arteries at the superior location. The 2D TOF sequence was qualitatively optimized to maximize the contrast between vessel and surrounding stationary tissue and achieve a minimum of ~10 voxels across each vessel at 38 °C [femoral: TR/TE 50/5 ms, FOV $(25.6\ mm)^2$, $\alpha\ 60^o$, matrix 256^2 zero-filled to 512^2, slice thickness 1 mm, NEX 8, resolution $(50\ \mu m)^2$, ~3 minutes ; popliteal and saphenous locations: TR/TE 20/3.4 ms, FOV $(25.6\ mm)^2$, $\alpha\ 60^o$, matrix 256^2 zero-filled to 512^2, slice thickness 1 mm, NEX 4, resolution $(50\ \mu m)^2$, ~1 minutes]. To null the signal from veins, a 5 mm thick saturation band was placed

distal to the imaging slice. Locations were similar to those described above. Data acquired at 38 °C were used to establish a threshold value that defined the size of the vessel based on user judgement and that was used for data at 35 °C.

Statistical Analysis

Data are plotted as mean ± standard error (SEM) with individual data points. To test whether temperature had an effect on a given metric within a group of animals, repeated measures one-way ANOVA and Tukey's post hoc test to account for multiple comparisons was used, with temperature treated as categorical. Two methods were used to evaluate differences between groups. First, to compare relative changes within a given one degree temperature interval (i.e. 35-36, 36-37, or 37-38 °C), the percent change per one degree increase in temperature (%/°C) was calculated for each metric to account for potential differences in the size of anatomical structures between groups. For example, percent change in vessel area in adult male mice for the interval 35-36 °C = (area36 – area35)/(area35)*100; and, similarly, for the other temperature intervals and each group. Using the %/°C values, the effects of sex and age were assessed via two-way ANOVA and Tukey's post hoc test. Second, to compare absolute changes over the four degree temperature interval, linear regression was applied to each metric of interest. For example for area, regression resulted in a fitted line with units of mm^2/°C. Slopes were assessed for linearity (R^2) and tested for being non-zero and different between groups. Significance was set at $p < 0.05$.

2.4 Results

Representative images from the four anatomical locations, acquired at 35 and 38 °C, are shown in Figure 2.2.

summarizes the results presented below as well as non-significant findings. Non-significant group comparisons of percent change per degree show adjusted means, for sex and age, averaged across the three temperature intervals. As a reference for area measurements, based on image resolution at each anatomical location: CoW, 10 voxels = 0.06 mm^2; infrarenal aorta, 10 voxels = 0.015 mm^2; peripheral vasculature, 10 voxels = 0.13 mm^2 and 5 voxels= 0.067 mm^2.

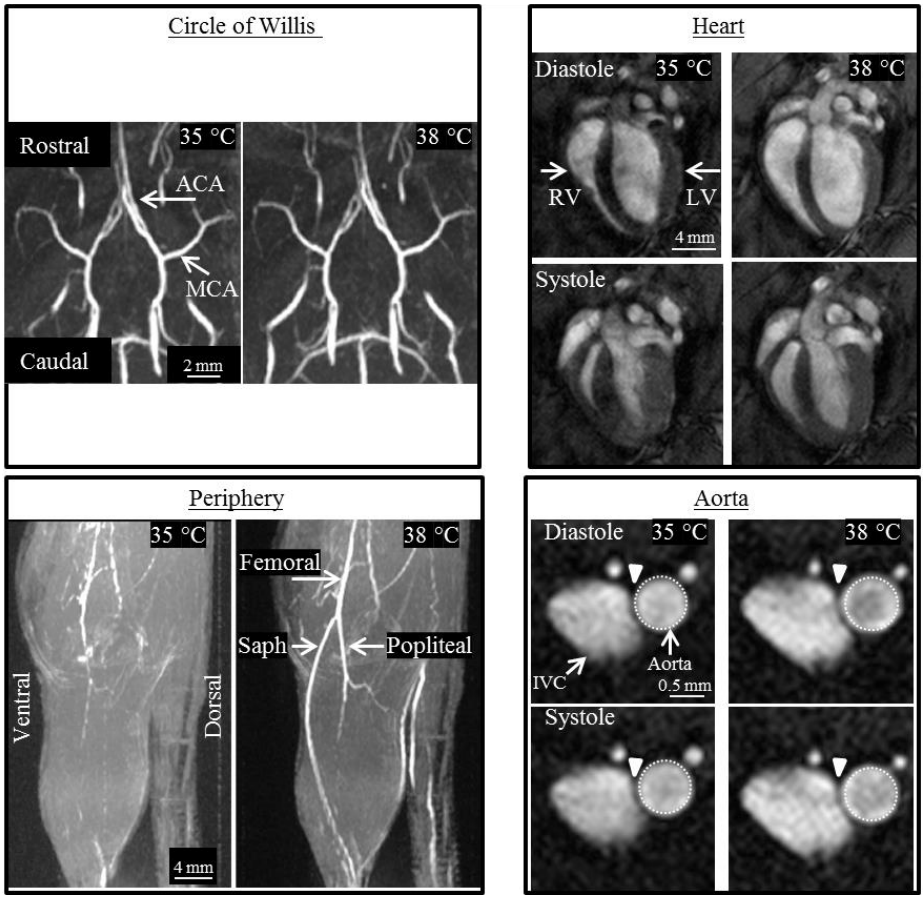

Figure 2.2 Representative images from the four anatomical locations of an adult male mouse at 35 and 38°C.

Cerebral vasculature has minimal response to increases in core temperature.

The ACA and MCA were readily visible at all temperatures, unlike superficial vessels of the periphery (Figure 2.2). Cerebral vasculature did not change with increasing core temperature. ACA and MCA vessel areas averaged across the four temperatures for each group were: adult

males, 0.06 ±0.005 mm^2 and 0.05 ±0.004 mm^2; adult females, 0.05±0.005 mm^2 and 0.04 ± 0.003 mm^2; aged males, 0.05 ±0.005 mm^2 and 0.05 ±0.005 mm^2; aged females, 0.04 ±0.004 mm^2 and 0.05 ±0.006 mm^2.

Table 2.1 Summary of results for arterial response across sex and age.
Data presented as mean ± SEM, or for group comparisons slopes and percent change per degree. Non-significant group comparisons of (%/°C) show adjusted means, for sex and age, averaged across the three temperature intervals. ACA = anterior cerebral artery, MCA = middle cerebral artery, bpm = beats per minutes, M = male, F = female, NS = not significant.

Location	Group (n = 5 each)	Temperature		Linear Regression			Group Comparisons
		Overall (p-value)	Pairwise Comparisons	Slope (unit/°C)	R^2	Slope ≠ 0 (p-value)	Slopes (unit/°C) Sex and Age (%/°C)
Head							
CoW (ACA, MCA: area, mm^2)	NS			NS			NS NS: M, F: 3.2 vs. -2.1%/°C Adult, Aged: 3.4 vs. -2.3 %/°C
Torso (Figures S1, S2, and 4)							
Heart (heart rate, bpm)	Adult F	0.04	None	19.9 ±3.6	0.94	0.03	NS
	Aged M	0.02	None	14.2 ±3.0	0.92	0.04	NS: M, F: 2.1 vs. 6.0 %/°C Adult, Aged: 2.4 vs. 3.3 %/°C
	Aged F	0.006	None	16.1 ±3.3	0.92	0.04	
Heart (stroke volume, µL/beat)	NS			NS			NS NS: M, F: 0.24 vs. -1.1 %/°C Adult, Aged: 0.063 vs. -0.93 %/°C
Heart (ejection fraction, %)	Adult F	0.008	35/38 p=0.03	NS			NS NS: M, F: -1.8 vs. -2.7 %/°C Adult, Aged: -2.7 vs. -0.48 %/°C
Heart (cardiac output, mL/min)	Adult F	0.049	None	NS			NS NS: M, F: 2.4 vs. 3.1 %/°C Adult, Aged: 2.4 vs. 2.3 %/°C
Infrarenal Aorta (area, mm^2)	Adult M	0.02	36/37 p=0.01	0.019 ±0.002	0.98	0.008	**p < 0.01** M, F: 0.018 and 0.018 mm^2/°C Adult, Aged: 0.022 and 0.014 mm^2/°C
	Adult F	0.003	35/38 p=0.01 36/38 p=0.02	0.024 ±0.001	0.99	0.003	
	Aged M	0.02	None	0.017 ±0.0008	0.99	0.002	NS: M, F: 4.8 vs.10.0 %/°C Adult, Aged: 6.4 vs. 3.9 %/°C
	Aged F	0.006	None	0.011 ±0.001	0.97	0.02	
Infrarenal Aorta (strain)	Adult M	NS		-2.0 ±0.1	0.99	0.004	NS NS: M, F: -7.8 vs. -4.7 %/°C Adult, Aged: -2.3 vs. -5.0 %/°C

Ejection fraction decreased, cardiac output increased with temperature in adult females.

Qualitatively, there is a discernable increase in both end-diastolic and end-systolic left ventricle volume with increasing temperature (Figure 2.2). Heart rate, stroke volume, ejection fraction, and cardiac output are presented in Figure 2.3. Except for adult males, temperature had an influence on heart rate for the other three groups ($p = 0.04$-0.006). Heart rate linearly increased with temperature (slopes > 0, $p = 0.03$-0.04, $R^2 = 0.92$-0.94), with no difference between slopes. In adult females, temperature had an influence on ejection fraction ($p = 0.008$; with a statistically significant difference between means for 35 and 38 °C, 73.6% vs. 68.7%, $p = 0.03$) and cardiac output ($p = 0.049$).

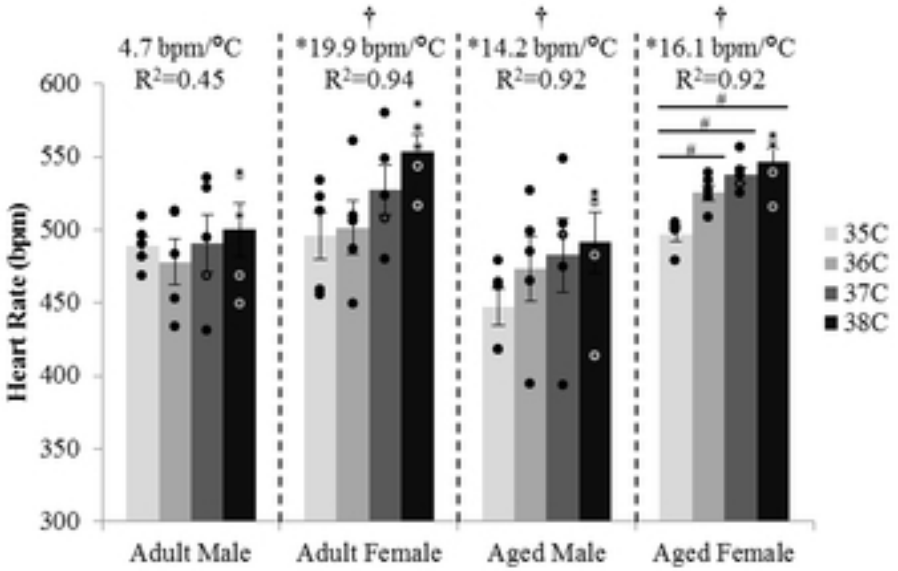

	Stroke Volume (µL/beat)		Ejection Fraction (%)		Cardiac Output (mL/min)	
	35°C	38°C	35°C	38°C	35°C	38°C
Adult Male	36.1 ±1.9	37.1 ±2.8	67.2 ±2.3	60.3 ±1.0	17.7 ±1.1	18.5 ±1.3
Adult Female	29.0 ±1.9	27.8 ±1.8	† 73.6 ±1.0*	68.7 ±1.0*	† 14.2 ±0.5	15.4 ±0.9
Aged Male	40.3 ±2.4	39.4 ±2.6	57.4 ±2.4	56.0 ±1.5	18.1 ±1.4	19.3 ±1.4
Aged Female	36.8±2.2	34.9 ±2.0	68.4 ±0.9	67.3 ±2.0	18.2 ±1.0	19.0 ±0.8

Figure 2.3 Cardiac response for male and female, adult and aged mice

Aortic area increased with temperature, but at a diminished rate for aged animals.

Qualitatively, there is a discernable increase in both diastolic and systolic area of the infrarenal aorta with increasing temperature (Figure 2.2). Figure 2.4 shows cross-sectional area of the infrarenal aorta across the cardiac cycle for all groups (error bars are omitted for clarity). Figure 2.5 shows cyclic strain of the infrarenal aorta across the cardiac cycle for all groups. In Figure 2.6, average area and maximum cyclic strain are plotted to highlight their relationship.

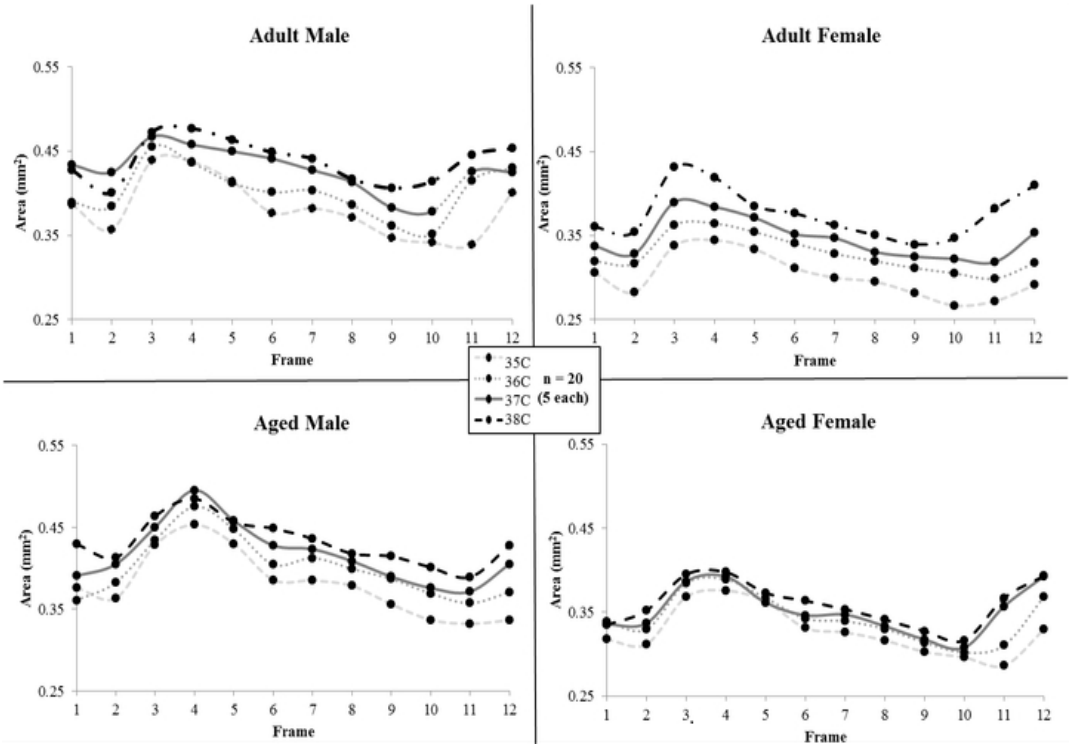

Figure 2.4 Cross-sectional area of the infrarenal aorta across the cardiac cycle for male and female, adult and aged mice

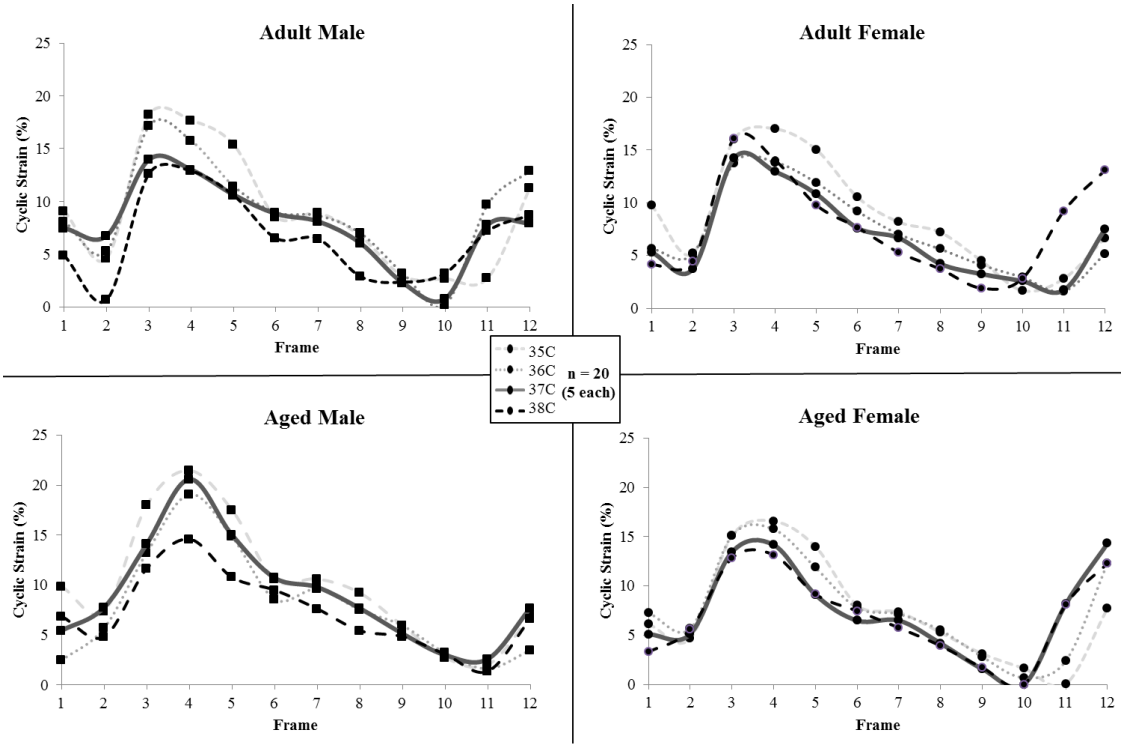

Figure 2.5 Cyclic strain of the infrarenal aorta across the cardiac cycle for male and female, adult and aged mice

Temperature had an influence on average vessel area for all groups (Figure 2.6,

, p = 0.02-0.003). There were statistically significant differences between means within a group for: adult male, 36/37 °C (p = 0.01); and, adult female, 35/38 °C (p = 0.01) and 36/38 °C (p = 0.02). Area linearly increased with temperature (slopes > 0, p = 0.02-0.003, R^2 = 0.97-0.99), and slopes were different between groups (p < 0.001; adjusted means: male vs. female, 0.018 and 0.018 mm^2/°C; adult vs. aged, 0.022 and 0.014 mm^2/°C). For adult males, cyclic strain linearly decreased with temperature (slope < 0, p = 0.004, R^2 = 0.99).

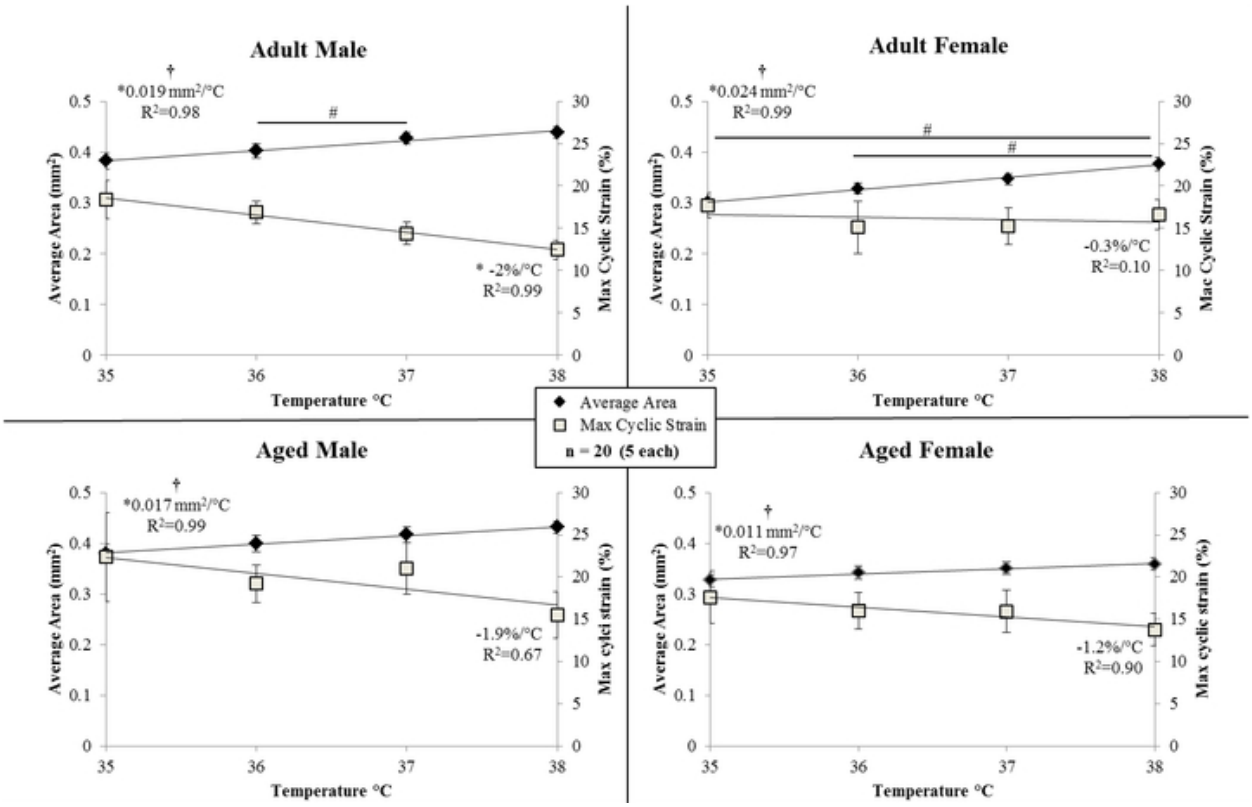

Figure 2.6 Average cross-sectional area and maximum circumferential cyclic strain of the infrarenal aorta for male and female, adult and aged mice at core temperatures.

Peripheral vessel areas and tracking length increased with temperature, with minimal or no response in aged males.

Although from the MIPs it appears there is no signal to quantify along large extents of the peripheral vasculature at 35 °C (Figure 2.2), in the 2D images from these 3D acquisitions there is signal visible throughout most of the regions of interest. When considering 2D versus 3D methods, there are several tradeoffs to consider, including non-perpendicular slice orientation relative to vessels vs. data acquisition efficiency. 3D acquisition allowed for the full leg to be imaged at four different temperatures in the least amount of time. Therefore, peripheral area data shown in Figure 2.7 are calculated from 2D axial slices of 3D acquisitions, with the caveat that the slices are only approximately perpendicular to the cross-sectional view of the artery

(particularly for the femoral location). Although this may cause a slight increase in the measured area, relative changes between temperatures account for this and provide relevant comparisons.

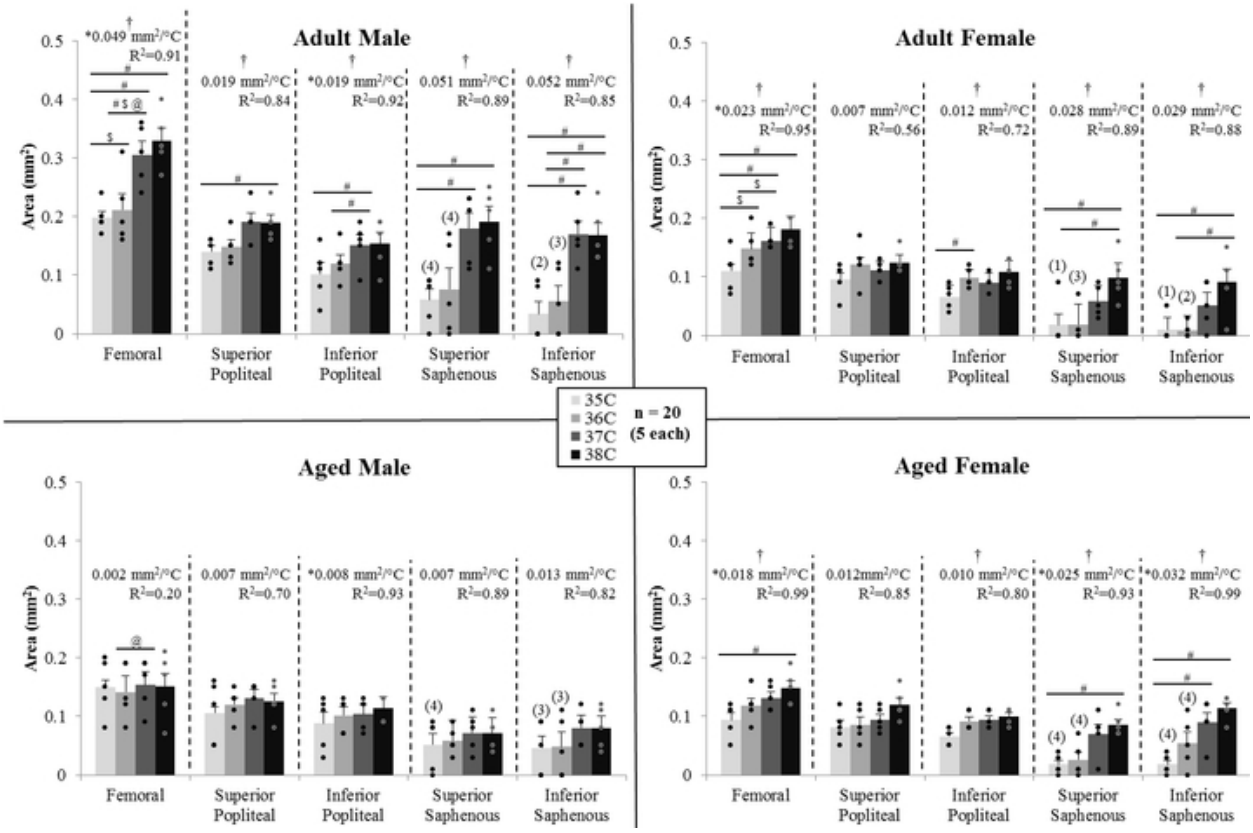

Figure 2.7 Cross sectional area of the peripheral arteries from 3D scans for male and female, adult and aged mice at core temperatures of 35, 36, 37, 38 °C.

Except for aged males, temperature had an influence on femoral artery area (p = 0.01-0.003), with statistically significant differences between means within a group for: adult male between 35/37, 35/38, and 36/37 °C (p = 0.02-0.03); adult female between 35/36 and 35/38 °C (p = 0.02 and 0.003); and, aged female 35/38 °C (p = 0.01). Except for aged males, femoral artery area linearly increased with temperature (slopes > 0, p = 0.04-0.007, R^2 = 0.91-0.99), and slopes were different between groups (p < 0.01; adjusted means: male vs. female 0.026 and 0.021 mm^2/°C; adult vs. aged 0.036 and 0.01 mm^2/°C). Relative changes within a given one degree temperature interval were influenced by sex and age. For the 35-36 °C interval, the adult female's response was over 7-fold larger than adult males (43.0 vs. 5.9 %/°C, p = 0.04). For the

36-37 °C interval, adult males had a larger response than adult females by 3.9-fold (48.7 vs. 12.6 %/°C, p = 0.05) and aged males by 4.7-fold (48.7 vs. 10.3 %/°C, p = 0.03). The average percent increase per degree temperature (averaged across all three intervals 35-36, 36-37, and 37-38) was 21.1%/°C for adult males, 22.6%/°C for adult females, 0.6%/ºC for aged males, and 19.8%/°C for aged females.

For adult males, temperature had an influence on the popliteal artery at the superior location (p = 0.01), with a statistically significant difference between means for 35 and 38 °C (p = 0.04). Except for aged males, temperature had an influence on inferior popliteal vessel area for all other groups (p = 0.045-0.01), with statistically significant differences between means within a group for: adult male between 35/37 and 36/37 °C (p = 0.005 and 0.04); and, adult female between 35/37 °C (p = 0.01). Area linearly increased with temperature for both male groups (slopes > 0, p = 0.04, R^2 = 0.92-.93).

For ten animals, the superior and/or inferior locations of the saphenous artery, both more superficial than the popliteal artery, did not have quantifiable signal at 35 and/or 36°C based on the threshold value set from the 38°C dataset. Therefore, values were recorded as zero, relative changes within a given one degree temperature interval could not be calculated, and, instead, changes in area per degree were used in sex and age comparisons. Except for aged males, temperature had an influence on superior saphenous vessel area for all other groups (p = 0.01-0.004), with statistically significant differences between means within a group for: adult male between 35/37 and 35/38 °C (p = 0.03); adult female between 35/38 and 36/38 °C (p = 0.005 and 0.003); and, aged female between 35/38 °C (p = 0.04). Only aged females demonstrated a linear increase in area with temperature (slope > 0, p = 0.03, R^2 = 0.93). Except for aged males, temperature had an influence on inferior saphenous vessel area for all other groups (p = 0.008-

.0002), with statistically significant differences between means within a group for: adult male between 35/37, 35/38, 37/38, 36/38 °C (p = 0.01, 0.02, 0.006, and 0.007); adult female between 35/38 and 36/38 °C (p = 0.04); and, aged female between 35/37 and 35/38 °C (p = 0.04 and 0.005). Like the superior location, only aged females demonstrated a linear increase in area with temperature (slope > 0, p = 0.004, R^2 = 0.99).

The tracking length of the saphenous artery is shown in Figure 2.8. Except for aged males, temperature had an influence on saphenous tracking length for all other groups (p = 0.02-0.007). Tracking length linearly increased with temperature (slopes > 0, p = 0.03-0.01, R^2 = 0.94-0.99), with no difference between slopes.

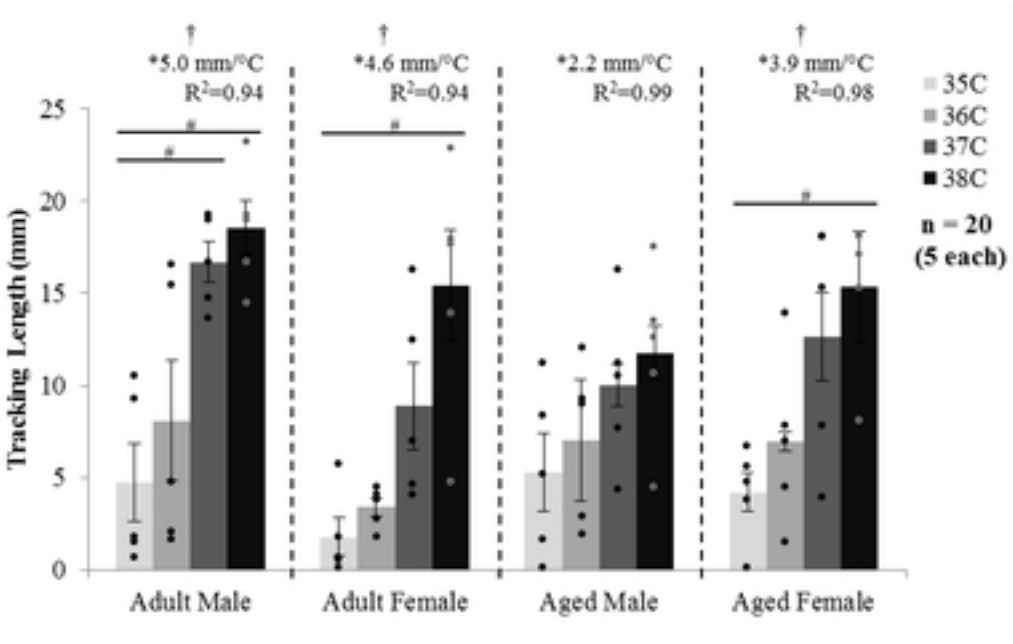

Figure 2.8 MRI tracking length of the saphenous artery for male and female, adult and aged mice at core temperatures of 35, 36, 37, 38 °C (n = 5 each).

Distal peripheral vessel area measurements differ between 2D and 3D acquisitions.

2D data was acquired in a second group of adult male mice to evaluate the contribution of blood flow velocity to visualization of peripheral vessels. With the 2D slices planned perpendicular to the vessel, as compared to the off-plane 3D acquisitions, absolute values of area

were different but percent changes can be compared. For the femoral location, the vessel areas from 2D data acquired at 35 and 38°C were 0.12±0.02 and 0.19±0.02 mm^2 (comparative 3D data shown in Figure 2.7), with increases of 59% (2D) compared to 63% (3D). For the superior popliteal location, the vessel areas were 0.07±0.006 and 0.09±0.01 mm^2 with percent increases of 34% (2D) compared to 57% (3D). For the superior saphenous location, the vessel areas were 0.03±0.002 and 0.06±0.01 mm^2 with percent increase of 47% (2D) compared to 235% (3D).

2.5 Discussion

Direct, non-invasive measurements of murine vascular structure and function with increasing temperature from minimally hypothermic to minimally hyperthermic conditions

This study provides quantitative insight into cardiovascular responses resulting from changes in core temperature, while illustrating an innovative non-invasive approach. Our data: show that the response in core vasculature depends on anatomical location; mimic human data in the head, heart, and periphery; and, include the novel finding that the aorta enlarges markedly with increasing core temperature. We have quantified sex- and age-dependent differences in the cardiovascular responses [44], harmonizing with the National Institutes of Health's recent communications regarding lack of sex diversity in preclinical experiments. The results presented here accentuate the need to closely control and report animal temperature in preclinical cardiovascular studies and provide foundational data (geometry of the vessels) to begin coupling empirical values of the body's physiological response to temperature (based on anatomical location, sex, and age) with bioheat and CFD modeling in order to better understand thermoregulation.

Infrarenal Aorta: Potential impact of changes in core vasculature on heat transfer.

Our primary endpoint for the aorta was measurements of area with a secondary outcome of cyclic strain, both of which are indicators of health and disease [45–48]. Increases in area would be hypothesized to impact conductive and convective heat transfer, while decreases in strain reflect a reduction in how much a vessel can expand across the cardiac cycle and are a representation of increased vascular stiffness [49].

The statistically significant temperature-induced enlargement we have quantified in the aorta, previously unknown and potentially underestimated, is biologically important because it may affect conductive and convective heat transfer. Heat conduction would be hypothesized to change due to an increase in surface area, closer proximity to surrounding tissue and vessels, and potential changes in velocity. In images acquired at 38°C, the aorta appears to be more closely juxtaposed to the infrarenal vena cava (Figure 2.2, arrowhead). Heat transfer via convection would be hypothesized to change based on potential changes in bulk flow and/or velocity. The large changes in geometry clearly illustrated in this work provide the motivation to pursue direct measurements of blood flow velocity by MRI in order to simultaneously quantify geometric and hemodynamic changes which could help elucidate conductive and convective processes and improve understanding of thermoregulation, directly, or by incorporating empirical values into subject-specific bioheat models.

Infrarenal Aorta: Age moderates the response of core vasculature to increases in temperature.

Even within a non-pathological range of core temperatures, as tested in this work, increases in the cross-sectional area of the infrarenal aorta were significant for all groups. This was not what we initially hypothesized due to the depth of this core vessel and thus limited heat exchange to the environment. Although relative changes within a particular one degree

temperature interval did not differ between groups, the rate of increase over the entirety of temperatures tested differed based on age (adult = 0.022 vs. aged = 0.014 $mm^2/°C$). This can be visualized in Figure 2.4, where area measurements across the cardiac cycle span a smaller range for aged animals, compared to adults, from 35 to 38 °C. The changes in area were linear for all groups (R^2 = 0.97-0.99), which would make their incorporation into mathematical models simpler.

Although not reaching statistical significance within the current temperature range, the biological effect of increased core temperature was a decrease in strain (Figure 2.5). The rate of decrease in maximum strain was similar between adult and aged animals (-1.2%/°C vs. -1.6%/°C, respectively, Figure 2.6) and implies, that with the enlargement of area due to increases in temperature, vessels are nearing their elastic limits. Favreau et al. saw a similar relationship between increased diastolic area and reduced strain in a murine model of arterial occlusive disease [50]. Larger increases in area but similar decreases in strain suggest there may be remaining reserve in adult animals, but not their aged counterparts, if we were to challenge the CV system further, for example if we were to explore exercise-like conditions in conjunction with heat stress.

Interestingly, adult females had the largest increase in area over the temperature range investigated (0.024 $mm^2/°C$), while having the smallest decrease in cyclic strain (-0.3%/°C, Figure 2.6). Large structural changes, while retaining the ability to expand over the cardiac cycle, may be a reflection of the sex-specific differences known to exist with respect to control of the baroreflex system [51].

Periphery: The compromised response in aged male mice parallels human data.

Although more cautious interpretation of data acquired in the periphery is warranted due to the greater influence of blood flow velocity on measurements (i.e. differences between percent changes in area for 3D versus 2D data) and the smaller vessel size beginning to challenge the spatial resolution of our MRI system, the peripheral vasculature undoubtedly enlarged with increasing core temperature. This was as we hypothesized due to its more superficial location and its role in carrying blood to the extremities. While Pearson et al. [12] found the human femoral artery diameter unchanged in a core temperature range of 37-39 °C, we quantified increases in the murine femoral artery area over the 35-38 °C range, with the largest increases between 36 and 37 °C [12]. The saphenous artery changed the most, consistent with it being the most superficial and its function of supplying blood to the hindlimb digits, one of the primary locations for heat exchange with the environment [52]. In aged male mice, the response was diminished, or in some locations absent entirely, and is consistent with data on the response of cutaneous vasculature of aged male humans [21,53]. Unlike aged male mice, aged females responded more similarly to adult animals of both sexes [54].

Head and Heart: Non-invasive quantification of cerebral and cardiac effects is consistent with previous results.

Temperature did not have an effect on cross-sectional area of the murine cerebral vasculature, as we hypothesized. This is likely due to the CoW not being superficial and thus not a site for large heat exchange with the environment as well as temperature-induced changes in the central nervous system being balanced with autoregulatory mechanisms [55]. Our results agree with previous work in humans showing cerebral blood flow was unchanged up to core

temperatures of ~38 °C and then began to decrease during more severe hyperthermia (core temperature ≥ 39.5 °C) [29,30,56].

Similar to previous cardiac data, females had smaller CO and larger EF than males of the same age [57] and contrary to previous findings [58] aged animals had larger SV and CO than younger groups of the same sex. The latter may be due to our aged mice just bordering senescence without frank declines in cardiac function, which would be consistent with findings in humans suggesting that age-related vascular changes (as we saw in the aorta and periphery) precede declines in cardiac function [59]. As we hypothesized based on the need to maintain blood pressure due to a large reduction in total vascular resistance [31], supported by our peripheral data, the response to increased temperature was an increase in CO. Although increases were statistically significant only for the adult female group, the qualitative differences in changes in CO based on sex and age parallel human data. The adult female and both aged groups increased CO via increased HR, whereas the adult male group increased CO via increases in both heart rate and stroke volume. Minson et al. showed that during passive heating male subjects demonstrated age-dependent differences in CO due to younger subjects having an initial increase in SV before a subsequent decline for both groups [24]. Also, SV and CO decreased in aged males between 37 and 38°C (heat stress), but not in aged females, which is consistent with heat stress research in humans in this temperature range [24,58,60].

Setpoints: Data support the idea of subject-specific core temperature setpoints.

Looking broadly across all metrics, the temperature interval at which the largest response occurred differed based on sex and age. Excluding measurements taken in the head, we considered twelve measurements for each group of animals. Adult males were focused around the 36-37 °C interval with the largest response in eight metrics, with two metrics each at the 35-

36 and 37-38 °C intervals. Adult females had the largest response in four and six metrics at the 35-36 °C and 36-37 °C intervals, respectively, and two at 37-38 °C. Aged males had the largest response at the 35-36 °C and 36-37 °C intervals for five metrics each, and 37-38 °C for two metrics. Aged females had the most distributed response with each of the three temperature intervals (35-36, 36-37, and 37-38 °C) having the largest response for four metrics. Physiologically, this could be an indicator of different animal core temperature setpoints as seen previously in C57BL6 mice [61].

2.6 Conclusions

Due to challenges associated with making measurements from core vasculature, there is a lack of empirical information regarding how it changes with changing core temperature and its role in thermoregulation. Researchers have begun to study this response in the leg [12,14], and we have expanded this to the whole body. With the non-invasive nature of MRI and our ability to tightly control our animals' temperature, data presented here begin to fill this gap. To our knowledge, this is the first work to quantify and compare temperature-induced changes in core vessels of the head, torso, and periphery of murine models. These data provide a broad view of physiological alterations of the murine cardiovascular system due to increases in core temperature, from head-to-toe. Our most important finding that the cross-sectional area of the infrarenal aorta increases significantly with increasing core temperature is biologically significant due to the potential impact these changes could have on conductive and convective processes involved in thermoregulation. This work provides further evidence of the effects of sex and age on CV responses and emphasizes the necessity to properly control an animal's temperature and report it in publications. In subsequent chapters, this thesis will consider additional structural and functional responses in the arteries and veins in Chapter 3, the velocity

and volumetric flow responses in Chapter 4, and the combination of a CV stressor and temperature for Chapter 5.

2.7 References

[1] Tucker R, Rauch L, Harley YR, et al. Impaired exercise performance in the heat is associated with an anticipatory reduction in skeletal muscle recruitment. Pflugers Arch. - Eur. J. Physiol. 2004;448:422–430.

[2] Stewart IB, Rojek AM, Hunt AP. Heat Strain During Explosive Ordnance Disposal. Mil. Med. 2011;176:959–963.

[3] Centers for Disease Control and Prevention U. Hypothermia-related deaths--United States, 1999-2002 and 2005. MMWR Morb. Mortal. Wkly. Rep. 2006;55:282–284.

[4] van der Zee J. Heating the patient: a promising approach? Ann. Oncol. Off. J. Eur. Soc. Med. Oncol. 2002;13:1173–1184.

[5] Polderman KH. Application of therapeutic hypothermia in the intensive care unit. Intensive Care Med. 2004;30:757–769.

[6] Parsons KC. Human thermal environments : the effects of hot, moderate, and cold environments on human health, comfort, and performance. 3rd ed. CRC Press/Taylor & Francis; 1993.

[7] Fiala D, Havenith G. Modelling Human Heat Transfer and Temperature Regulation. Springer International Publishing; 2015. p. 265–302.

[8] Rowell LB. Human Cardiovascular Adjustments to Exercise and Thermal Stress. Physiol. Rev. 1974;54:75–159.

[9] González-Alonso J. Human thermoregulation and the cardiovascular system. Exp. Physiol. 2012;97:340–346.

[10] Dastre A, Morat J. Influence du sang asphyxique sur l'appareil nerveux de la circulation [Influence of asphyxial blood on the nervous system of circulation]. Arch. Physiol. Norm. Pathol. 1884;3:1–45.

[11] Akyürekli D, Gerig LH, Raaphorst GP. Changes in muscle blood flow distribution during hyperthermia. Int. J. Hyperth. 1997;13:481–496.

[12] Pearson J, Low DA, Stöhr E, et al. Hemodynamic responses to heat stress in the resting and exercising human leg: insight into the effect of temperature on skeletal muscle blood flow. Am. J. Physiol. - Regul. Integr. Comp. Physiol. 2011;300:663–673.

[13] Binzoni T, Tchernin D, Richiardi J, et al. Haemodynamic responses to temperature changes of human skeletal muscle studied by laser-Doppler flowmetry. Physiol. Meas. 2012;33:1181–1197.

[14] Chiesa ST, Trangmar SJ, González-Alonso J. Temperature and blood flow distribution in the human leg during passive heat stress. J. Appl. Physiol. 2016;120:1047–1058.

[15] González-Alonso J, Calbet JAL, Boushel R, et al. Blood temperature and perfusion to exercising and non-exercising human limbs. Exp. Physiol. 2015;100:1118–1131.

[16] Brody GM. Hyperthermia and hypothermia in the elderly. Clin. Geriatr. Med. 1994;10:213–229.

[17] McDonald RB, Day C, Carlson K, et al. Effect of age and gender on thermoregulation. Am. J. Physiol. 1989;257:R700-4.

[18] Kaciuba-Uscilko H, Grucza R. Gender differences in thermoregulation. Curr. Opin. Clin. Nutr. Metab. Care. 2001;4:533–536.

[19] Collins KJ, Exton-Smith AN. 1983 Henderson Award Lecture. Thermal homeostasis in old age. J. Am. Geriatr. Soc. 1983;31:519–524.

[20] Noe RS, Jin JO, Wolkin AF. Exposure to Natural Cold and Heat: Hypothermia and Hyperthermia Medicare Claims, United States, 2004–2005. Am. J. Public Health. 2012;102:e11–e18.

[21] Van Someren EJW. Chapter 22 – Age-Related Changes in Thermoreception and Thermoregulation. Handb. Biol. Aging. 2011. p. 463–478.

[22] Chen CH, Nakayama M, Nevo E, et al. Coupled systolic-ventricular and vascular stiffening with age: implications for pressure regulation and cardiac reserve in the elderly. J. Am. Coll. Cardiol. 1998;32:1221–1227.

[23] O'Toole ML. Gender differences in the cardiovascular response to exercise. Cardiovasc. Clin. 1989;19:17–33.

[24] Minson CT, Wladkowski SL, Cardell AF, et al. Age alters the cardiovascular response to direct passive heating. J. Appl. Physiol. 1998;84:1323–1332.

[25] Johnson JM, Rowell LB, Brengelmann GL. Modification of the skin blood flow-body temperature relationship by upright exercise. J. Appl. Physiol. 1974;37.

[26] Savage M V, Brengelmann GL. Control of skin blood flow in the neutral zone of human body temperature regulation. J. Appl. Physiol. 1996;80:1249–1257.

[27] Swain ID, Grant LJ. Methods of measuring skin blood flow. Phys. Med. Biol. 1989;34:151–175.

[28] Nybo L, Møller K, Volianitis S, et al. Effects of hyperthermia on cerebral blood flow and metabolism during prolonged exercise in humans. J. Appl. Physiol. 2002;93:58–64.

[29] Bain AR, Nybo L, Ainslie PN. Cerebral Vascular Control and Metabolism in Heat Stress. Compr. Physiol. Hoboken, NJ, USA: John Wiley & Sons, Inc.; 2015. p. 1345–1380.

[30] Qian S, Jiang Q, Liu K, et al. Effects of short-term environmental hyperthermia on patterns of cerebral blood flow. Physiol. Behav. 2014;128:99–107.

[31] Crandall CG. Heat stress and baroreflex regulation of blood pressure. Med. Sci. Sports Exerc. 2008;40:2063–2070.

[32] Siddiqui A. Effects of Vasodilation and Arterial Resistance on Cardiac Output. J. Clin. Exp. Cardiolog. 2011;02.

[33] Kuhn LA, Turner JK. Alterations in Pulmonary and Peripheral Vascular Resistance in Immersion Hypothermia. Circ. Res. 1959;7:366–374.

[34] Wissler EH. Pennes' 1948 paper revisited. J. Appl. Physiol. 1998;85:35–41.

[35] Bhowmik A, Singh R, Repaka R, et al. Conventional and newly developed bioheat transport models in vascularized tissues: A review. J. Therm. Biol. 2013;38:107–125.

[36] Leon LR. The use of gene knockout mice in thermoregulation studies. J. Therm. Biol. 2005;30:273–288.

[37] Cuomo F, Roccabianca S, Dillon-Murphy D, et al. Effects of age-associated regional changes in aortic stiffness on human hemodynamics revealed by computational modeling. Aliseda A, editor. PLoS One. 2017;12:e0173177.

[38] Ducharme MB, Tikuisis P. Role of blood as heat source or sink in human limbs during local cooling and heating. J. Appl. Physiol. 1994;76:2084–2094.

[39] FLURKEY K, MCURRER J, HARRISON D. Mouse Models in Aging Research. Mouse Biomed. Res. Elsevier; 2007. p. 637–672.

[40] Constantinides C, Mean R, Janssen BJ. Effects of isoflurane anesthesia on the cardiovascular function of the C57BL/6 mouse. ILAR J. 2011;52:e21-31.

[41] Teng D, Hornberger TA. Optimal Temperature for Hypothermia Intervention in Mouse Model of Skeletal Muscle Ischemia Reperfusion Injury. Cell. Mol. Bioeng. 2011;4:717–723.

[42] Duhan V, Joshi N, Nagarajan P, et al. Protocol for long duration whole body hyperthermia in mice. J. Vis. Exp. 2012;e3801.

[43] Goergen CJ, Barr KN, Huynh DT, et al. In vivo quantification of murine aortic cyclic strain, motion, and curvature: Implications for abdominal aortic aneurysm growth. J. Magn. Reson. Imaging. 2010;32:847–858.

[44] Hinson JM, Laprairie KN, Cundiff JM. One Size Does NOT Fit ALL. J Appl Physiol. 2005;32:26–30.

[45] Liu X, Peyton KJ, Durante W. Physiological cyclic strain promotes endothelial cell survival via the induction of heme oxygenase-1. Am. J. Physiol. Heart Circ. Physiol. 2013;304:H1634-43.

[46] Schad JF, Meltzer KR, Hicks MR, et al. Cyclic strain upregulates VEGF and attenuates proliferation of vascular smooth muscle cells. Vasc. Cell. 2011;3:21.

[47] Shimizu K, Mitchell RN, Libby P. Inflammation and Cellular Immune Responses in Abdominal Aortic Aneurysms. Arterioscler. Thromb. Vasc. Biol. 2006;26:987–994.

[48] Smith JD, Davies N, Willis AI, et al. Cyclic stretch induces the expression of vascular endothelial growth factor in vascular smooth muscle cells. Endothelium. 2001;8:41–48.

[49] Goergen CJ, Azuma J, Barr KN, et al. Influences of Aortic Motion and Curvature on Vessel Expansion in Murine Experimental Aneurysms. Arterioscler. Thromb. Vasc. Biol. 2011;31:270–279.

[50] Favreau JT, Liu C, Yu P, et al. Acute reductions in mechanical wall strain precede the formation of intimal hyperplasia in a murine model of arterial occlusive disease. J. Vasc. Surg. 2014;60:1340–1347.

[51] Huxley VH. Sex and the cardiovascular system: the intriguing tale of how women and men regulate cardiovascular function differently. Adv. Physiol. Educ. 2007;31:17–22.

[52] Kochi T, Imai Y, Takeda A, et al. Characterization of the Arterial Anatomy of the Murine Hindlimb: Functional Role in the Design and Understanding of Ischemia Models. Gaetano C, editor. PLoS One. 2013;8:e84047.

[53] Rooke GA, Savage M V, Brengelmann GL. Maximal skin blood flow is decreased in elderly men. J. Appl. Physiol. 1994;77:11–14.

[54] Drinkwater BL, Bedi JF, Loucks AB, et al. Sweating sensitivity and capacity of women in relation to age. J. Appl. Physiol. 1982;53:671–676.

[55] Eric Kandle, Jame Schwartz, Thomas Jessell, Steven Siegelbaum AJH. PRINCIPLES OF NEURAL SCIENCE. 5th ed. 2012.

[56] Ogoh S, Sato K, Okazaki K, et al. Blood Flow Distribution during Heat Stress: Cerebral and Systemic Blood Flow. J. Cereb. Blood Flow Metab. 2013;33:1915–1920.

[57] Chung AK, Das SR, Leonard D, et al. Women Have Higher Left Ventricular Ejection Fractions Than Men Independent of Differences in Left Ventricular Volume: The Dallas Heart Study. Circulation. 2006;113:1597–1604.

[58] Kenney WL, Munce TA. Physiology of Aging Invited Review: Aging and human temperature regulation. Pandolf KB. Exp Aging Res Ageing Res Rev Exp Aging Res. 1997;17:41–76.

[59] Houghton D, Jones TW, Cassidy S, et al. The effect of age on the relationship between cardiac and vascular function. Mech. Ageing Dev. 2016;153:1–6.

[60] Dunbar SL, Kenney WL. Effects of hormone replacement therapy on hemodynamic responses of postmenopausal women to passive heating. J. Appl. Physiol. 2000;89:97–103.

[61] Sanchez-Alavez M, Alboni S, Conti B. Sex- and age-specific differences in core body temperature of C57Bl/6 mice. Age (Dordr). 2011;33:89–99.

Chapter 3
Comparison of arterial and venous response to increases in core body temperature

3.1 Abstract

Purpose: Deep core veins, due to their large size and role in returning blood to the heart, are an important part of CV system. The response of veins to increasing core temperature has not been adequately studied *in vivo*. Our objective was to non-invasively quantify in C57BL/6 mice the response of artery-vein pairs to increases in body temperature.

Methods: Adult male mice were anesthetized and underwent magnetic resonance imaging. Data were acquired from three co-localized vessel pairs (the neck [carotid/jugular], torso [aorta/inferior vena cava (IVC)], periphery [femoral artery/vein]) at core temperatures of 35, 36, 37, and 38 °C.

Results: Cross-sectional area increased with increasing temperature for all vessels, excluding the carotid. Average area of the jugular, aorta, femoral artery and vein linearly increased with temperature (0.10, 0.017, 0.017, and 0.027 mm^2/°C, respectively; $p<0.05$). On average, the IVC has the largest venous response for area (18.2 %/°C, vs. jugular 9.0 and femoral 10.9 %/°C). Increases in core temperature from 35 to 38 °C resulted in an increase in contact length between the aorta/IVC of 29.3% ($p=0.007$) and between the femoral artery/vein of 28.0% ($p=0.03$).

Conclusion: Previously unidentified increases in the IVC area due to increasing core temperature are biologically important because they may affect conductive and convective heat transfer. Vascular response to temperature varied based on location and vessel type. Leveraging

non-invasive methodology to quantify vascular responses to temperature could be combined with bioheat modeling to improve understanding of thermoregulation.

3.2 Introduction

Increasing core temperature has been observed to result in: either increases or decreases in cerebral blood flow depending on the temperature range [7–9], increased cardiac output [10,11], and decreased total peripheral resistance [10,12]. Absent from this previous work was empirical data regarding geometric (size and shape) and functional (deformation across cardiac cycle) changes in core vessels, which are necessary for improved parameterization and validation of mathematical and computational models [13,14]. Chapter 2 quantified cardiac output and the arterial response (area and cyclic strain) to increases in core temperature from head-to-toe [15]. However, data regarding changes in the core (alternatively, deep) veins are still missing from this body of work. Literature suggests that with a decrease in temperature, the cross-sectional area of core veins in the torso will increase [16]. It is proposed that this is due to the shunting of blood away from the periphery and subcutaneous vessels to minimize heat exchanged with the environment and to increase venous return flow while decreasing blood velocity to increase the heat exchanged between artery-vein pairs, via the process of counter-current heat exchange [16–18].

It is important to study both arteries and veins because of their differential influence on convective and conductive processes as well as counter-current heat exchange. For example: 65-75% of total blood volume is distributed in the venous system [19,20]; in the arteries, there is high-pressure flow, and thus higher blood flow velocity, compared to the low-pressure/slower flow in the veins; and, differences in wall composition and thickness (e.g. the amount, location, and orientation of elastin, collagen, smooth muscle cells (SMC)) affect the stress-strain

relationship and thus how an artery or vein will respond to stimuli, such as temperature, as well as the thermal conductivity of the vessel wall itself [21].

Using C57BL/6 mice [22] and MRI, we noninvasively quantified changes in artery-vein pairs in the neck (carotid/jugular), torso (infrarenal aorta/inferior vena cava (IVC)), and periphery (femoral artery/vein) at four target core temperatures. We hypothesized that as core temperature was increased from minimally hypothermic at 35 °C to minimally hyperthermic at 38 °C vascular response would vary based on location in the body from cranial to caudal (e.g. neck < torso < periphery) as well as depth (e.g. femoral artery > carotid artery and aorta, jugular and femoral veins > IVC). To our knowledge, these data are the first to empirically quantify the spatially and temporally resolved response of artery-vein pairs of core vasculature to changes in core temperature in vivo from head-to-toe. This geometric and functional data could be used to couple bioheat modeling and computational fluid dynamics (CFD) to improve understanding of thermoregulation.

3.3 Methods

All experiments were carried out with local Institutional Animal Care and Use Committee approval. Animals were housed in a room with temperature (22 ± 2 °C) and humidity (~27%) control and an alternate 12 hour light/dark cycle.

Healthy adult male (12- to 20-weeks-old, ~22-30 human years [23]) C57BL/6 mice, purchased from Charles River Laboratories, were used in this study. Male mice were chosen in this initial study of artery-vein pairs because this sex showed the smallest response in the aorta in our previous work (male: 0.019 mm^2/°C vs. female: 0.024 mm^2/°C, [15]). Mice were anesthetized with 1.25-2% isoflurane in 1 L/min of oxygen [24]. Animals were imaged in the supine position at 7T using a Direct Drive console (Agilent Technologies, Santa Clara, CA) and

a 40 mm inner diameter transmit-receive volume coil (Morris Instruments, Ontario, Canada). The four target core temperatures, ranging from minimally hypothermic (35 °C) to minimally hyperthermic (38 °C), were controlled within ± 0.2 °C using forced convection and were selected to avoid pathological changes [25,26]. The system included a heater blowing warm air through the bore of the magnet and over the animal, a rectal temperature probe, and a custom-built proportional-integral-derivative (PID) controller (Labview, National Instruments, Austin TX). Heart rate and respiration were monitored (SA Instruments, Stony Brook, NY).

Figure 3.1 illustrates the locations investigated in this study. CINE data was acquired in the neck (carotid artery and jugular vein), torso (infrarenal aorta and inferior vena cava), and periphery (femoral artery and vein). To acquire all locations for a given animal, with four target core temperatures tested at each location, three imaging sessions were required (approximately two hours each). Each region was completed within two weeks before acquiring data from the next region; therefore, ages ranged 1-2 weeks within a region and 2-8 weeks between regions. To verify that changes observed in the vasculature were not due to long exposures to anesthesia, the same data acquisition and analysis procedures were repeated every 30 minutes with animal's core temperature maintained at 37 °C for two hours (n = 2, adult males). Data were acquired at the carotid artery and jugular vein, aorta and IVC, and femoral artery and vein. To acquire preliminary data regarding the thermal environment while imaging, skin and rectal temperatures were recorded using two tissue implantable thermocouple microprobes, IT-23 (Physitemp Instruments Inc, Clifton, NJ), inserted subcutaneously on the ventral and dorsal side of mice (n = 2, adult males), and a rectal temperature probe. Because the thermocouples are not MRI compatible, a set-up to mimic the magnet bore was used for testing outside the 5 Gauss line in the MR room. The set-up included a polyvinyl chloride (PVC) pipe size 6 with approximately

same diameter and cut to same length as magnet bore and the same PID controlled heater and fan.

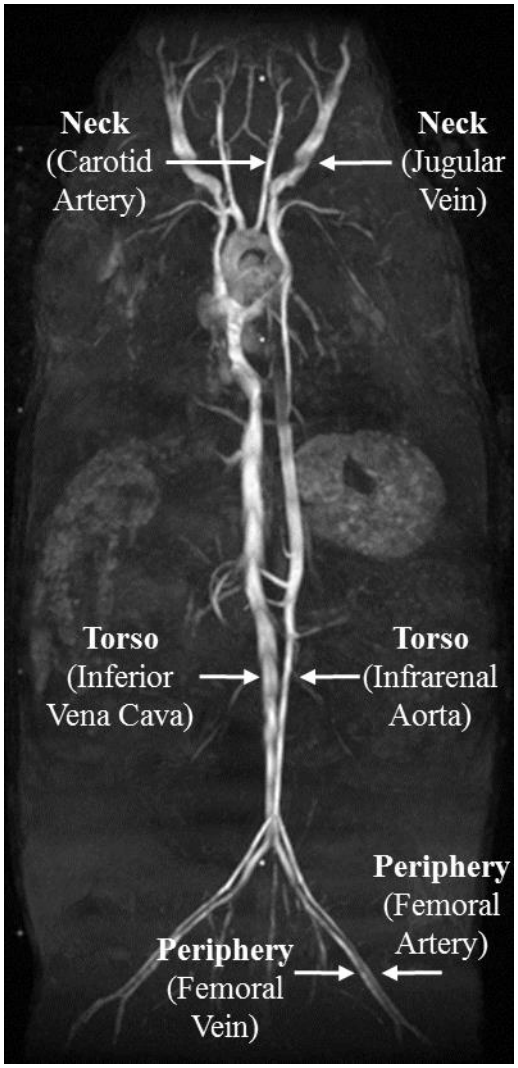

Figure 3.1 Coronal MIP illustrating arterial and venous locations where imaging data was acquired and quantified.

Neck: Carotid Artery and Jugular Vein

Sagittal 2D and axial 3D acquisitions were used to plan slices perpendicular to the carotid artery and to the jugular vein. A cardiac-gated and velocity compensated 2D CINE sequence with 12 frames was used to acquire data at each location. Parameters for the carotid artery were [TR/TE ~120/4 ms depending on heart rate, flip angle (α) 60º, FOV (20 mm)2, matrix 256^2 zero-

filled to 512^2, in-plane resolution $(39\ \mu m)^2$, slice thickness 1 mm, NEX 6]. Parameters for the jugular vein were [TR/TE ~120/6 ms depending on heart rate, α 30º, FOV $(25.6\ mm)^2$, matrix 512 x 256 zero-filled to 512^2, in-plane resolution $(50\ \mu m)^2$, slice thickness 1 mm, NEX 6]. The difference in parameters (reduced flip angle and resolution, respectively) reflects the slower blood flow and larger size of the veins. These parameters were optimized in a separate, independent study focused on the venous system and allowed us to compare data from the present work [27]. Typically, there were 14 voxels across the carotid artery and 24 voxels across the jugular vein.

The CINE images were analyzed for vessel cross-sectional area and cyclic strain using an in-house semi-automated process previously described in Equation 6.

Torso: Infrarenal Aorta and Inferior Vena Cava (IVC)

Coronal 2D and sagittal 3D acquisitions were used to plan slices perpendicular to the aorta and to the IVC. Image acquisition parameters and analysis were identical to that performed for the carotid artery and jugular vein. Typically, there were 18 voxels across the artery and 24 voxels across the vein. Using manual tracing along the contiguous border between the artery and vein, the contact length between the aorta and IVC was measured at 35 and 38 °C for both systole and diastole from data acquired from the IVC (MRVision, MA).

Peripheral: Femoral Artery and Vein

Coronal 2D and sagittal 3D acquisitions were used to plan slices perpendicular to the artery and to the vein. Data acquisition and analysis were identical to that performed for the carotid artery and jugular vein. Typically, there were 10 voxels across the artery and 12 voxels across the vein. The contact length between the artery and vein was measured at 35 and 38 °C for systole and diastole from data acquired from the femoral vein (MRVision, MA).

Statistical Analysis

Data are plotted as mean ± standard error (SEM) with individual data points. To compare areas (average, maximum, minimum) or maximum cyclic strain derived from a given vessel, repeated measures one-way ANOVA was used to test for an overall effect of temperature and Tukey's post hoc test was used to account for multiple comparisons while testing for pairwise differences between temperatures. To investigate the relationship between temperature and area or strain over the full temperature range tested, linear regression was used and fitted slopes were tested for whether they differed from zero. Two methods were used to compare artery-vein pairs. Firstly, the slopes from the linear regression analysis were compared between co-localized artery-vein pairs. Secondly, the percent change per one degree increase in temperature (%/°C) was calculated for average area and maximum cyclic strain of each vessel and compared using two-way ANOVA with Tukey's post hoc test to determine main group effects of location and vessel type. A relative difference (the percent change) was used to account for differences in the size of anatomical structures. To test if the contact length differed between 35 and 38 °C at the aorta/IVC and the femoral artery/vein, a two-tailed paired t-test was used. Significance was set at $p < 0.05$.

3.4 Results

Representative images from the three regions of the body, acquired at 35 and 38 °C, are shown in Figure 3.2. Qualitatively, with increasing temperature, there is no discernable increase in either diastolic (minimum) or systolic (maximum) area of the carotid artery. However, there is a noticeable increase in both areas for all other vessels.

Figure 3.3 summarizes area averaged across the cardiac cycle and maximum cyclic strain for the three pairs of co-localized vessels. In Figure 3.4, average area and maximum cyclic strain

are plotted together to highlight their relationship. Table 3.1 summarizes the results of average area and maximum cyclic strain, including non-significant findings.

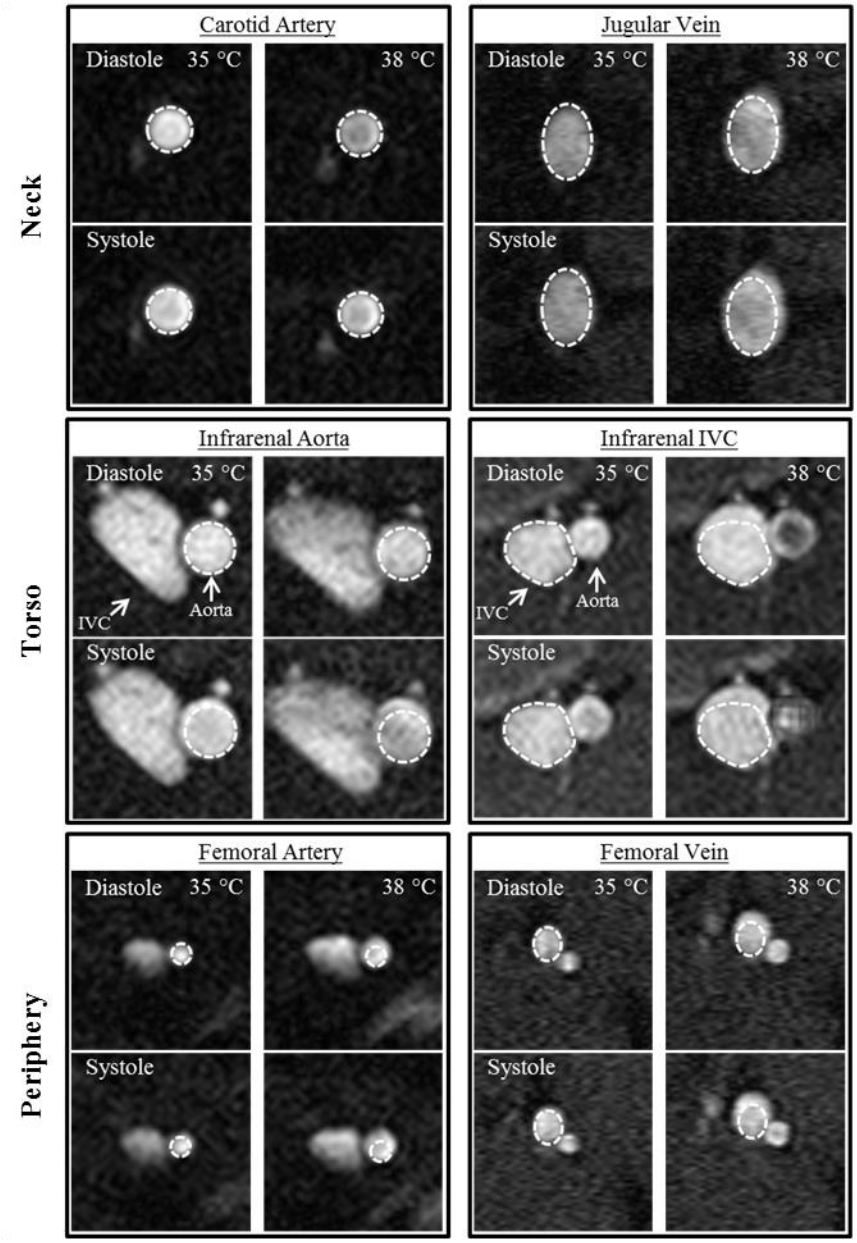

Figure 3.2 Cross-sectional view of the artery-vein pairs at 35 and 38°C with the same-sized region of interest drawn around the vessel for all four panels (diastole/systole; 35/38°C).

Table 3.1 Summary of results of response in arterial and venous pairs.
Data presented as mean ± SEM, or for location comparisons percent change per degree. Temperature-interval specific data are listed below with the only significant findings at the 35-36 °C interval, and p-value is denoted in parentheses. IVC: inferior vena cava, NS = not significant.

Location	ANOVA (Figure 3)		Linear Regression (Figure 4)		
	Overall (p-value)	Pairwise Comparisons	Slope (unit/°C)	R^2	Significance of Slope (p-value)
Average Area (mm^2)					
Carotid	NS (0.07)	None	-0.004 ±0.003	0.50	NS (0.3)
Jugular	0.006	35/38 p=0.03	0.10 ±0.003	0.99	0.0007
Aorta	0.02	35/36 p=0.03 35/37 p=0.002	0.017 ±0.003	0.94	0.03
IVC	0.049	None	0.14 ±0.05	0.83	NS (0.09)
Femoral Artery	0.002	35/37 p=0.003 35/38 p=0.0004	0.017 ±0.004	0.90	0.05
Femoral Vein	0.05	None	0.027 ±0.006	0.92	0.04
Max Cyclic Strain (%)					
Carotid	NS (0.6)	None	-0.31 ±0.6	0.11	NS (0.7)
Jugular	NS (0.9)	None	-0.02 ±0.1	0.01	NS (0.9)
Aorta	NS (0.5)	None	-0.49 ±0.8	0.16	NS (0.6)
IVC	NS (0.1)	None	-1.05 ±0.4	0.80	NS (0.1)
Femoral Artery	0.03	None	-2.45 ±1.7	0.52	NS (0.3)
Femoral Vein	0.01	35/37 p=0.008	-1.29 ±1.2	0.38	NS (0.4)

Location Comparisons		
Relative Changes in Average Area (%/°C) Pairwise (p-value)		
35-36 °C	36-37 °C (NS)	37-38 °C (NS)
IVC>Aorta, 39.2 vs. 5.42 %/°C (p=0.04) IVC>Carotid, 39.2 vs. -3.23 %/°C (p= 0.004) Femoral Artery>Carotid, 52.7 vs. -3.23 %/°C (p<0.0001) Femoral Artery>Aorta, 52.7 vs. 5.42 %/°C (p=0.0009) Femoral Artery> Jugular, 52.7 vs. 11.3 %/°C (p=0.005) Femoral Vein: 21.5 %/°C	Carotid vs. Jugular: -4.75 vs. 12.2 %/°C Aorta vs. IVC: 6.00 vs. -0.04 %/°C Femoral Artery vs. Vein: 16.7 vs. 7.63 %/°C	Carotid vs. Jugular: 3.58 vs. 8.11 %/°C Aorta vs. IVC: 1.29 vs. 15.5 %/°C Femoral Artery vs. Vein: 6.03 vs. 3.50 %/°C
Max Cyclic Strain (%/°C) Pairwise (p-value)		
35-36 °C (NS)	36-37 °C (NS)	37-38 °C (NS)
Carotid vs. Jugular: -14.9 vs. 23.8 %/°C Aorta vs. IVC: 8.55 vs. -14.5 %/°C Femoral Artery vs. Vein: -40.1 vs. -21.2 %/°C	Carotid vs. Jugular: 4.21 vs. 9.34 %/°C Aorta vs. IVC: -18.6 vs. -17.7 %/°C Femoral Artery vs. Vein: 26.9 vs. -37.0 %/°C	Carotid vs. Jugular: -12.3 vs. -1.03 %/°C Aorta vs. IVC: 12.9 vs. 9.85 %/°C Femoral Artery vs. Vein: -17.4 %/°C vs. 79.7 %/°C

Heart rate linearly increased with temperature: 515.3 ± 6.8 at 35 °C, 533 ± 21 at 36 °C, 535.4 ± 24.4 at 37 °C, 554.2 ± 24.6 at 38 °C (or 11.9 bpm/°C, $p = 0.03$, $R^2=0.93$). Two hours of isoflurane exposure at normothermic conditions (37 °C) resulted in minimal changes in heart rate (mouse 1: 431, 429, 423, 426 bpm; and, mouse 2: 534, 545, 553, 530 bpm) or vessel area (avg. -0.95%/30 min). With the animal in the supine position, warm air passes over the ventral surface of the animal. Throughout the temperature range tested, ventral and dorsal skin temperature averaged 0.1 and 0.94 °C less than core temperature, respectively.

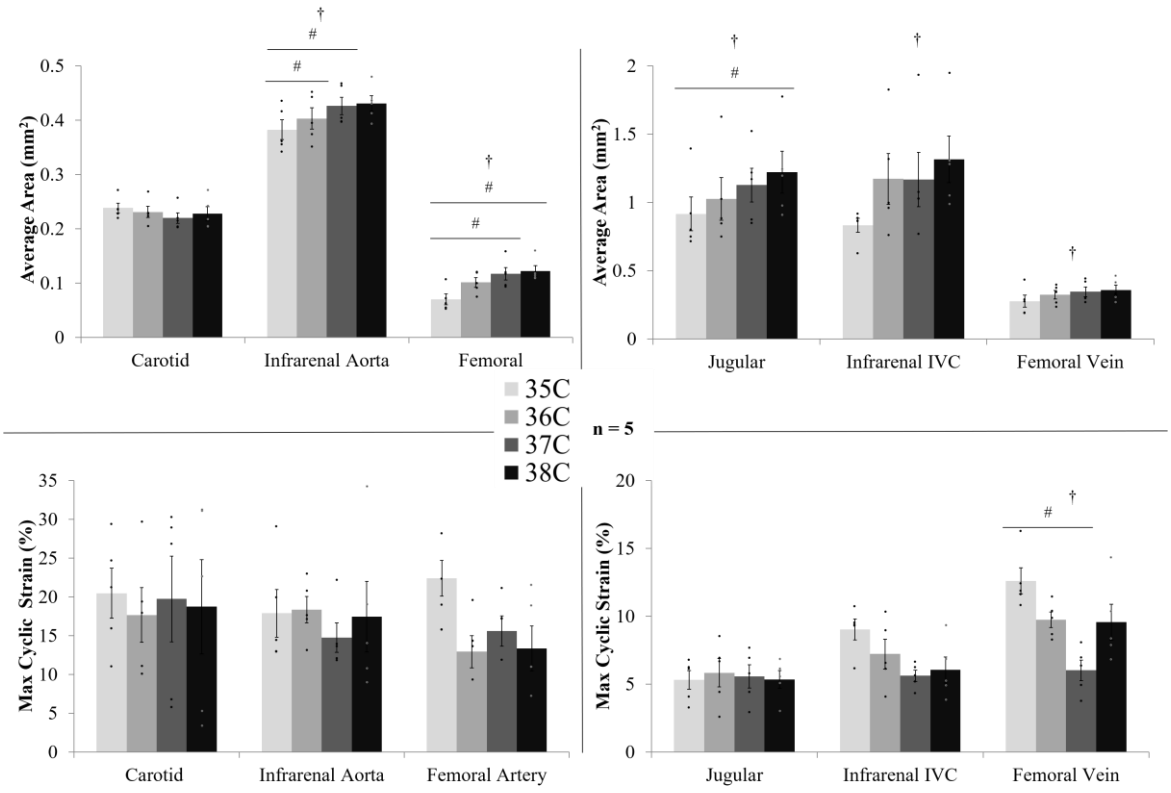

Figure 3.3 Vessel area averaged (top) and maximum cyclic strain (bottom) across the cardiac cycle for arteries (left) and veins (right) at four core body temperatures.

Cross-sectional area of the jugular vein increased with increasing core temperature.

Temperature did not have an effect on average area of the carotid artery (Figure 3.3). Temperature did influence average area of the jugular vein ($p = 0.006$), with statistically

significant differences between means at 35/38 °C (p = 0.03, Figure 3.3). The cross-sectional area of the jugular vein linearly increased with temperature by 0.10 mm^2/°C, or ~40 voxels/°C (slope > 0, p=0.0007, R^2=0.99, Figure 3.4). Cross-section area of the jugular vein but not the carotid artery, increased with increasing temperature for all timepoints across the cardiac cycle. The average percent change in maximum and minimum areas for the carotid were 2.1 and -0.7 %/°C, respectively, and for the jugular were 10.5 and 10.5 %/°C, respectively. With minimal change or similar increases in maximum and minimum vessel area in the carotid and jugular, respectively, maximum cyclic strain did not change with core temperature (Figure 3.3).

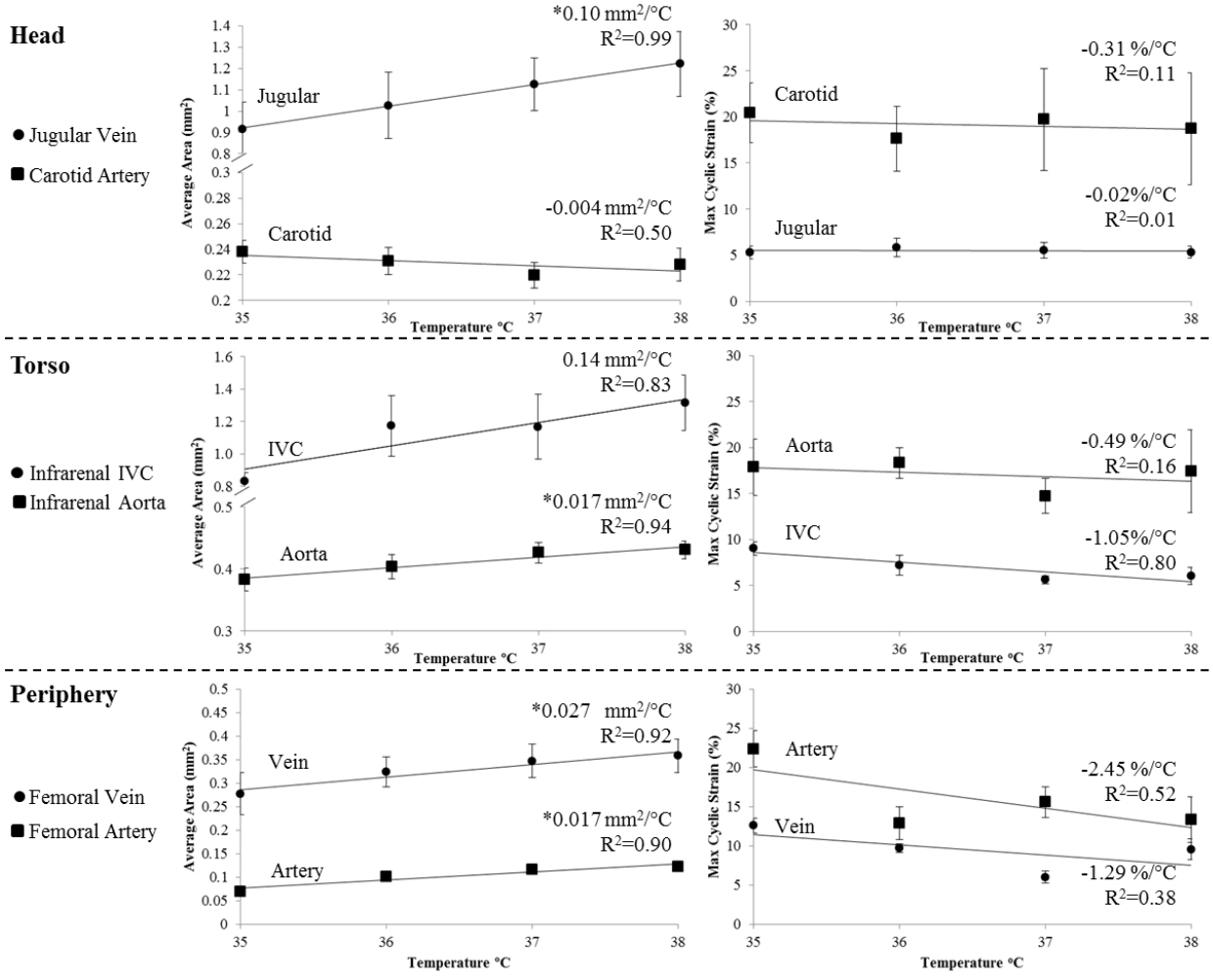

Figure 3.4 Average vessel area (left) and maximum cyclic strain (right) for artery-vein pairs at four core body temperatures: 35, 36, 37, 38 ºC (n=5 adult male mice).

Cross-sectional area of the aorta and IVC increased with increasing core temperature.

Temperature had an influence on average vessel area for both the aorta ($p = 0.02$) and IVC ($p = 0.05$, Figure 3.3) with statistically significant differences between means for the aorta at 35/36 °C and 35/37 °C ($p = 0.03$, $p = 0.002$). The average area of the aorta linearly increased by 0.017 mm^2/°C or ~11 voxels/°C (slope > 0, $p=0.03$, $R^2=0.94$, Figure 3.4). Although the slope was not found to be significantly different from zero, the average area of the IVC increased 0.14 mm^2/°C or ~56 voxels/°C, $R^2= 0.83$.

Cross-sectional area of the aorta and IVC, increased with increasing temperature for nearly all timepoints across the cardiac cycle, with the exception of the IVC at 36 and 37 °C where values were nearly identical. The average percent increase in maximum and minimum areas for the aorta were 4.3 and 6.6 %/°C, respectively, and for the IVC were 17.9 and 18.8 %/°C, respectively. Although the slope was not found to be different from zero, the maximum cyclic strain of the IVC decreased -1.05 %/°C, $R^2= 0.80$.

Cross-sectional area of the femoral artery and vein increased with increasing core temperature.

Temperature had an influence on average vessel area for the artery ($p = 0.002$) and vein ($p = 0.05$), with statistically significant differences between means for the artery at 35/37 °C and 35/38 °C ($p = 0.003$ and 0.0004, respectively, Figure 3.3).The average area of the femoral artery and vein linearly increased by 0.017 mm^2/°C or ~11 voxels/°C (slope > 0, $p = 0.05$, $R^2 = 0.90$) and 0.027 mm^2/°C or ~11 voxels/°C (slope > 0, $p=0.04$, $R^2=0.92$, Figure 3.4), respectively. When comparing slopes, the slope of area versus temperature for the femoral vein was larger than for the femoral artery ($p = 0.02$). Cross-sectional area of the artery and vein increased with increasing temperature for nearly all timepoints across the cardiac cycle. The average percent

increase in maximum and minimum areas for the artery were 22.0 and 28.6 %/°C, respectively, and for the vein were 10.5 and 11.3 %/°C, respectively. Temperature had an influence on maximum cyclic strain for the artery ($p = 0.03$) and the vein ($p = 0.01$), with statistically significant differences between means for the vein at 35/37 °C ($p = 0.008$, Figure 3.3).

Response as measured by relative changes in average area was location-dependent for 35-36 °C

Relative changes in average area over a one degree temperature interval (%/°C), compared using two-way ANOVA with Tukey's post hoc test, were influenced by location and vessel type at the 35-36°C interval (Table 3.1). The IVC response (39.2 %/°C) was 7.4-fold larger than the aorta response (5.42 %/°C, $p = 0.04$) and over 12-fold larger than the carotid response (-3.23 %/°C, $p = 0.004$). The femoral artery response (52.7 %/°C) was over 16-fold larger than the carotid response (-3.23 %/°C, $p<0.0001$), 9.8-fold larger than aorta response (5.42 %/°C, $p=0.0009$), and 4.6-fold larger than the jugular response (11.3 %/°C, $p=0.005$). Location and vessel type did not have an effect on response as measured by changes in maximum cyclic strain.

Contact length between artery and vein increased between 35 and 38 °C

Qualitatively, the contact length between the infrarenal and femoral artery-vein pairs increased between 35 and 38 °C (Figure 3.2). In Figure 3.5, the contact length is plotted for the aorta/IVC and femoral artery/vein at 35 and 38 °C at diastole and systole. Increases in core temperature resulted in an increase of 29.3% in contact length between the aorta and IVC for systole ($p = 0.007$) and an increase of 28.0% in contact length between the femoral artery and vein for diastole ($p = 0.03$).

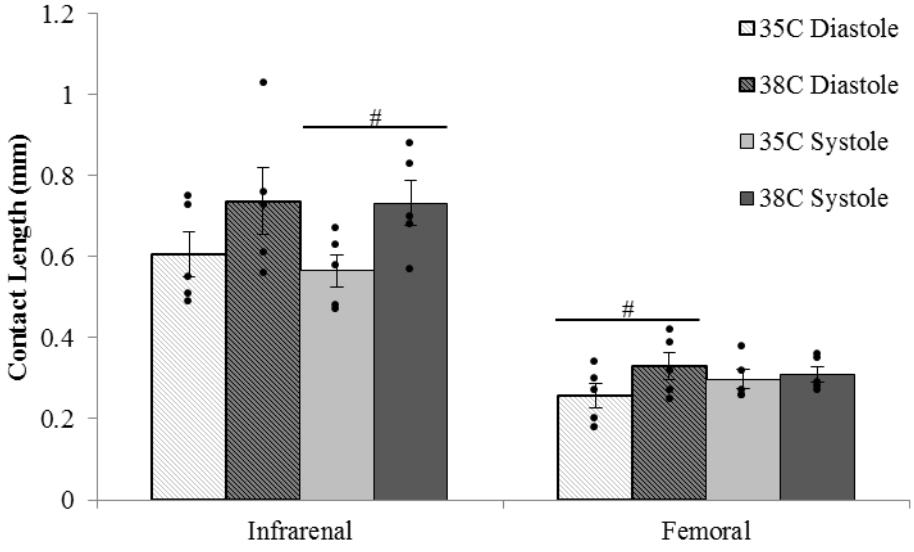

Figure 3.5 Contact length of contiguous (touching) portion of vessel calculated for core body temperatures of 35 and 38 °C at diastole and systole for the infrarenal and femoral locations

3.5 Discussion

In contrast to our previous study [15], adult males showed a linear increase in heart rate with increasing temperature. However, the slopes are not statistically different between the two studies ($p = 0.17$), and one slope can be calculated from all 10 animals: 8.3 bpm/°C. Also from our previous study, although not statistically significant, there was a trend of increased stroke volume with increasing temperature (36.1 vs. 37.1 µL/beat, $p = 0.5$ [15]). With an increase in heart rate and either no change or an increase in stroke volume, cardiac output would increase. Temperature-induced increases in cardiac output would cause an increase in volumetric flow rate in the body, and may also be necessary to maintain blood pressure subsequent to large reductions in total vascular resistance resulting from cutaneous vasodilation [10].

Femoral artery and infrarenal vena cava exhibit the largest relative changes in area

When comparing the relative vascular response between locations (Table 3.1), statistically significant differences were seen at the 35-36 °C interval. However, different

patterns of response between core arteries and veins, based on cranial-caudal location and depth, are apparent.

Arterial responses to temperature are consistent with previous findings. Lack of change in the carotid artery is reminiscent of our initial work showing minimal vascular response in the Circle of Willis with changes in core temperature. Furthermore, increases in cross-sectional area of the aorta due to increasing core temperature are in close accord with Chapter 2 data (0.017 $mm^2/°C$, Figure 3.4; compared to 0.019 $mm^2/°C$ [15]). As expected, the largest effects of temperature were seen in the femoral artery when comparing relative data (%/°C) [10,12]. Averaged across the temperature range investigated here, the arterial response increased from cranial to caudal and the more superficial femoral artery had a larger response than the deeper aorta, (carotid -1.4 %/°C, aorta 4.2 %/°C, and femoral 25.2 %/°C; Table 3.1). This would be consistent with the periphery and more superficial vessels being a site for heat exchange with the environment [10,12]. Two patterns of response were seen in the veins with respect to cranial-caudal location. First, relative increases in area were larger in the torso for 35-36 °C (jugular, IVC, femoral vein: 11.3, 39.2, 21.5%) and 37-38 °C (jugular, IVC, femoral vein: 8.1, 15.5, 3.5%; Table 3.1). Relative increases in area were larger away from the torso for 36-37 °C (jugular, IVC, femoral vein: 12.2, -0.04, 7.6%). An increase in area of the jugular vein with an increase in temperature was expected since there is limited conduction through the skull, and therefore, heat must be removed from the brain via the venous blood [28,29]. Increases in the area of the infrarenal IVC have not been identified previously and would be predicted to affect conductive and convective heat transfer. Changes in the femoral vein reinforce the concept that peripheral and more superficial vessels constrict with decreased temperature to minimize heat loss and, conversely, dilate with increased temperature to maximize heat loss [12]. Compared to arteries,

veins had a different pattern of response based on depth. Previous research suggests that with a decrease in temperature, core veins in the torso vasodilate to keep blood centrally and away from the skin and periphery where it might lose heat to the environment [16,17,30]. Researchers hypothesized that this mechanism would lead to an increase in venous return flow with a subsequent decrease in blood velocity, due to increased cross-sectional area of the vein. This, in turn, would promote heat transfer from the artery to the vein (increased counter-current heat exchange [18]). Our results illustrate the opposite (Figure 3.3).S The infrarenal IVC had the largest relative increase in area for veins (18.2 %/°C, compared to 9.0 and 10.9 %/°C for the jugular and femoral vein, respectively). This suggests that there is a decrease in venous return flow with decreased temperature. This could result from reduced cardiac output [15] and aortic flow at lower temperatures (as implied by reduced aortic area at lower temperatures). Additionally, recent research has revealed that the enteric nervous system, coined the "second brain", controls more than just digestion and has large blood flow demands [31,32]. At lower core temperatures, arterial blood may be redistributed to the gastrointestinal tract in order to maintain its temperature. The gut's venous return occurs at a location superior to the infrarenal IVC, and thus, increases in venous return flow with decreases in core temperature may still occur in the IVC superior to the location investigated in this work.

With no other physiological adjustments, the enlargement of the infrarenal IVC with increasing core temperature that we quantified here would act to minimize increases in blood velocity with increased cardiac output [10,11,15], and increase counter-current heat exchange, potentially leading to deleterious effects as more heat is transferred centrally. However, the hemodynamically inactive blood volume (60-70% of total blood volume [33]) may decrease with

increased core temperature and cardiac output. This would lead to increases in bulk flow at all depths and, thus, greater heat exchange with the environment.

Increases in contact length between artery-vein pairs could increase conductive heat transfer

Vessel composition affects the thermal conductivity of the vessel wall. Heat conduction between tissues depends on their thermal conductivities as well as the area of contact between the two tissues. Changes in contact length between artery-vein pairs due to changing temperature have not been investigated previously. Assuming that contact length also increases proximally and distally to the location at which imaging data were acquired, the increased contact lengths for the aorta/IVC and femoral artery/vein (Figure 3.5) suggest an increase in surface area between these artery-vein pairs. And, heat transfer via conduction would be hypothesized to increase between the artery and vein. Quantifying arterial/venous blood and tissue temperatures, while altering core temperature, will be essential to verify this.

Considerations for bioheat modeling

Data presented here can direct where and when temperature-dependent changes in geometry and strain need to be considered when coupling CFD and bioheat modeling [14,34,35]. For example, the carotid is an anatomical location where you would not need to incorporate geometric changes due temperature. By contrast, changes in geometry would be pertinent for the aorta, femoral artery, and all the veins studied here. With respect to implementation, we show a nearly linear dependence between vessel area and temperature in the jugular vein, infrarenal aorta, femoral artery, and femoral vein (Figure 3.4). In the infrarenal IVC there is not a linear relationship due to the large increase between 35-36 °C and, again, between 37-38 °C. However, there is a clear overall increase in vessel area with temperature. A larger temperature range, and thus more data points, is necessary to appropriately fit the non-linear data. Changes in contact

length should also be considered, due to their potential contribution to heat transfer via conduction. Strain data, even if not dependent on temperature, is important for deformable wall models in CFD [36] and data provided here illustrate large differences in cyclic strain between arteries and veins, which is consistent with previous work [27].

3.6 Conclusions

Challenges in measuring core vasculature have resulted in a lack of empirical information regarding how it might change with core temperature and its role in thermoregulation. Researchers have begun to study the response of core vessels in the leg [41,42]. In Chapter 2, we expanded this to the whole body for the arterial system in C57BL/6 mice [15], describing geometric and functional changes in the infrarenal aorta that demonstrate the importance of studying core arteries in response to changes in core temperature. In this chapter, we extend our investigations to the venous system by optimizing our non-invasive MRI data acquisition methods. The veins are an important part of the cardiovascular system's role in thermoregulation since blood returning to the heart must be warmed to core temperature via the activation of brown adipose tissue (BAT), countercurrent heat exchange, or other means of heat generation [22,43,44]. Although cutaneous veins are undoubtedly involved in thermoregulation [16,20,45], our data show that changes in the IVC, despite its depth, must also be considered. Our most important finding that the cross-sectional area of the core veins, particularly the IVC, is significantly smaller at lower temperatures is biologically significant due to the potential impact these changes could have on conductive and convective processes involved in thermoregulation. Changes in vasculature quantified in this chapter, motivated further study of the core vasculature's response to temperature including blood velocity and volumetric flow (Chapter 4) as well as combination studies (Chapter 5).

3.7 References

[1] van der Zee J. Heating the patient: a promising approach? Ann. Oncol. Off. J. Eur. Soc. Med. Oncol. 2002;13:1173–1184.

[2] Tucker R, Rauch L, Harley YR, et al. Impaired exercise performance in the heat is associated with an anticipatory reduction in skeletal muscle recruitment. Pflugers Arch. - Eur. J. Physiol. 2004;448:422–430.

[3] Stewart IB, Rojek AM, Hunt AP. Heat Strain During Explosive Ordnance Disposal. Mil. Med. 2011;176:959–963.

[4] Polderman KH. Application of therapeutic hypothermia in the intensive care unit. Intensive Care Med. 2004;30:757–769.

[5] Centers for Disease Control and Prevention U. Hypothermia-related deaths--United States, 1999-2002 and 2005. MMWR Morb. Mortal. Wkly. Rep. 2006;55:282–284.

[6] Fiala D, Havenith G. Modelling Human Heat Transfer and Temperature Regulation. Springer International Publishing; 2015. p. 265–302.

[7] Nybo L, Møller K, Volianitis S, et al. Effects of hyperthermia on cerebral blood flow and metabolism during prolonged exercise in humans. J. Appl. Physiol. 2002;93:58–64.

[8] Bain AR, Nybo L, Ainslie PN. Cerebral Vascular Control and Metabolism in Heat Stress. Compr. Physiol. Hoboken, NJ, USA: John Wiley & Sons, Inc.; 2015. p. 1345–1380.

[9] Qian S, Jiang Q, Liu K, et al. Effects of short-term environmental hyperthermia on patterns of cerebral blood flow. Physiol. Behav. 2014;128:99–107.

[10] Crandall CG. Heat stress and baroreflex regulation of blood pressure. Med. Sci. Sports Exerc. 2008;40:2063–2070.

[11] Siddiqui A. Effects of Vasodilation and Arterial Resistance on Cardiac Output. J. Clin. Exp. Cardiolog. 2011;02.

[12] Kuhn LA, Turner JK. Alterations in Pulmonary and Peripheral Vascular Resistance in Immersion Hypothermia. Circ. Res. 1959;7:366–374.

[13] Wissler EH. Pennes' 1948 paper revisited. J. Appl. Physiol. 1998;85:35–41.

[14] Bhowmik A, Singh R, Repaka R, et al. Conventional and newly developed bioheat transport models in vascularized tissues: A review. J. Therm. Biol. 2013;38:107–125.

[15] Crouch AC, Manders AB, Cao AA, et al. Cross-sectional area of the murine aorta linearly increases with increasing core body temperature. Int. J. Hyperth. 2018;34(7):1121-1113

[16] Shepherd J, Vanhoutte P. Veins and their control. London-Philadephia: W.B. Saunders Co.; 1975.

[17] Flavahan N, Vanhoutte P. Thermosensitivity of cutaneous and deep veins. Phlebology. 1988;3:41–45.

[18] Vanhoutte P. Return circulation and norepinephrine: an update. Paris; 1991.

[19] Milnor WR. Cardiovascular Physiology. New York: Oxford University Press; 1990.

[20] Rothe C. Venous system: physiology of the capacitance vessels. In: Shepard J, Abboud F, editors. Handb. Physiol. Cardiovasc. Syst. Peripher. Circ. organ blood flow. Bethesda, MD: American Physiological Society; 1983. p. 397–452.

[21] Mattson JM, Zhang Y. Structural and Functional Differences Between Porcine Aorta and Vena Cava. J. Biomech. Eng. 2017;139:071007.

[22] Leon LR. The use of gene knockout mice in thermoregulation studies. J. Therm. Biol. 2005;30:273–288.

[23] FLURKEY K, MCURRER J, HARRISON D. Mouse Models in Aging Research. Mouse Biomed. Res. Elsevier; 2007. p. 637–672.

[24] Constantinides C, Mean R, Janssen BJ. Effects of isoflurane anesthesia on the cardiovascular function of the C57BL/6 mouse. ILAR J. 2011;52:e21-31.

[25] Teng D, Hornberger TA. Optimal Temperature for Hypothermia Intervention in Mouse Model of Skeletal Muscle Ischemia Reperfusion Injury. Cell. Mol. Bioeng. 2011;4:717–723.

[26] Duhan V, Joshi N, Nagarajan P, et al. Protocol for long duration whole body hyperthermia in mice. J. Vis. Exp. 2012;e3801.

[27] Palmer OR, Chiu CB, Cao A, et al. In vivo characterization of the murine venous system before and during dobutamine stimulation: implications for preclinical models of venous disease. Ann. Anat. - Anat. Anzeiger. 2017;214:43–52.

[28] Nybo L, Secher NH, Nielsen B. Inadequate heat release from the human brain during prolonged exercise with hyperthermia. J. Physiol. 2002;545:697–704.

[29] Mariak Z, White MD, Lewko J, et al. Direct cooling of the human brain by heat loss from the upper respiratory tract. J. Appl. Physiol. 1999;87:1609–1613.

[30] Shepherd J, Vanhoutte P. The Human Cardiovascular System. Facts and Concepts. New York: Raven Press; 1979.

[31] Gershon M. The Second Brain : The Scientific Basis of Gut Instinct and a Groundbreaking New Understanding of Nervous Disorders of the Stomach and Intestines. New York: HarperCollins; 1998.

[32] Carabotti M, Scirocco A, Maselli MA, et al. The gut-brain axis: interactions between enteric microbiota, central and enteric nervous systems. Ann. Gastroenterol. 2015;28:203–209.

[33] Greenway C V., Lautt WW. Blood volume, the venous system, preload, and cardiac output. Can. J. Physiol. Pharmacol. 1986;64:383–387.

[34] Coccarelli A, Boileau E, Parthimos D, et al. An advanced computational bioheat transfer model for a human body with an embedded systemic circulation. Biomech. Model. Mechanobiol. 2016;15:1173–1190.

[35] Shitzer A, Stroschein L a, Vital P, et al. Numerical analysis of an extremity in a cold environment including countercurrent arterio-venous heat exchange. J. Biomech. Eng. 1997;119:179–186.

[36] Figueroa CA, Vignon-Clementel IE, Jansen KE, et al. A coupled momentum method for modeling blood flow in three-dimensional deformable arteries. Comput. Methods Appl. Mech. Eng. 2006;195:5685–5706.

[37] Støen R, Sessler DI. The Thermoregulatory Threshold is Inversely Proportional to Isoflurane Concentration. Anesthesiology. 1990;72:822–827.

[38] Matta BF, Heath KJ, Tipping K, et al. Direct cerebral vasodilatory effects of sevoflurane and isoflurane. Anesthesiology. 1999;91:677–680.

[39] Hartley CJ, Reddy AK, Madala S, et al. Effects of isoflurane on coronary blood flow velocity in young, old and ApoE(-/-) mice measured by Doppler ultrasound. Ultrasound Med. Biol. 2007;33:512–521.

[40] Frank SM, Raja SN, Bulcao CF, et al. Relative contribution of core and cutaneous temperatures to thermal comfort and autonomic responses in humans. J. Appl. Physiol. 1999;86:1588–1593.

[41] Pearson J, Low DA, Stöhr E, et al. Hemodynamic responses to heat stress in the resting and exercising human leg: insight into the effect of temperature on skeletal muscle blood flow. Am. J. Physiol. - Regul. Integr. Comp. Physiol. 2011;300:663–673.

[42] Chiesa ST, Trangmar SJ, González-Alonso J. Temperature and blood flow distribution in the human leg during passive heat stress. J. Appl. Physiol. 2016;120:1047–1058.

[43] Vosselman MJ, van Marken Lichtenbelt WD, Schrauwen P. Energy dissipation in brown adipose tissue: From mice to men. Mol. Cell. Endocrinol. 2013;379:43–50.

[44] Walløe L. Arterio-venous anastomoses in the human skin and their role in temperature control. Temp. (Austin, Tex.). 2016;3:92–103.

[45] Rowell LB. Cardiovascular aspects of human thermoregulation. Circ. Res. 1983;52:367–379.

Chapter 4
Blood flow distribution with increasing core temperature

4.1 Abstract

Purpose: To fully understand the cardiovascular system's role in thermoregulation, blood distribution (influenced by cardiac output, vessel size, blood flow, and pressure) must be quantified, ideally across sex and age. The purpose of this study is to determine the influence of sex and age on the CV response to temperature.

Methods: Male and female, adult and aged, mice were anesthetized and imaged at 7T. Data were acquired from four co-localized vessel pairs (the neck [carotid/jugular], torso [suprarenal and infrarenal aorta/inferior vena cava (IVC)], periphery [femoral artery/vein]) at core temperatures of 35, 36, 37, and 38 °C. Sixteen CINE, ECG-gated, phase contrast frames with one-directional velocity encoding (through plane) were acquired perpendicular to each vessel: TR/TE ~180/5ms, field of view arteries/veins (20/25.6 mm)2, flip angle arteries/veins (60º/20º), matrix 1282 zero-filled to 2562, slice thickness 1 mm, 2 excitations, VENC 20-120 depending on the vessel). Each frame was blood velocity and volumetric flow using a semi-automated in-house MATLAB script.

Results: Blood velocity and volumetric flow were quantified in eight vessels at four core body temperatures. Flow in the infrarenal IVC linearly increased with temperature for all groups ($p = 0.002$; adjusted means: male vs. female, 0.37 and 0.28 mL/(min • °C); adult vs. aged, 0.22 and 0.43 mL/(min • °C)).Comparing average volumetric flow response to temperature, groups differed for the suprarenal aorta (adult < aged, $p<0.05$), femoral artery (adult < aged, $p<0.05$), and femoral vein (adult male < aged male, $p<0.001$).

Conclusions: With this work, we have been able to distinguish contributions from changes in area and blood velocity which would be important for more accurate bioheat modeling. In aged animals, flow increases were driven primarily by velocity changes suggesting a diminished ability for structural changes in area. These changes in blood velocity are also likely causing changes in wall shear stress which is an important metric in cardiovascular disease progression.

4.2 Introduction

As described in section 3.2, literature suggests that with a decrease in temperature, the blood flow in the core veins in the torso will increase [22] due to the shunting of blood away from the periphery and subcutaneous vessels to minimize heat exchanged with the environment [22–24], Chapters 2 and 3 illustrated an increase in the cross-sectional area of arteries and veins, from head-to-toe, due to increases in core temperature [25,26]. These geometric results imply flow would decrease with a decrease in temperature. However, data regarding velocity, and hence volumetric flow in the core (alternatively, deep) veins and arteries are necessary to confirm our initial findings.

Using healthy C57B/6 mice [27] and MRI, we noninvasively quantified blood velocity and calculated volumetric flow changes in artery-vein pairs in the neck (carotid/jugular), torso (suprarenal and infrarenal aorta/inferior vena cava (IVC)), and periphery (femoral artery/vein) at four target core temperatures. We hypothesized that: blood flow would increase as core temperature increased from minimally hypothermic at 35 °C to minimally hyperthermic at 38 °C; the magnitude of blood flow increase would vary based on anatomical location; and, aged males would have a diminished response [25]. To our knowledge, these data are the first to empirically quantify the spatially and temporally resolved blood velocity/flow response of artery-vein pairs

of core vasculature to changes in core temperature in vivo from head-to-toe. This functional data could be used to couple bioheat modeling and computational fluid dynamics (CFD) to improve understanding of the complex process of thermoregulation.

4.3 Methods

All experiments were carried out with local Institutional Animal Care and Use Committee approval. Animals were housed in a room with temperature (22 ± 2 °C) and humidity (~27%) control and an alternate 12 hour light/dark cycle.

Animals and normothermic data were collected in a previous study [Crouch 2019, pending acceptance]. Methods for imaging are briefly repeated here. For both studies, healthy adult (12- to 14-weeks-old, ~20-25 human years) and aged (52- to 58-weeks-old, ~50 human years [28]), male and female, C57BL/6 mice, purchased from Charles Rivers Laboratory, were used in this study (n = 5 each, total = 20). Mice were anesthetized with 1.25-2% isoflurane in 1 L/min of oxygen [29]. Animals were imaged in the supine position at 7T using a Direct Drive console (Agilent Technologies, Santa Clara, CA) and a 40 mm inner diameter transmit-receive volume coil (Morris Instruments, Ontario, Canada).

In this study, the four target core temperatures, selected to avoid pathological changes [30,31], ranged from minimally hypothermic (35 °C) to minimally hyperthermic (38 °C) within ± 0.2 °C. The forced convection system included a heater blowing warm air through the bore of the magnet and over the animal, a rectal temperature probe, and a custom-built proportional-integral-derivative (PID) controller (Labview, National Instruments, Austin TX). Heart rate and respiration were monitored (SA Instruments, Stony Brook, NY).

Figure 4.1 illustrates the locations investigated in this study [25,26]. CINE phase contrast data was acquired in the neck (carotid artery and jugular vein), torso (suprarenal/infrarenal aorta

and inferior vena cava), and periphery (femoral artery and vein). To acquire all four locations for a given animal, with four target core temperatures tested at each location, two imaging sessions were required (approximately two hours each). To verify that changes observed in the vasculature were not due to long exposures to anesthesia, the same data acquisition and analysis procedures were repeated every 30 minutes with animal's core temperature maintained at 37 °C for two hours (n = 2, adult males) [26]. Data were acquired at the carotid artery and jugular vein, suprarenal and infrarenal aorta and IVC, and femoral artery and vein.

MRI Slice planning and parameters

Sixteen cardiac-gated 2D CINE, phase contrast frames with one-directional velocity encoding (through plane) were acquired perpendicular to each vessel with methods reported in full elsewhere [Crouch 2019, pending acceptance]. The PCMRI sequence involved repeated measurements using reversed, bipolar, linear gradients. Parameters for the arteries were [TR/TE ~180/5 ms depending on heart rate, flip angle (α) 60º, FOV $(20\ mm)^2$, matrix 128^2 zero-filled to 256^2, in-plane resolution $(78\ \mu m)^2$, slice thickness 1 mm, NEX 2]. Parameters for the jugular vein were [TR/TE ~180/5 ms depending on heart rate, α 20º, FOV $(25.6\ mm)^2$, matrix 128^2 zero-filled to 256^2, in-plane resolution $(100\ \mu m)^2$, slice thickness 1 mm, NEX 2]. The difference in parameters (reduced flip angle and resolution, respectively) reflects the slower blood flow and larger size of the veins.

Velocity encoding (VENC) parameter was optimized for each vessel, data not shown: carotid 100 cm/sec, jugular 20 cm/sec, suprarenal aorta 120 cm/sec, suprarenal IVC 20 cm/sec, infrarenal aorta 80 cm/sec, infrarenal IVC 20 cm/sec, femoral artery 40 cm/sec, and femoral vein 20 cm/sec.

MRI Analysis: Cross-sectional area, velocity, volumetric flow

The CINE images were analyzed for vessel cross-sectional area, average and maximum blood velocity, and volumetric flow using an in-house semi-automated Matlab code [Crouch 2018, pending acceptance]. Volumetric flow of the entire vessel was calculated by the following Equation 7.

Equation 7

$$Volumetric\ Flow = \sum Area_{voxel} * Velocity_{voxel}$$

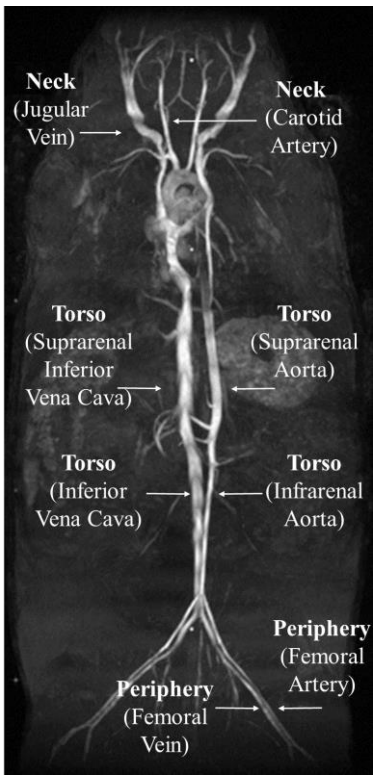

Figure 4.1 Coronal maximum intensity projection (MIP) (Crouch et al. 2018) illustrating arterial and venous locations where imaging data was acquired and quantified.

Statistical Analysis

Data are plotted as mean ± standard error (SEM). Velocity and volumetric flow were positive for flow in the positive Z-direction (carotid, IVC, femoral vein) and negative for flow in the negative Z-direction (jugular, aorta, and femoral artery). However, all results were tested and

are reported as the absolute value to be able to compare locations. To test whether temperature had an effect on a given metric within a group of animals, repeated measures one-way ANOVA and Tukey's post hoc test to account for multiple comparisons was used, with temperature treated as categorical.

Three methods were used to evaluate differences between groups. First, to compare relative changes within a given one degree temperature interval (i.e. 35-36, 36-37, or 37-38 °C), the percent change per one degree increase in temperature (%/°C) was calculated for each metric to account for potential differences due to size between groups [25]. Using the %/°C values, the effects of sex and age were assessed via two-way ANOVA and Tukey's post hoc test. Secondly, to compare absolute changes over the four degree temperature interval, linear regression was applied to mean velocity and mean volumetric flow averaged across the cardiac cycle. For example for mean velocity, regression resulted in a fitted line with units of cm/(s • °C). Slopes were assessed for linearity (R^2) and tested for being non-zero and different between groups. Finally to determine sex and age differences at each temperature, the metrics at each temperature were tested via repeated measured two-way ANOVA and Tukey's post hoc test (i.e for a given metric, adult male 35 °C vs. adult female 35°C). Significance was set at $p < 0.05$. Data were analyzed using GraphPad Prism version 7.0 (GraphPad Software, La Jolla, CA).

4.4 Results

Average body weights increased with age (adult: 21.9 ± 0.6 vs. aged: 32.4 ± 0.9 g, $p < 0.0001$) and were greater in males compared to females (male: 29.8 ± 1.4 vs. female: 24.5 ± 1.1 g, $p < 0.001$).

Heart rate linearly increased with temperature for adult males: 19.2 ± 2.4 bpm/°C, adult females: 26.9 ± 5.0 bpm/°C, aged males: 10.4 ± 0.6 bpm/°C, and aged females: 26.2 ± 2.0

bpm/°C (R^2: 0.93-0.99, p: 0.003-0.02). Two hours of isoflurane exposure at normothermic conditions (37 °C) resulted in minimal changes in heart rate and vessel area [26] and volumetric flow in the infrarenal IVC, femoral artery and vein: 6.9, 7.0, and 0.9 %/30 min, respectively.

For the carotid artery, the left and right carotid artery were compared for n=15 animals, and there was no statistical difference between the left and right for area, velocity, or volumetric flow ($p > 0.05$). However, for this study, the right carotid was used for temperature testing.

Mean velocity across the lumen increased with temperature in the femoral artery and effect of temperature was dependent on location, sex, and age.

Figure 4.2 shows the mean velocity averaged across the cardiac cycle (average velocity) at four arterial locations for the four groups studied here. Temperature had an influence on the average velocity in the femoral artery for the adult animals and aged males (Figure 4.2, $p < 0.03$) with statistically significant differences between means for: adult females, 35/37 °C ($p = 0.03$), 35/38 °C ($p = 0.01$) 36/38 °C ($p = 0.02$) and 37/38 °C ($p = 0.01$), aged males, 35/37 °C ($p = 0.04$), 35/38 °C ($p = 0.02$), and 36/37 °C ($p = 0.01$). In the femoral artery, average velocity linearly increased with temperature for adult animals and aged males (slopes > 0, $p = 0.01$-0.03, $R^2 = 0.92$-0.97); however the slopes were not different between group ($p > 0.05$; adjusted slope 1.2 cm/(s • °C)).

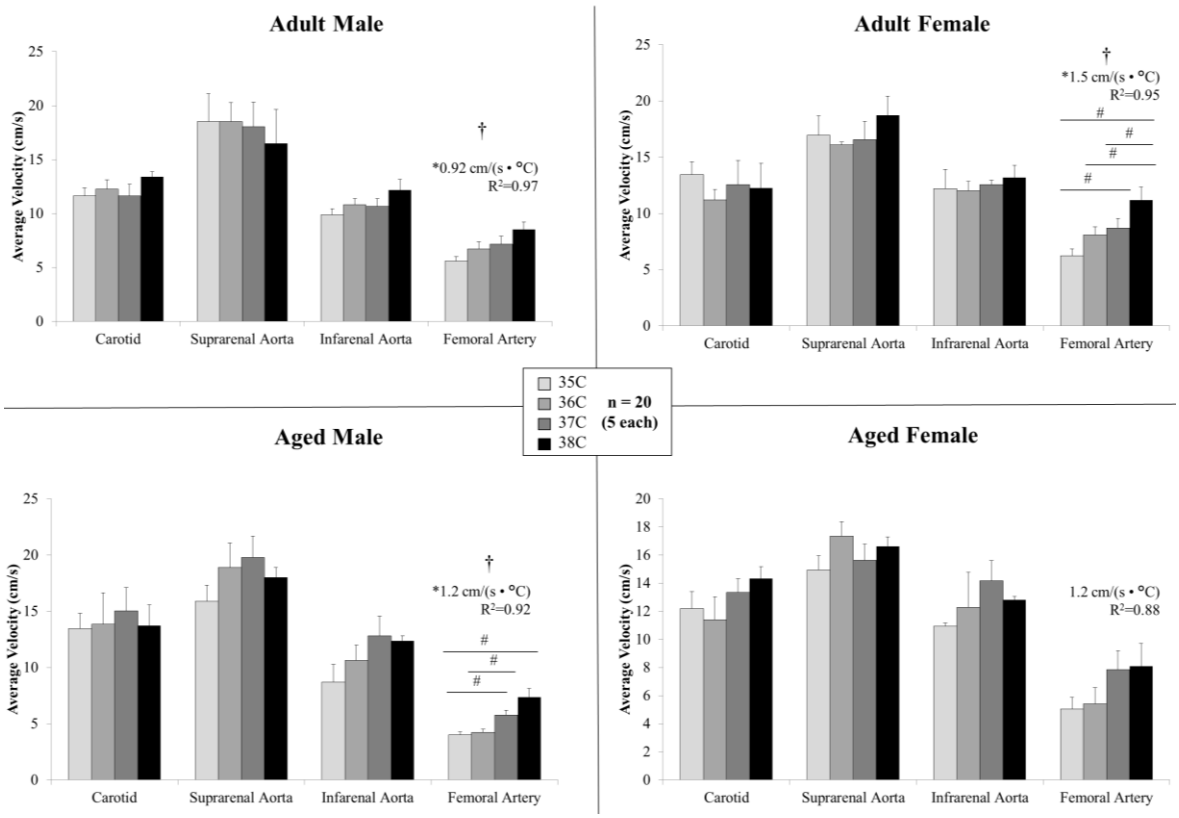

Figure 4.2 Mean velocity averaged across the cardiac cycle (mean ± SEM) in the arteries for male and female, adult and aged mice (n=5 each) at core temperatures of 35, 36, 37, 38 °C.
Response varied by location and across sex and age. Significance set at $p < 0.05$: for temperature effect overall (†), pairwise comparisons between temperatures within a group(#), relative changes to same age group but opposite sex ($), relative changes to same sex but different age group (@), non-zero slope (*).

Figure 4.3 shows the mean velocity averaged across the cardiac cycle at four venous locations for each group. Temperature had an influence on the average velocity for the infrarenal IVC for aged males ($p = 0.03$) and for the femoral vein for aged females ($p = 0.04$). In the jugular and infrarenal IVC, average velocity linearly increased with temperature for the aged males (slope > 0, $p < 0.04$, $R^2 = 0.92$-0.99).

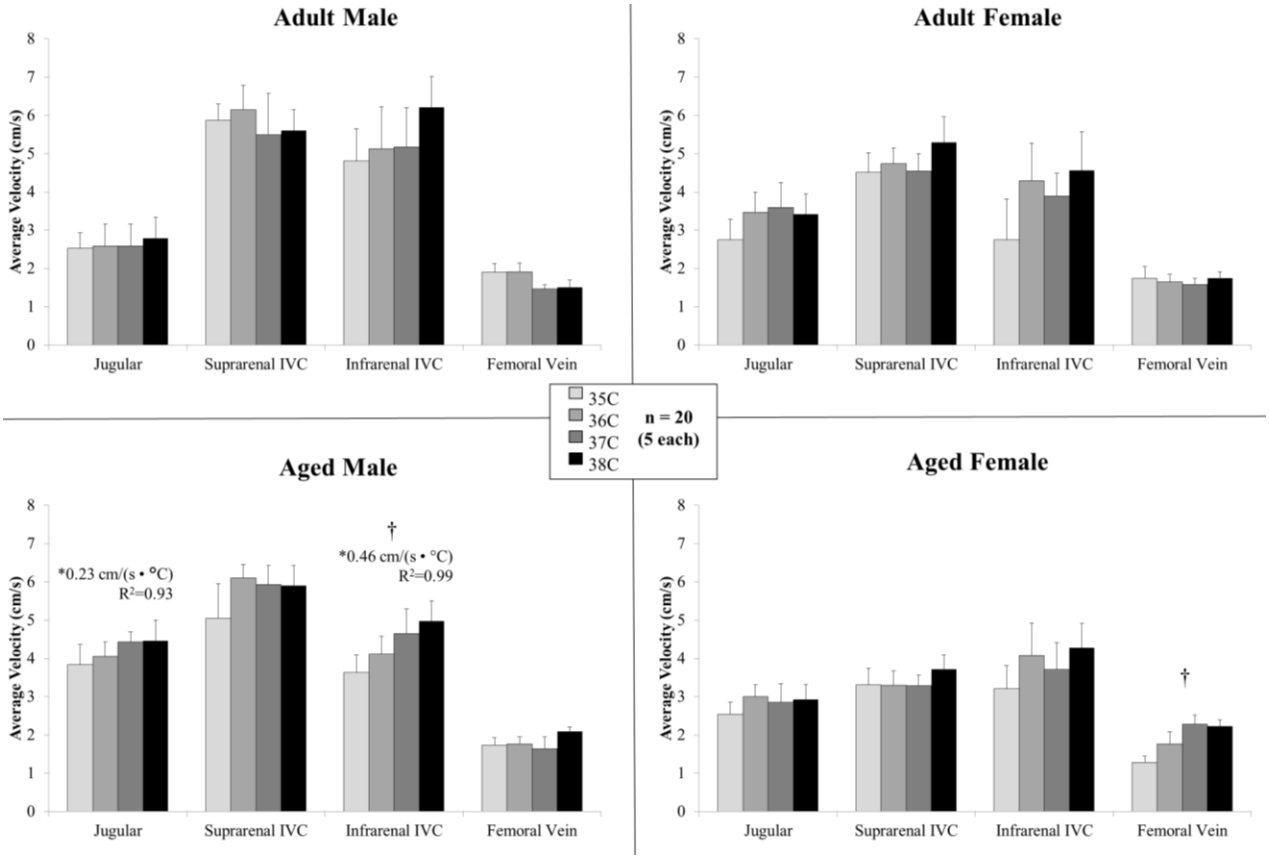

Figure 4.3 Mean velocity averaged across the cardiac cycle (mean ± SEM) in the veins for male and female, adult and aged mice (n=5 each) at core temperatures of 35, 36, 37, 38 °C.
Response varied by location and across sex and age. Significance set at $p < 0.05$: for temperature effect overall (†), pairwise comparisons between temperatures within a group(#), relative changes to same age group but opposite sex ($), relative changes to same sex but different age group (@), non-zero slope (*).

The mean velocity across the lumen at systole and diastole are referred to here as mean systolic and mean diastolic velocities, and the maximum velocity across the lumen during peak-systole is referred to as or peak velocity. A summary of the mean systolic and diastolic velocities and peak velocity for all animal groups at every location is presented in Table 4.1. If there were no statistical difference between temperatures, the values are averaged across the four temperatures.

For mean systolic velocities, temperature had an influence at the carotid, suprarenal and infrarenal aorta for aged females (Table 4.1, $p < 0.05$) with statistically significant differences

between means for: suprarenal aorta, 35/36 °C ($p = 0.04$) and 35/38 °C ($p = 0.03$); infrarenal aorta, 35/38 °C ($p = 0.03$). Temperature had an influence at the infrarenal IVC for aged males (Table 4.1, $p = 0.04$) with statistically significant differences between means for 35/38 °C ($p = 0.03$). Figure 4.4 shows the mean velocity across the lumen plotted across the cardiac cycle for the femoral artery for the four groups. Temperature had an influence on femoral artery mean systolic velocity for all groups (Table 4.1 Figure 4.4, $p < 0.01$) with statistically significant differences between means within a group for: adult male, 35/36 °C ($p=0.046$), 35/38 °C ($p=0.04$), and 37/38 °C ($p=0.02$); adult female, 35/36 °C ($p = 0.006$), 35/37 °C ($p = 0.001$), 35/38 °C ($p = 0.007$), 36/38 °C ($p = 0.03$), and 37/38 °C ($p < 0.05$); aged males, 35/37 °C ($p < 0.05$) and 35/38 °C ($p = 0.02$); and aged females, 36/37 °C ($p=0.02$) and 36/38 °C ($p = 0.03$). When comparing relative response for mean systolic velocity, sex and age had an influence on response at the suprarenal aorta ($p = 0.03$).

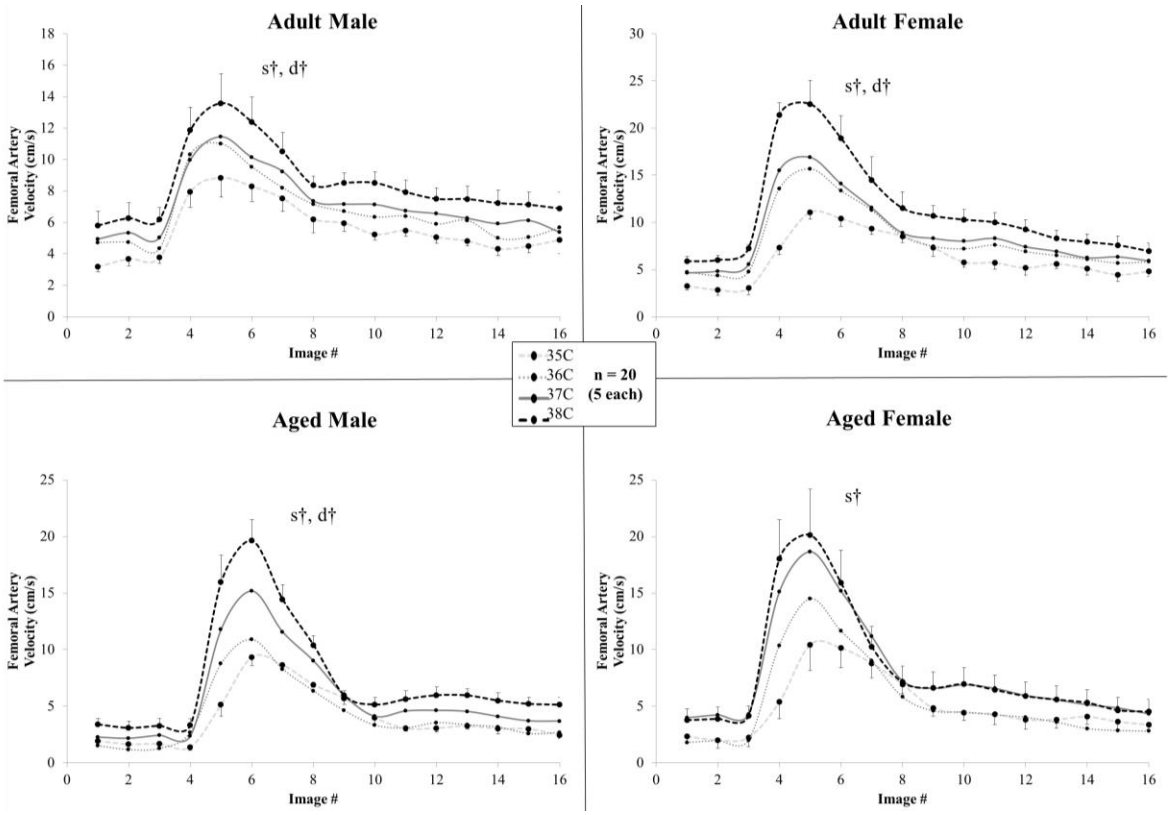

Figure 4.4 Mean velocity of femoral artery across the cardiac cycle for male and female, adult and aged mice (n=5 each) at core temperatures of 35, 36, 37, 38 °C.
Error bars shown only for 38C and 35C for clarity, and plotted on different y-scales to better highlight temperature effect. Significance set at $p < 0.05$: for temperature effect overall at mean systole (s†) and mean diastole (d†).

For mean diastolic velocities, temperature had an influence at suprarenal aorta and femoral vein for aged females (Table 4.1, $p < 0.03$) with statistically significant differences between means for the suprarenal aorta, 35/37 °C ($p = 0.04$). Temperature had an influence on femoral artery mean diastolic velocity for all groups except aged females ($p < 0.02$) with statistically significant differences between means within a group for adult females, 35/38 °C ($p = 0.04$) and 36/38 °C ($p = 0.004$), and aged males, 36/37 °C ($p = 0.03$) and 36/38 °C ($p < 0.05$).

Table 4.1 Summary table of mean systolic, mean diastolic, and peak velocity.

		Velocity (cm/s)		
Location	Group (n=5 each)	Mean systolic	Mean diastolic	Peak
Carotid	Adult Male	27.7 ± 3.4	6.3 ± 1.1	53.8 ± 5.9
	Adult Female	40.8 ± 4.3	3.2 ± 1.9	81.1 ± 6.7
	Aged Male	37.0 ± 3.9	4.6 ± 2.5	83.5 ± 9.0
	Aged Female	**37.7** ± 2.5, **36.7** ± 1.9, **43.1** ± 2.8, **45.4** ± 3.4	3.0 ± 2.1	88.1 ± 4.9
Jugular	Adult Male	1.7 ± 0.6	0.7 ± 0.4	6.7 ± 0.7
	Adult Female	2.1 ± 0.8	0.8 ± 0.8	8.1 ± 1.4
	Aged Male	5.4 ± 0.6	2.2 ± 0.4	9.6 ± 0.7
	Aged Female	1.7 ± 0.4	1.1 ± 0.3	6.6 ± 0.7
Suprarenal Aorta	Adult Male	25.4 ± 8.0	1.4 ± 1.7	89.7 ± 12.9
	Adult Female	27.0 ± 2.0	1.0 ± 2.2	100.3 ± 4.4
	Aged Male	24.9 ± 3.0	1.7 ± 1.4	102.5 ± 6.5
	Aged Female	**40.4** ± 3.1, **46.6** ± 3.0, **43.7** ± 4.0, **49.9** ± 3.0	**2.2** ± 1.5, **6.8** ± 0.7, **4.9** ± 1.0, **5.8** ± 0.5	91.7 ± 8.2
Suprarenal IVC	Adult Male	7.6 ± 0.8	2.8 ± 1.0	13.3 ± 1.4
	Adult Female	6.7 ± 0.8	2.0 ± 0.6	11.8 **±** 1.6
	Aged Male	7.7 ± 0.7	2.8 ± 0.7	14.3 ± 1.4
	Aged Female	5.1 ± 0.7	1.1 ± 0.3	10.7 ± 1.5
Infrarenal Aorta	Adult Male	18.8 ± 5.3	1.9 ± 1.3	60.8 ± 9.7
	Adult Female	16.8 ± 2.4	2.1 ± 0.6	**58.3** ± 6.2, **64.6** ± 4.7, **71.1** ± 0.7, **73.6** ± 3.9
	Aged Male	17.0 ± 2.9	1.1 ± 1.1	**63.2** ± 6.0, **73.4** ± 4.6, **75.8** ± 3.8, **79.3** ± 0.6
	Aged Female	**29.3** ± 2.3, **33.4** ± 3.6, **36.0** ± 2.3, **37.5** ± 1.4	1.7 ± 1.1	**60.0** ± 3.8, **66.1** ± 3.2, **71.3** ± 3.3, **72.5** ± 3.3
Infrarenal IVC	Adult Male	6.2 ± 1.0	4.5 ± 0.9	10.7 ± 1.6
	Adult Female	4.9 ± 0.8	2.9 ± 0.9	8.8 **±** 1.0
	Aged Male	**4.5** ± 0.5, **5.0** ± 0.6, **5.6** ± 0.8, **5.9** ± 0.7	3.1 ± 0.5	**7.9** ± 0.7, **9.0** ± 1.1, **9.8** ± 1.4, **10.5** ± 1.1
	Aged Female	4.5 ± 0.7	2.8 ± 0.7	8.2 ± 1.1
Femoral Artery	Adult Male	**9.1** ± 1.0, **11.4** ± 1.5, **11.5** ± 1.5, **14.0** ± 1.9	**3.0** ± 0.3, **4.1** ± 0.6, **4.8** ± 0.7, **5.6** ± 0.8	**10.8** ± 1.1, **13.8** ± 1.7, **14.1** ± 1.6, **17.6** ± 2.3
	Adult Female	**11.1** ± 0.7, **15.7** ± 1.1, **17.1** ± 0.8, **23.1** ± 2.2	**2.7** ± 0.6, **4.3** ± 0.5, **4.5** ± 0.6, **5.9** ± 0.5	**14.2** ± 1.3, **19.5** ± 1.5, **20.4** ± 0.8, **28.0** ± 0.5
	Aged Male	**9.9** ± 0.4, **11.5** ± 0.9, **15.2** ± 1.0, **19.6** ± 1.9	**1.1** ± 0.4, **0.9** ± 0.3, **1.9** ± 0.4, **2.9** ± 0.6	**12.6** ± 0.4, **15.4** ± 0.5, **23.2** ± 2.3, **33.3** ± 2.9
	Aged Female	**11.0** ± 1.9, **14.5** ± 3.0, **18.7** ± 3.3, **20.6** ± 3.7	0.8 ± 0.9	**13.5** ± 2.4, **18.4** ± 3.4, **25.0** ± 2.9, **27.2** ± 3.7
Femoral Vein	Adult Male	2.2 ± 0.2	1.2 ± 0.2	**4.1** ± 0.3, **4.3** ± 0.3, **3.7** ± 0.3, **3.5** ± 0.3
	Adult Female	2.1 ± 0.2	1.3 ± 0.2	4.2 ± 0.2
	Aged Male	2.3 ± 0.2	1.4 ± 0.2	5.1 ± 0.3
	Aged Female	2.4 ± 0.2	**0.8** ± 0.1, **1.1** ± 0.2, **1.7** ± 0.2, **1.6** ± 0.2	5.1 ± 0.4

Peak velocity increased with temperature in the femoral artery with varied relative response between groups in the suprarenal aorta and femoral artery

Temperature had an influence on peak velocity at the infrarenal aorta for adult females and aged animals (Table 4.1, $p < 0.03$) with statistically significant differences between means for aged females for 36/37 °C ($p = 0.04$). Temperature had an influence on peak velocity at the infrarenal IVC for aged males (Table 4.1, $p = 0.02$) with statistically significant differences for 35/38 °C ($p = 0.03$). For the femoral artery, temperature had an influence on peak velocity for all groups ($p < 0.008$) with statistically significant differences between means within a group for: adult male, 35/36 °C ($p = 0.02$), 35/37 °C ($p= 0.007$), and 35/38 °C ($p = 0.03$); adult females, 35/36 °C ($p = 0.045$), 35/37 °C ($p = 0.006$), 35/38 °C ($p = 0.004$), and 36/38 °C ($p = 0.047$); aged males, 35/37 °C ($p = 0.045$), 35/38 °C ($p = 0.006$), and 36/38 °C ($p = 0.01$); and aged females, 35/37 °C ($p = 0.007$), 35/38 °C ($p = 0.01$), 36/37 °C ($p = 0.02$), and 36/38 °C ($p = 0.004$). For the femoral vein, temperature had an influence on peak velocity for adult males ($p = 0.03$) with statistically significant differences for 36/38 °C ($p = 0.0006$). When comparing relative response for peak velocity, sex and age had an influence on response at the suprarenal aorta ($p = 0.03$) and the femoral artery ($p = 0.004$), and aged males had a larger response in the femoral artery for the 36-37 °C interval than adult males by nearly 20-fold (52.2 vs. 2.7 %/°C, $p = 0.02$).

Volumetric flow response to temperature was larger in aged animals

Figure 4.5 shows the volumetric flow averaged across the cardiac cycle in the neck and torso vessels for male and female, adult and aged mice. Temperature had an influence on average volumetric flow for the infrarenal aorta (aged males, $p = 0.03$) and for the infrarenal IVC (aged males, $p = 0007$; aged females, $p = 0.02$) with statistically significant differences between means for the infrarenal IVC: aged males, 35/38 °C ($p = 0.006$) and 36/38 °C ($p = 0.01$); aged females,

35/38 (p = 0.04). For aged males, flow in the suprarenal IVC and infrarenal aorta (slopes > 0, p < 0.007, R^2 = 0.98-0.99) linearly increase with temperature. Flow in the infrarenal IVC linearly increased with temperature for all groups (slopes > 0, p < 0.02, R^2 = 0.94-0.98) with slopes differing between groups (p = 0.002; adjusted means: male vs. female, 0.37 and 0.28 cm/(s • °C); adult vs. aged, 0.22 and 0.43 cm/(s • °C)). When comparing relative response for volumetric flow, sex and age had an influence on response at the suprarenal aorta (p = 0.005) with statistically significant differences between adult and aged animals at 35-36 °C interval (adult male: -1.2 %/°C vs aged male: 20.5 %/°C, p = 0.04; adult female: -7.5 %/°C vs. aged female: 15.1 %/°C, p = 0.02).

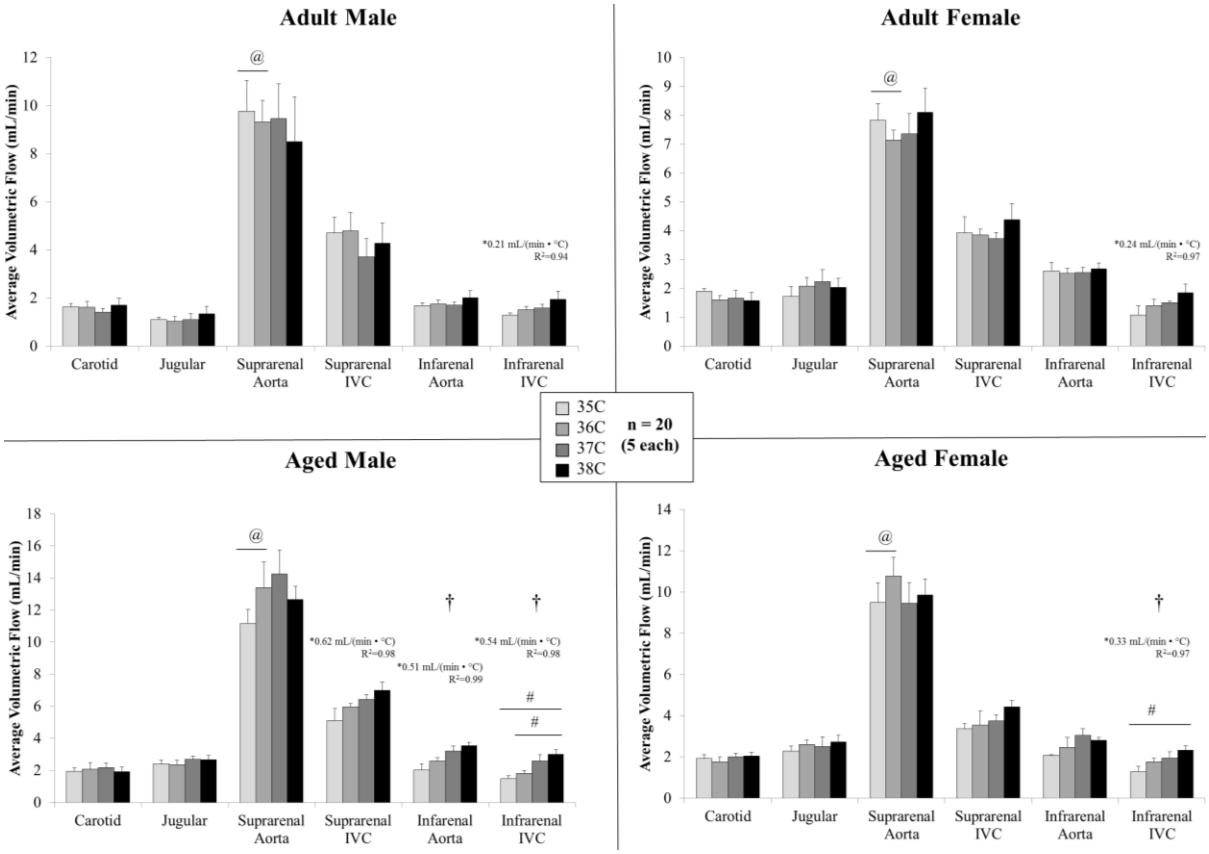

Figure 4.5 Volumetric flow averaged across the cardiac cycle (mean ± SEM) in the neck and torso vessels for male and female, adult and aged mice (n=5 each) at core temperatures of 35, 36, 37, 38 °C.
Response varied by location and across sex and age. Significance set at p < 0.05: for temperature effect overall (†), pairwise comparisons between temperatures within a group(#), relative changes to same age group but opposite sex ($), relative changes to same sex but different age group (@), non-zero slope (*).

Figure 4.6 shows the volumetric flow averaged across the cardiac cycle in the peripheral vessels for male and female, adult and aged mice. Temperature had an influence on average volumetric flow for the femoral artery for all groups ($p < 0.04$). There were statistically significant differences between means within a group for: adult females, 35/36 °C ($p = 0.03$), 35/37 °C ($p = 0.0006$), 35/38 °C ($p = 0.02$), and 36/38 °C ($p = 0.046$); aged males, 35/36 °C ($p = 0.01$), 35/37 °C ($p = 0.01$), 35/38 °C ($p = 0.005$), 36/37 °C ($p = 0.03$), and 36/38 °C ($p = 0.008$); and aged females, 35/37 °C ($p = 0.01$), 35/38 °C ($p = 0.03$), and 36/37 °C ($p = 0.03$).

Temperature had an influence on average volumetric flow for the femoral vein only for aged animals $p < 0.001$ with statistically significant difference between means within a group for: aged males, 35/38 °C ($p = 0.003$), 36/38 °C ($p = 0.02$), and 37/38 °C ($p = 0.047$); and aged females, 35/37 °C ($p = 0.005$) and 35/38 °C ($p = 0.008$). Flow in the femoral artery linearly increased with temperature for adult females and aged males (slopes > 0, $p < 0.05$, $R^2 = 0.90$-0.95). Flow in the femoral vein linearly increased with temperature for aged females (slope > 0, $p = 0.01$, $R^2 = 0.98$). Comparing volumetric flow response to temperature, sex and age had an influence on relative response at the femoral artery ($p = 0.001$) and femoral vein ($p = 0.048$) with statistically significant differences between adult and aged animals at 36-37 °C interval for the femoral artery (adult male: 5.7 %/°C vs aged male: 92 %/°C, $p = 0.01$; adult female: 6.6 %/°C vs. aged female: 106 %/°C, $p = 0.002$).

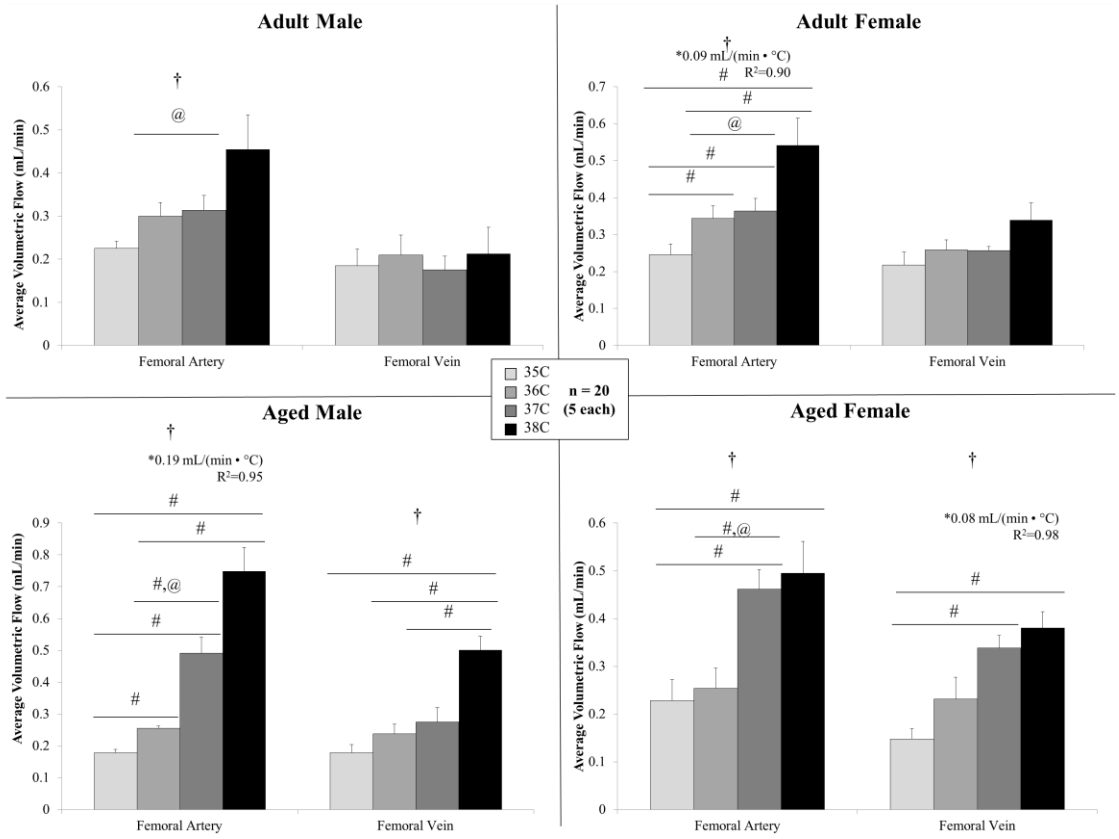

Figure 4.6 Volumetric flow averaged across the cardiac cycle (mean ± SEM) in the peripheral vessels for male and female, adult and aged mice (n=5 each) at core temperatures of 35, 36, 37, 38 °C.
Response varied by location and across sex and age. Significance set at $p < 0.05$: for temperature effect overall (†), pairwise comparisons between temperatures within a group(#), relative changes to same age group but opposite sex ($), relative changes to same sex but different age group (@), non-zero slope (*).

Velocity and volumetric flow differed between groups at each core body temperature

Comparison of normothermic metrics between groups is reported in Crouch 2019_pending. Comparing velocity average across the lumen (average across cardiac cycle, mean systolic, and mean diastolic) between groups at each temperature, 5 instances of differences between ages (male: 4, female: 1) and 10 instances of differences between sexes (adult: 3, aged: 7) were found. Comparing volumetric flow (average across cardiac cycle, mean systolic, and mean diastolic) between groups at each temperature, 28 instances of differences between ages (males only) and 9 instances of differences between sexes (adult: 2, aged: 7) were found.

4.5 Discussion

In agreement with previous studies, adult males [26], adult females and aged animals [25] showed a linear increase in heart rate with increasing temperature. Also from our previous study, although not statistically significant, there was a trend of increased stroke volume with increasing temperature 36.1 vs. 37.1 µL/beat, p = 0.5 [25]. With an increase in heart rate and either no change or an increase in stroke volume, cardiac output increases. Temperature-induced increases in cardiac output causes an increase in volumetric flow rate in the body, and may also be necessary to maintain blood pressure subsequent to large reductions in total vascular resistance resulting from cutaneous vasodilation [17].

Volumetric flow tended to increase in the torso and periphery with increased core body temperature

For nearly all vessels and aged groups (excluding carotid, suprarenal aorta and IVC in adult males), there was a trend of increased velocity and increased volumetric flow from 35 °C to 38 °C suggesting that increases in cardiac output, and thus increases in volumetric flow (Q), are mediated through both area changes [26] and velocity changes (Volumetric Flow=Area • Velocity). The increases in peripheral blood flow with temperature is consistent with the periphery and more superficial vessels being a site for heat exchange with the environment [17,19]. As discussed in Crouch et al., previous researchers suggested that with a decrease in core body temperature, core veins, such as the infrarenal IVC, vasodilate to keep blood centrally and away from the skin and periphery where it might lose heat to the environment [22,23,32]. In the infrarenal IVC our results illustrate the opposite [26] for all animal groups. This could result from reduced cardiac output [25] and aortic flow at lower temperatures. Our work further supports the theory that the enteric nervous system, coined the “second brain”, controls more

than just digestion and has large blood flow demands [33,34]. The gut's venous return occurs at a location superior to the infrarenal IVC, and for adult males, we see a slight increase in venous return flow in the suprarenal IVC with decreases in core temperature.

An increase in volumetric flow in this many locations without a subsequent decrease in flow in other large vessels, further suggests that the hemodynamically inactive blood volume (60-70% of total blood volume [35]) may decrease with increased core temperature and increased cardiac output leading to increases in bulk flow at all depths and, thus, greater heat exchange with the environment. The differences in volumetric flow at each location may be due, in part, to the ability of individual vessels to sense changes in heat and temperature thermosensitivity [11,23,36].

Sex and age mediate vascular response to temperature

Aged males showed the largest response in volumetric flow due to large increases in velocity in the infrarenal IVC, femoral artery, and femoral vein in contrast to adult males that had larger increases in vessel area that lead to increases in volumetric flow for those locations. This contrasts with our theory from Crouch et al. 2018 that predicted aged males had a diminished vascular response to temperature in the femoral location [25]. In Crouch et al., the resolution was limited in the periphery vessels and with the 3D acquisition were unable to plan slices perpendicular to the vessel. In this present study, we were able to plan slices perpendicular to the vessel to decrease partial-volume effects and quantify velocity as well as cross-sectional area. It appears, from this study, that aged animals are responding more than adult animals. However, it remains unclear if this larger response in the cardiovascular system contributes to the aged animals diminished thermoregulatory ability [11,37]. We hypothesize that if too much blood is shifted to the periphery, and thus superficial vessels, and the animals have a diminished

ability to remove that heat (in aged mice, too much fat [28] that is not as thermally conductive [38]), then this could lead to diminished heat removal. An increase in fat content and thermal insulation inside the body also lead to a slight increase in imaging time.

Although not apparent in average velocity or volumetric flow response (Figures 2, 5, and 6), aged females responded more to temperature than the other groups in the carotid, suprarenal aorta, and infrarenal vessels for mean systolic velocity suggesting differences in systolic function [39]. In agreement with Crouch et al., aged females in the periphery had similar response to adult females [25,40]. Differences in sex and age at normothermia are further discussed in Crouch_2019_pending.

Considerations for bioheat modeling

With changes in volume flow and/or velocity, heat transfer via convection would be hypothesized to change. Data presented here can direct where and when temperature-dependent changes in hemodynamics need to be considered when coupling CFD and bioheat modeling [21,45,46]. For example, the carotid is an anatomical location where you would not need to incorporate hemodynamic changes due temperature. By contrast, velocity and volumetric changes would be pertinent for the infrarenal and peripheral vessels aorta. Differences in mean systolic/diastolic and peak velocity (Table 4.1) are also important considerations, not only for heat transfer, but also because of their influence on wall shear stress, a biomarkers for cardiovascular health. This work provides further evidence of the effects of sex and age on CV responses, and these differences should be incorporated into models.

Analogy between exercise and temperature

The healthy mammalian cardiovascular system is sensitive and highly adaptive as evident in our study because we are able to quantify not insubstantial cardiovascular changes despite

relatively small changes in body temperature. For this study, core body temperature ranged from marginally hypothermic (35°C) to marginally hyperthermic (38°C), and yet we see volumetric changes of the vasculature of over 30% in core vessels. For further context, we compare our results to another common cardiovascular stressor, exercise. The active homeostasis system responds differently at rest compared to during a bout of exercise. In a human study, there was a 67% change in volume flow rate in the aorta, and, in comparison, we quantified an increase of 17% volume flow rate in the infrarenal aorta for adult males from 35 to 38 °C[41]. For the peripheral vessels during exercise, there was a 50% increase in area for the anterior tibial artery after acute exercise, and we see a 100% increase in volumetric the femoral artery from 35 to 38 °C [42]. Thermoregulation has a large impact on the cardiovascular system, and we hypothesize temperature will compound the stress of exercise due to the temperature gradients addressed in this work [2,43,44]. Heat transfer by flowing blood is the most important pathway for heat-exchange in the body, and this is particularly evident during exercise because of the conflicting demand for blood [43].

Limitations

As discussed in Crouch_2019_pending, the non-circular geometries and vessel curvature in the veins made image planning perpendicular to the vessel more challenging, and complex vessel curvature could introduce partial volume effect biases. However, slice planning, optimized in previous work with parameters for slower blood flow for anatomical landmarks, provided reproducible planning and slices were perpendicular to flow [47]. We also must use anesthetized mice for imaging, leading to a slight reduction in cardiac output under anesthesia, but heart rates are closer to those recorded in conscious mice using isoflurane [29]. For the isoflurane control in adult males, volumetric flow did slightly increase in the infrarenal IVC, femoral artery and vein:

6.9, 7.0, and 0.9 %/30 min, respectively.; however, compared to the increase with temperature 14.9, 35.3, and 7.2 %/°C, the results are minimal and are not statistically significant different between 30 minute intervals.

4.6 Conclusion

Overall, the results demonstrate that there are differences in velocity and volumetric flow response to temperature, and this response varies across sex and age. With this work, we have been able to distinguish contributions from changes in area and blood velocity which would be important for more accurate bioheat modeling. In aged animals, flow increases were driven primarily by velocity changes suggesting a diminished ability for structural changes in area. These changes in blood velocity are also likely causing changes in wall shear stress which is an important metric in cardiovascular disease progression.

To our knowledge, this is the first time that the effect of core body temperature on velocity and volumetric blood flow of the murine arterial and venous systems has been studied non-invasively, at multiple locations across age and sex. Age, in particular, had a significant impact on hemodynamic response. Future work incorporating pressure measurements and/or computational fluid dynamics (CFD) would be useful for examining stress-strain properties and luminal biomechanical forces such as wall shear stress in vivo. Our data can provide physiologically-relevant parameters to CFD models and provide baseline data for the healthy murine vasculature to use as a benchmark for investigation of a variety of physiological and pathophysiological conditions of the cardiovascular system. This chapter concludes our work on the effect of temperature on the CV system. In the subsequent chapter, we combine temperature and a CV stressor and quantified response.

4.7 References

[1] van der Zee J. Heating the patient: a promising approach? Ann. Oncol. Off. J. Eur. Soc. Med. Oncol. 2002;13:1173–1184.

[2] Tucker R, Rauch L, Harley YR, et al. Impaired exercise performance in the heat is associated with an anticipatory reduction in skeletal muscle recruitment. Pflugers Arch. - Eur. J. Physiol. 2004;448:422–430.

[3] Stewart IB, Rojek AM, Hunt AP. Heat Strain During Explosive Ordnance Disposal. Mil. Med. 2011;176:959–963.

[4] Polderman KH. Application of therapeutic hypothermia in the intensive care unit. Intensive Care Med. 2004;30:757–769.

[5] Centers for Disease Control and Prevention U. Hypothermia-related deaths--United States, 1999-2002 and 2005. MMWR Morb. Mortal. Wkly. Rep. 2006;55:282–284.

[6] Fiala D, Havenith G. Modelling Human Heat Transfer and Temperature Regulation. Springer International Publishing; 2015. p. 265–302.

[7] Brody GM. Hyperthermia and hypothermia in the elderly. Clin. Geriatr. Med. 1994;10:213–229.

[8] Collins KJ, Exton-Smith AN. 1983 Henderson Award Lecture. Thermal homeostasis in old age. J. Am. Geriatr. Soc. 1983;31:519–524.

[9] Noe RS, Jin JO, Wolkin AF. Exposure to Natural Cold and Heat: Hypothermia and Hyperthermia Medicare Claims, United States, 2004–2005. Am. J. Public Health. 2012;102:e11–e18.

[10] McDonald RB, Day C, Carlson K, et al. Effect of age and gender on thermoregulation. Am. J. Physiol. 1989;257:R700-4.

[11] Van Someren EJW. Chapter 22 – Age-Related Changes in Thermoreception and Thermoregulation. Handb. Biol. Aging. 2011. p. 463–478.

[12] Chen CH, Nakayama M, Nevo E, et al. Coupled systolic-ventricular and vascular stiffening with age: implications for pressure regulation and cardiac reserve in the elderly. J. Am. Coll. Cardiol. 1998;32:1221–1227.

[13] Minson CT, Wladkowski SL, Cardell AF, et al. Age alters the cardiovascular response to direct passive heating. J. Appl. Physiol. 1998;84:1323–1332.

[14] Nybo L, Møller K, Volianitis S, et al. Effects of hyperthermia on cerebral blood flow and metabolism during prolonged exercise in humans. J. Appl. Physiol. 2002;93:58–64.

[15] Bain AR, Nybo L, Ainslie PN. Cerebral Vascular Control and Metabolism in Heat Stress. Compr. Physiol. Hoboken, NJ, USA: John Wiley & Sons, Inc.; 2015. p. 1345–1380.

[16] Qian S, Jiang Q, Liu K, et al. Effects of short-term environmental hyperthermia on patterns of cerebral blood flow. Physiol. Behav. 2014;128:99–107.

[17] Crandall CG. Heat stress and baroreflex regulation of blood pressure. Med. Sci. Sports Exerc. 2008;40:2063–2070.

[18] Siddiqui A. Effects of Vasodilation and Arterial Resistance on Cardiac Output. J. Clin. Exp. Cardiolog. 2011;02.

[19] Kuhn LA, Turner JK. Alterations in Pulmonary and Peripheral Vascular Resistance in Immersion Hypothermia. Circ. Res. 1959;7:366–374.

[20] Wissler EH. Pennes' 1948 paper revisited. J. Appl. Physiol. 1998;85:35–41.

[21] Bhowmik A, Singh R, Repaka R, et al. Conventional and newly developed bioheat transport models in vascularized tissues: A review. J. Therm. Biol. 2013;38:107–125.

[22] Shepherd J, Vanhoutte P. Veins and their control. London-Philadelphia: W.B. Saunders Co.; 1975.

[23] Flavahan N, Vanhoutte P. Thermosensitivity of cutaneous and deep veins. Phlebology. 1988;3:41–45.

[24] Vanhoutte P. Return circulation and norepinephrine: an update. Paris; 1991.

[25] Crouch AC, Manders AB, Cao AA, et al. Cross-sectional area of the murine aorta linearly increases with increasing core body temperature. Int. J. Hyperth. 2018;34:1121–1133.

[26] Crouch AC, Scheven UM, Greve JM. Cross-sectional areas of deep/core veins are smaller at lower core body temperatures. Physiol. Rep. 2018;6:e13839.

[27] Leon LR. The use of gene knockout mice in thermoregulation studies. J. Therm. Biol. 2005;30:273–288.

[28] FLURKEY K, MCURRER J, HARRISON D. Mouse Models in Aging Research. Mouse Biomed. Res. Elsevier; 2007. p. 637–672.

[29] Constantinides C, Mean R, Janssen BJ. Effects of isoflurane anesthesia on the cardiovascular function of the C57BL/6 mouse. ILAR J. 2011;52:e21-31.

[30] Teng D, Hornberger TA. Optimal Temperature for Hypothermia Intervention in Mouse Model of Skeletal Muscle Ischemia Reperfusion Injury. Cell. Mol. Bioeng. 2011;4:717–723.

[31] Duhan V, Joshi N, Nagarajan P, et al. Protocol for long duration whole body hyperthermia in mice. J. Vis. Exp. 2012;e3801.

[32] Shepherd J, Vanhoutte P. The Human Cardiovascular System. Facts and Concepts. New York: Raven Press; 1979.

[33] Gershon M. The Second Brain : The Scientific Basis of Gut Instinct and a Groundbreaking New Understanding of Nervous Disorders of the Stomach and Intestines. New York: HarperCollins; 1998.

[34] Carabotti M, Scirocco A, Maselli MA, et al. The gut-brain axis: interactions between enteric microbiota, central and enteric nervous systems. Ann. Gastroenterol. 2015;28:203–209.

[35] Greenway C V., Lautt WW. Blood volume, the venous system, preload, and cardiac output. Can. J. Physiol. Pharmacol. 1986;64:383–387.

[36] BLIGH J. THE THERMOSENSITIVITY OF THE HYPOTHALAMUS AND THERMOREGULATION IN MAMMALS. Biol. Rev. 1966;41:317–365.

[37] Rooke GA, Savage M V, Brengelmann GL. Maximal skin blood flow is decreased in elderly men. J. Appl. Physiol. 1994;77:11–14.

[38] Stolwijk JAJ, Hardy JD. Section 9: Reaction to Environmental Agents. Handb. Physiol. Bethesda, MD: American Physiological Society; 1977.

[39] Carroll JD, Carroll EP, Feldman T, et al. Sex-Associated Differences in Left Ventricular Function in Aortic Stenosis of the Elderly. 1992.

[40] Drinkwater BL, Bedi JF, Loucks AB, et al. Sweating sensitivity and capacity of women in relation to age. J. Appl. Physiol. 1982;53:671–676.

[41] Weber TF, von Tengg-Kobligk H, Kopp-Schneider A, et al. High-resolution phase-contrast MRI of aortic and pulmonary blood flow during rest and physical exercise using a MRI compatible bicycle ergometer. Eur. J. Radiol. 2011;80:103–108.

[42] Meyer RA, Foley JM, Harkema SJ, et al. Magnetic resonance measurement of blood flow in peripheral vessels after acute exercise. Magn. Reson. Imaging. 1993;11:1085–1092.

[43] Nybo L, Secher NH, Nielsen B. Inadequate heat release from the human brain during prolonged exercise with hyperthermia. J. Physiol. 2002;545:697–704.

[44] González-Alonso J. Human thermoregulation and the cardiovascular system. Exp. Physiol. 2012;97:340–346.

[45] Coccarelli A, Boileau E, Parthimos D, et al. An advanced computational bioheat transfer model for a human body with an embedded systemic circulation. Biomech. Model. Mechanobiol. 2016;15:1173–1190.

[46] Shitzer A, Stroschein L a, Vital P, et al. Numerical analysis of an extremity in a cold environment including countercurrent arterio-venous heat exchange. J. Biomech. Eng. 1997;119:179–186.

[47] Palmer OR, Chiu CB, Cao A, et al. In vivo characterization of the murine venous system before and during dobutamine stimulation: implications for preclinical models of venous disease. Ann. Anat. - Anat. Anzeiger. 2017;214:43–52.

Chapter 5
Effect of temperature and adrenergic stress on arterial system

5.1 Abstract

***Purpose*:** Because of the importance of adrenoreceptors in regulating the cardiovascular system and the role of the CV system in thermoregulation, understanding the response to these two stressors is of interest. The purpose of this study was to assess changes of arterial geometry and function in vivo during thermal and β-adrenergic stress induced in mice and quantified by MRI.

Methods: Male mice were anesthetized and imaged at 7T. Anatomical and functional data were acquired from the neck (carotid artery), torso (suprarenal and infrarenal aorta and iliac artery), and periphery (femoral artery). Intravenous dobutamine (tail vein catheter, 40 μg/kg/min, 0.12 mL/hr) was used as β-adrenergic stressor. Baseline and dobutamine data were acquired at minimally hypothermic (35°C) and minimally hyperthermic (38°C) core temperatures. Cross-sectional vessel area and maximum cyclic strain were measured across the cardiac cycle.

Results: Vascular response varied by location and by core temperature. For minimally hypothermic conditions (35°C), average, maximum, and minimum areas decreased with dobutamine only at the suprarenal aorta (avg: -17.9%, max: -13.5%, min: -21.4%). For minimally hyperthermic conditions (38°C), vessel areas decreased between baseline and dobutamine at the carotid (avg: -19.6%, max: -15.5%, min: -19.3%) and suprarenal (avg: -24.2%, max: -17.4%, min: -17.3%); whereas, only the minimum vessel area decreased for the iliac (min:

-14.4%). Maximum cyclic strain increased between baseline and dobutamine at the iliac artery for both conditions and at the suprarenal aorta at hyperthermic conditions.

Conclusion: At hypothermic conditions the vessel area response to dobutamine is diminished compared to hyperthermic conditions where the vessel area response mimics normothermic dobutamine conditions. The varied response has implications in critical care treatment.

5.2 Introduction

Various pathological conditions and treatments, including sepsis [6] and the treatment of cardiogenic shock [7], can cause core body temperature to deviate from normothermia. Clinically, dobutamine is used in critical care for acute treatment of congestive heart failure, cardiogenic and septic shock, and as a pharmacological surrogate to exercise [8–10]. Dobutamine's primary mechanism is direct stimulation of β1-adrenergic receptors thus increasing cardiac contractility and output, with more mild β2 stimulation resulting in peripheral vasodilation [11].

To improve parameterization and validation of mathematical and computational models [12,13], Chapters 2-4 focused on geometric (cross-sectional area),functional (Green-Lagrange circumferential strain), and hemodynamic (velocity and volumetric flow) changes in core arteries (Chapter 2) and veins (Chapter 3) due to increases in core temperature [14,15]. Other work in the Greve lab quantified changes in arterial and venous mechanics due to the administration of dobutamine [16,17]. Combining these two cardiac stressors is of interest because of the differential response of core vasculature to changing temperature or administering dobutamine alone. Temperature increased area [15], while dobutamine decreased area and increased strain [17]. Researchers are also interested in the combined effects of temperature and dobutamine

because of the detrimental consequences of decreased peripheral resistance after dobutamine administration in hypothermic patients [18,19].

Preclinical animal models play a vital role in the advancement of therapeutic development and optimization of current treatment paradigms. It is important to understand the results of cardiac stressors in the healthy murine condition before studying their effects in preclinical CV disease models. With magnetic resonance imaging (MRI), core vasculature geometry and function can be investigated non-invasively due to high spatial and temporal resolution. The purpose of this study was to assess physiological changes of arterial geometry and function in vivo during thermal and β-adrenergic stress via dobutamine using murine models and MRI. MRI data were acquired under hypothermic (35 °C) and hyperthermic (38 °C) conditions at the carotid artery, suprarenal and infrarenal aorta, iliac artery, and femoral artery of C57BL/6 male mice, prior to and during dobutamine infusion.

We hypothesized that: 1) at hypothermic conditions (35 °C), dobutamine would not elicit changes in cross-sectional area and strain, due to temperature-induced vasoconstriction; and, 2) at hyperthermic conditions (38 °C) cross-sectional area would decrease and strain would increase, mirroring dobutamine responses at normothermic conditions (37 °C). To our knowledge, these data are the first to empirically quantify the spatially and temporally resolved response of core vasculature to dobutamine at hypo- and hyper-thermic conditions in vivo from head-to-toe.

5.3 Methods

All experiments were carried out with local Institutional Animal Care and Use Committee approval. Animals were housed in a room with temperature (22°C ± 2°C) and humidity (~27%) control with an alternate 12-hour light/dark cycle.

Healthy adult male (13- to 15-weeks-old, ~20 human years [20]) C57BL/6 mice, purchased from Charles River Laboratory, were used in this study. Male mice were chosen in this initial study combining hypo- and hyper-thermic states with dobutamine stimulation because this sex showed the smallest response to increases in core temperature in the aorta in our previous work in Chapter 2 (male: 0.019 $mm^2/°C$ vs. female: 0.024 $mm^2/°C$, [14]). A dobutamine dosage of 40 µg/kg of body weight (Hospira, Inc., Lake Forest, IL) was prescribed at an infusion rate of 2 µL/min (Cole Parmer, Vernon Hills, IL) and pre-mixed assuming an average murine body weight of 25 g (actual mean and SEM of our animals was 26.4±0.7 g). Prior to imaging, a tail vein catheter was placed using a 30-gauge needle, connected to an ~5 cm length of PE10 tubing prefilled with saline, followed by the dobutamine solution [17]. Mice were anesthetized with 1.25-2% isoflurane in 1 L/min of oxygen [21]. Animals were imaged in the supine position at 7T field strength using a Direct Drive console (Agilent Technologies, Santa Clara, CA) and a 40 mm inner diameter transmit-receive volume coil (Morris Instruments, Ontario, Canada).

Figure 5.1 illustrates the locations investigated in this study. CINE data were acquired in the neck (carotid artery), torso (suprarenal and infrarenal aorta, iliac artery), and periphery (femoral artery). The two target core temperatures were minimally hypothermic (35 °C) and minimally hyperthermic (38 °C), controlled within ± 0.2 °C using forced convection [14]. These temperatures were selected to avoid pathological changes [22,23]. Baseline and dobutamine data were acquired at all five locations for a given animal in two separate imaging sessions, corresponding to the two target core temperatures. Heart rate (HR) and respiration were monitored (SA Instruments, Stony Brook, NY). After acquiring baseline data at all five locations for the given target core temperature, dobutamine infusion was initiated. After a plateau in

increased HR was achieved, slices planned at each of the five locations were acquired a second time during the infusion of dobutamine (referred to as 'dobutamine' in this paper). The total imaging time for each animal was approximately 90 minutes with approximately 60 minutes of dobutamine infusion (~120 μL infused). Time to reach maximum heart rate plateau was 12 min of dobutamine infusion for hypothermic state compared to 19 minutes for hyperthermic state. In a previous study at normothermic conditions, approximately the same volume of saline was infused as a control and demonstrated minimal changes to arterial area or strain due to these small increases in blood volume [17].

Sagittal 2D and axial 3D acquisitions were used to plan slices perpendicular to the carotid artery. Coronal 2D and sagittal 3D acquisitions were used to plan slices perpendicular to the aorta, iliac and femoral arteries. A cardiac-gated and velocity compensated 2D CINE sequence with 16 frames was used to acquire data at each location. Parameters were: TR/TE ~120/4 ms depending on HR, flip angle (α) 60^{o}, FOV $(20\ mm)^2$, matrix 256^2 zero-filled to 512^2, zero-filled in-plane resolution $(39\ \mu m)^2$, slice thickness 1 mm, NEX 6. The CINE images were analyzed for vessel cross-sectional area and circumferential cyclic strain (Equation 6) using an in-house semi-automated process previously described on page 22.

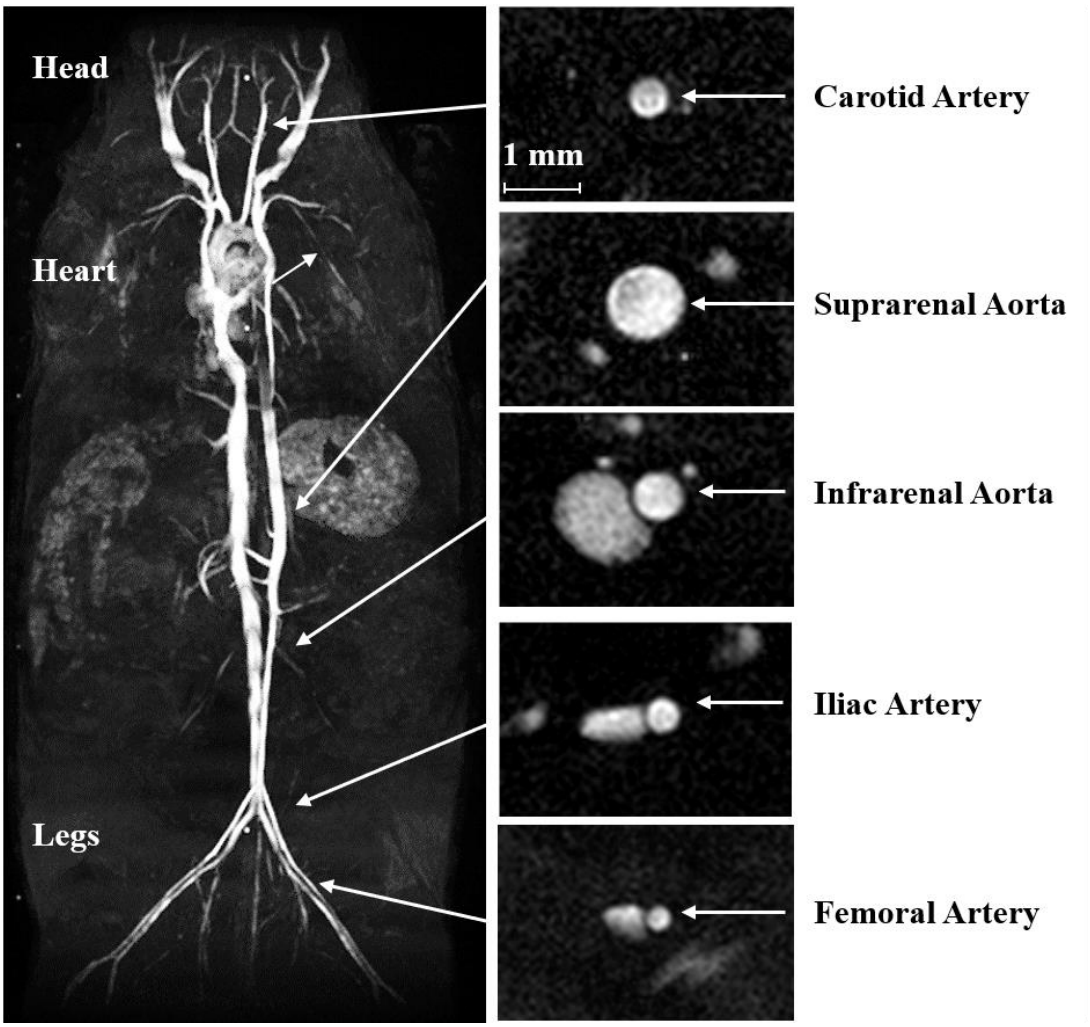

Figure 5.1 Coronal MIP and cross-sectional view of the arteries illustrating arterial locations where imaging data were acquired and quantified.

Statistical Analysis

Data are reported and plotted as mean ± standard error (SEM). To test if areas (average, maximum, minimum) and maximum cyclic strain differed significantly between baseline and dobutamine at a given target core temperature and location, a two-tailed paired t-test was used. To test if the response to dobutamine (average_areadobutamine – average_areabaseline) differed between the two temperatures for a given location, a two-tailed paired t-test was used. Two methods were used to compare the response at different locations. The response at different locations was compared using two-way ANOVA with Tukey's post hoc test. The relative

response ((average_areadobutamine – average_areabaseline) /average_areabaseline) was calculated to account for size-differences between vessels and was compared between locations using two-way ANOVA with Tukey's post hoc test. Significance was set at $p < 0.05$.

5.4 Results

Heart rate (HR)

Dobutamine resulted in an elevated HR in all mice at 35 °C (baseline: 419 ± 6 to dobutamine: 541 ± 5 beats per minute, $p < 0.0001$) and at 38 °C (baseline: 482 ± 20 to dobutamine: 594 ± 9 beats per minute, $p = 0.0003$). HR was higher at 38 °C compared to 35 °C for both baseline ($p = 0.002$) and dobutamine ($p = 0.007$).

Effect of dobutamine at different core temperatures, within a location

Baseline vs. Dobutamine during hypothermic or hyperthermic conditions

The first comparison was baseline versus dobutamine for vessel area (average, maximum, minimum) and maximum cyclic strain. Statistically significant results for cross-sectional area across the cardiac cycle at baseline and during dobutamine for 35 and 38 °C are shown in Figure 5.2. For the hypothermic condition (35 °C), dobutamine resulted in a decrease in vessel area in the suprarenal aorta by 17.9 ± 1.8% ($p < 0.0001$), 13.5 ± 3.3% ($p = 0.005$), and 21.4 ± 5.2% ($p = 0.006$) for average, maximum, and minimum areas, respectively. For the hyperthermic condition (38 °C), dobutamine resulted in a decrease in vessel area in the carotid by 19.4 ± 5.7% ($p = 0.006$), 15.5 ± 6.7% ($p = 0.04$), and 19.6 ± 4.2% ($p = 0.01$) for average, maximum, and minimum areas, respectively. In the suprarenal aorta, the vessel area decreased by 24.2 ± 2.8% ($p = 0.0002$), 17.4 ± 4.4% ($p = 0.005$), and 33.6 ± 2.2% ($p < 0.0001$) for average, maximum and

minimum areas, respectively. In the iliac artery, the vessel area decreased by 14.4 ± 5.2% (p = 0.03) for the minimum area.

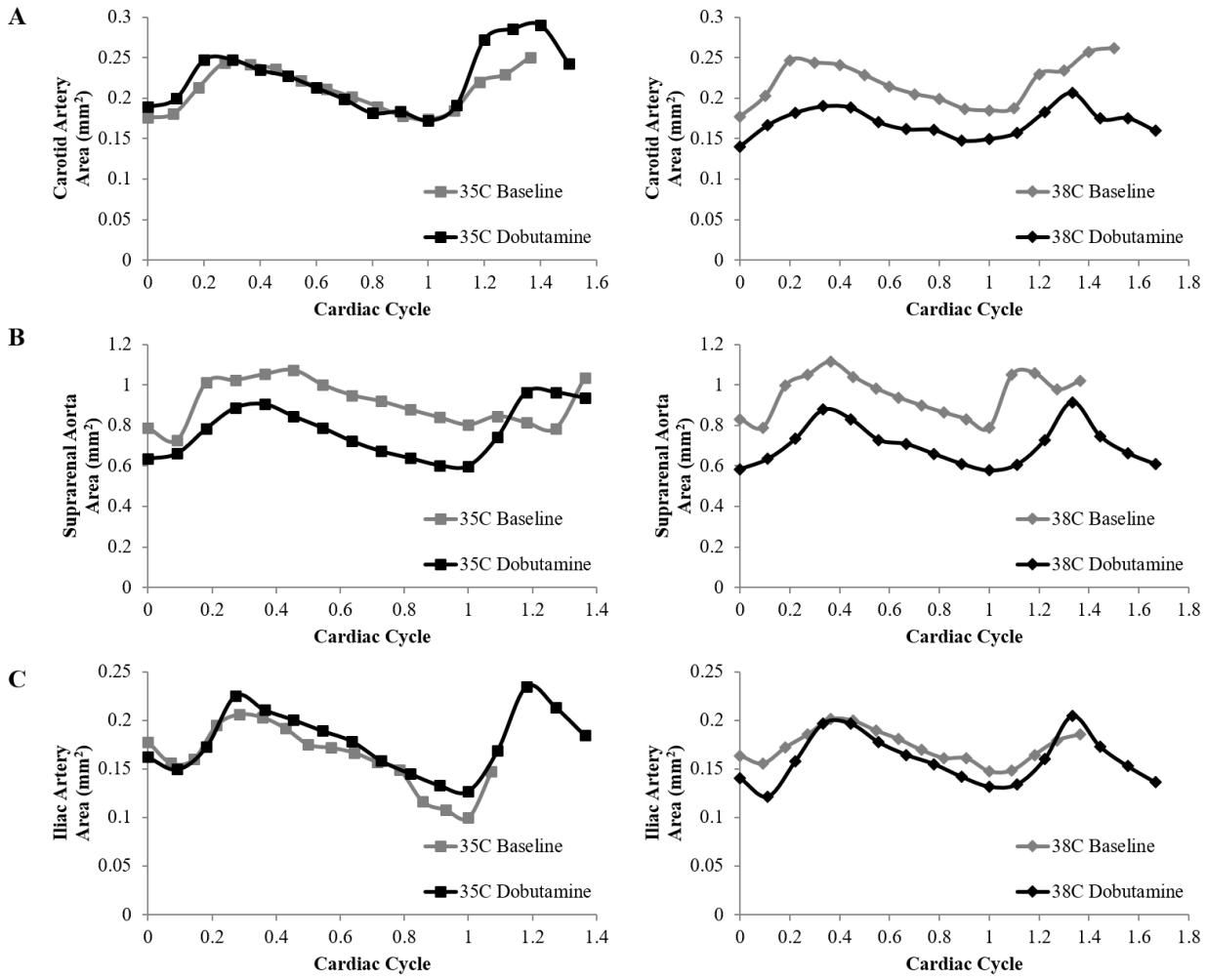

Figure 5.2 Cross-sectional area across the cardiac cycle for the (A) carotid artery, (B) suprarenal aorta, and (C) iliac artery at 35 and 38 °C (left and right) for baseline and dobutamine.

Statistically significant results for maximum cyclic strain at baseline and during dobutamine for 35 and 38 °C are shown in Figure 5.3. For the hypothermic condition (35 °C), maximum cyclic strain increased with dobutamine in the iliac artery 20.3 ± 4.5% (p = 0.003). For the hyperthermic condition (38 °C), maximum cyclic strain increased with dobutamine in the suprarenal artery by 21.0 ± 3.6% (p = 0.0006) and in the iliac artery by 17.3 ± 5.5% (p = 0.02).

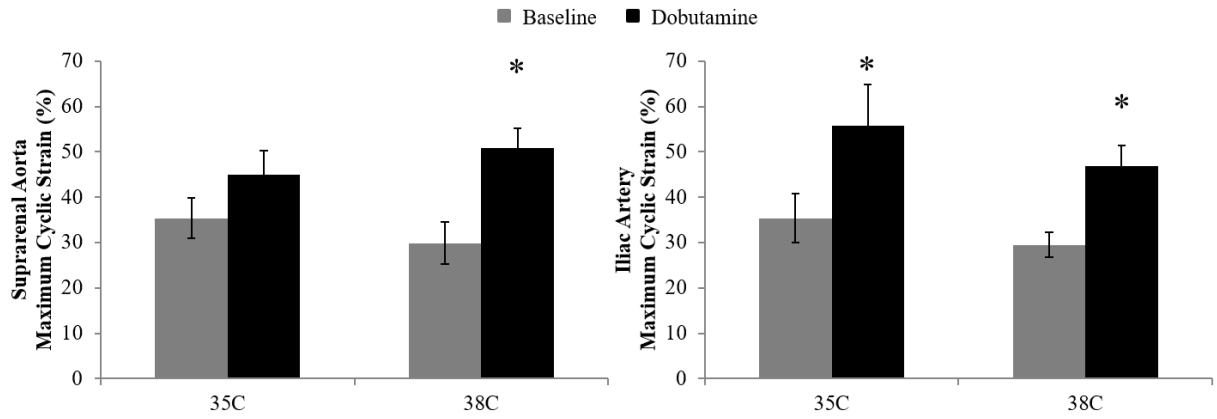

Figure 5.3 Maximum cyclic strain across the cardiac cycle for suprarenal aorta (left) and iliac artery (right) at baseline and dobutamine for two core body temperatures 35 and 38 °C.

Comparison of the response during hypothermic vs. hyperthermic conditions

The response (dobutamine-baseline) at 35 °C was compared to the response at 38 °C for vessel areas and strain. The change in areas for all locations at 35 and 38 °C is shown from head-to-toe in Figure 5.4. The response to dobutamine as measured by area varied between the temperatures. Statistically significant differences were seen at the carotid artery and suprarenal aorta. The change in carotid average area at 35 °C was an increase of 0.01± 0.01 mm^2 compared to a decrease of -0.04 ± 0.01 mm^2 ($p = 0.005$) at 38 °C. The change in carotid maximum area at 35 °C was an increase of 0.02± 0.01 mm^2 compared to a decrease of -0.04 ± 0.01 mm^2 ($p = 0.004$) at 38 °C. The change in suprarenal aorta minimum area at 35 °C was a decrease of -0.16 ± 0.04 mm^2 compared to a decrease of -0.25 ± 0.03 mm^2 ($p = 0.03$) at 38 °C.

The maximum cyclic strain response for all locations at 35 and 38 °C is shown in Figure 5.5. Maximum cyclic strain tended to increase with dobutamine at all locations and for both temperatures. However, there were no statistically significant differences when comparing the response at 35 to that at 38 °C.

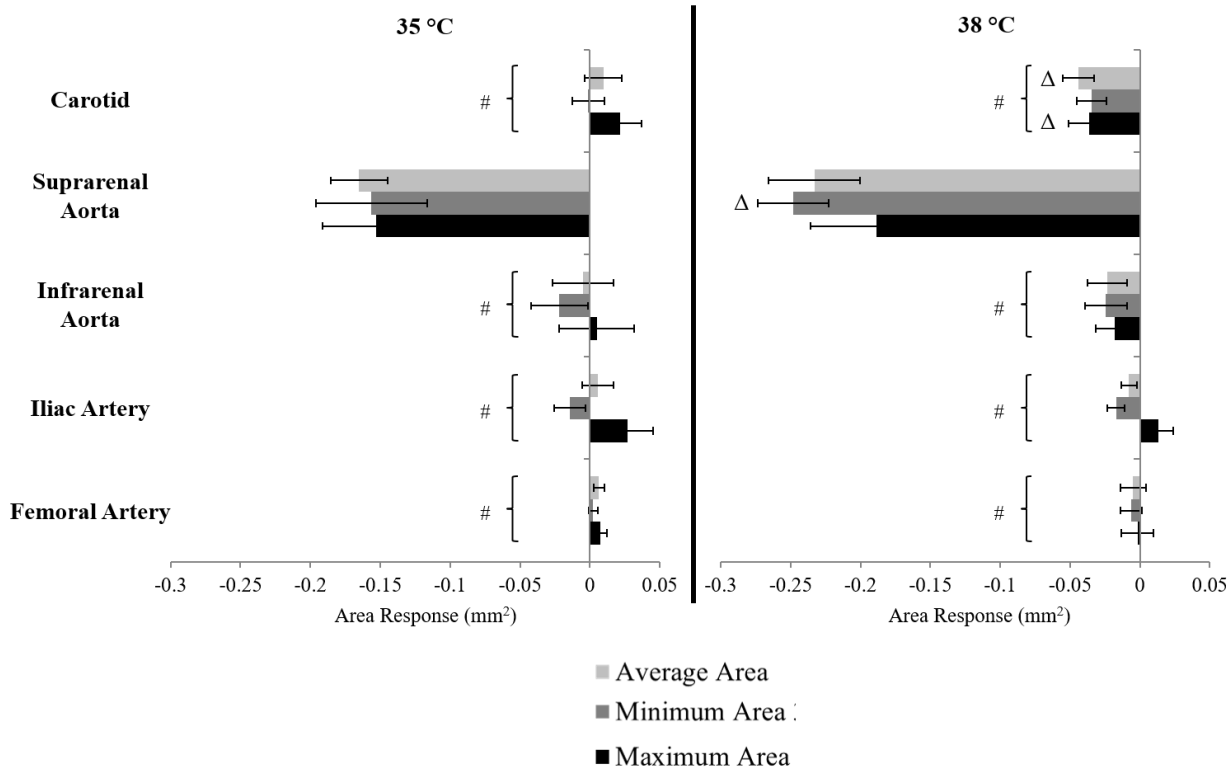

Figure 5.4 The response to dobutamine (dobutamine – baseline) for average, minimum, and maximum areas at 35 °C (left) and 38 °C (right).

Effect of dobutamine at different core temperatures and across locations

To determine the effect of location on overall response, two comparisons were made: absolute response and relative response. For the absolute difference in response (Figure 5.4), changes in area were dependent on location for average ($p = 0.0001/0.005$; location/temp), maximum ($p = 0.0001$/N.S.), and minimum ($p = 0.0001/0.007$) areas. For the hypothermic condition (35 °C), pairwise comparisons were significantly different ($p < 0.0001$, all) between the suprarenal aorta (avg: -0.17 ± 0.02, max: -0.15 ± 0.04, min: -0.16 ± 0.04 mm^2) and the carotid (0.01 ± 0.01, 0.02 ± 0.01, -0.001 ± 0.01 mm^2), infrarenal aorta (-0.005 ± 0.02, $0.005 \pm$

0.03, -0.02 ± 0.02 mm^2), iliac artery (0.006 ± 0.01, 0.03 ± 0.01, -0.01 ± 0.01 mm^2), and femoral artery (0.006 ± 0.004, 0.007 ± 0.005, -0.002 ± 0.003 mm^2). For the hyperthermic condition (38 °C), pairwise comparisons were also significantly different ($p < 0.001$, all) between the suprarenal aorta (avg: -0.23 ± 0.03, max: -0.19 ± 0.04, min: -0.25 ± 0.02 mm^2) and the carotid (-0.04 ± 0.01, -0.04 ± 0.01, -0.03 ± 0.01 mm^2), infrarenal aorta (-0.023 ± 0.01, -0.02 ± 0.01, -0.02 ± 0.01 mm^2), iliac artery (-0.008 ± 0.006,0.01 ± 0.01, -0.02 ± 0.006 mm^2), and femoral artery (-0.005 ± 0.009, -0.002 ± 0.01,-0.006 ± 0.008 mm^2).

Strain responses were not dependent on location (Figure 5.5). However, the vessels varied in the magnitude of the change between 35 and 38 °C. For example, the carotid, suprarenal aorta, and femoral artery had a larger increase during hyperthermic conditions, while the infrarenal aorta and iliac artery had a smaller increase.

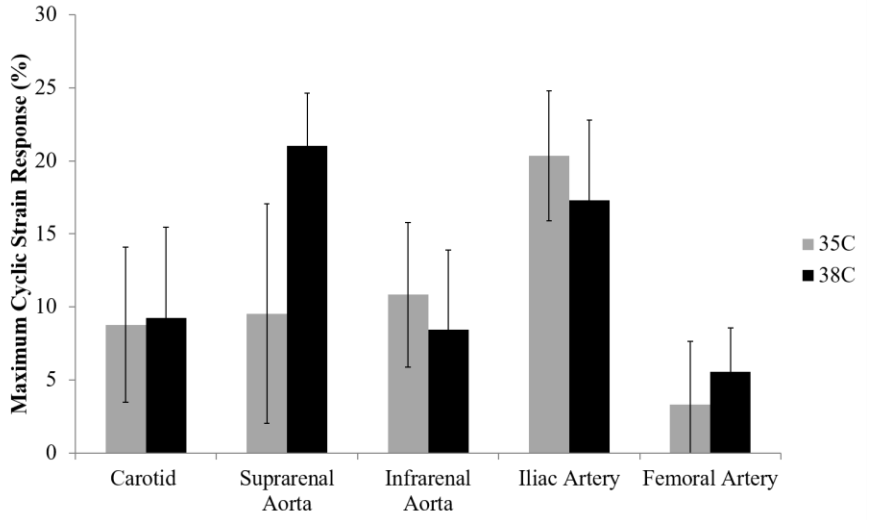

Figure 5.5 The response to dobutamine (dobutamine – baseline) for maximum cyclic strain at 35 and 38 °C.

Size-differences between the vessels were accounted for by calculating the relative response. The relative changes for average, maximum, and minimum areas for all locations at 35 and 38 °C are shown in Figure 5.6. All relative changes in area were dependent on location and temperature for average ($p = 0.004/0.003$; location/temp), maximum ($p = 0.02/0.009$), and

minimum (p = 0.004/0.01) areas. For average area, pairwise comparisons were significantly different at 35 °C between the suprarenal aorta and iliac artery (-0.18 vs. 0.07, p = 0.03) and the suprarenal aorta and femoral artery (-0.18 vs. -0.09, p = 0.003). For minimum area, significant differences occurred at 35 °C between the suprarenal aorta and femoral artery (-0.21 vs. 0.14, p = 0.02). For maximum area, significant differences occurred at 35 °C between the suprarenal aorta and iliac artery (-0.14 vs. 0.17, p = 0.03).

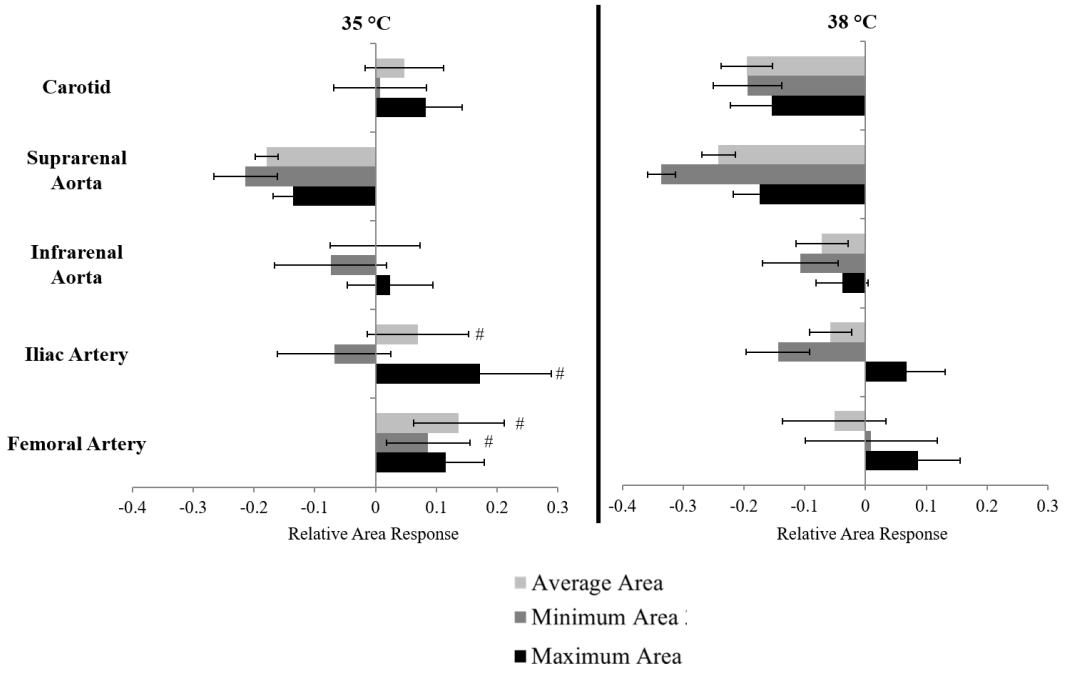

Figure 5.6 The relative response to dobutamine for average, minimum, and maximum areas at 35 °C (left) and 38 °C (right).

5.5 Discussion

Two cardiovascular stressors, deviations from normothermia and dobutamine administration, have been combined in this study. Because of the importance of adrenoreceptors in regulating the cardiovascular system and the role of the CV system in thermoregulation, understanding the response to these two stressors is of interest. To our knowledge, these data are the first to empirically quantify the spatially and temporally resolved response of arterial vasculature to a pharmacological stressor at different core body temperatures.

Previous work by Crouch et al. showed that under hypothermic conditions (35 °C) the average area was significantly smaller in the infrarenal aorta and femoral artery by -12% and -72%, respectively, and larger for hyperthermic conditions (38 °C) by 1.3 and 6.0%, respectively, compared to normothermic conditions (37 °C) [15]. While cross-sectional area tended to increase with temperature, with larger changes occurring inferiorly, previous work by Castle et al. showed that cross-sectional area at normothermic conditions decreased with dobutamine for the carotid, suprarenal and infrarenal aorta, and iliac artery by -19%, -16%, -14%, and -12%, respectively, with larger changes occurring superiorly in the body [17]. For either increases in core temperature or dobutamine administration, the end-diastolic/minimum areas experienced larger changes than the peak-systolic/maximum areas, resulting in changes in maximum cyclic strain. Temperature's effect on strain varied by location with a general overall decrease in strain from 35 to 38 °C [14,15], whereas dobutamine caused an increase in maximum cyclic strain for all vessels [17].

In this study, the two cardiac stressors, core temperature variations and dobutamine administration, were combined. For both temperature conditions, dobutamine resulted in elevated HR consistent with previous findings [24,25]. The hypothermic condition resulted in a slightly larger increase in HR of 29% compared to an increase of 23% in the hyperthermic condition, likely due to an increase in baseline heart rate at 38 °C [14,26]. Although not statistically significant for all vessels, dobutamine-induced decreases in area were more consistent across location during hyperthermic conditions. The suprarenal aorta exhibited distinct and greater decreases during both hypothermic and hyperthermic states. The unique response of the suprarenal aorta may be due to its position as the most superior vessel located below the heart. Another factor that may be influencing results at the suprarenal aorta is the influence of the

gut. Interest in the brain-gut connection has grown after research has revealed that the enteric nervous system, coined the “second brain”, controls more than just digestion [27,28]. Due to the large nervous network, this location may be more susceptible to dobutamine. Further studies in the connection of the enteric nervous system and thermoregulation and dobutamine could provide interesting results.

Data presented here show that the vessel area response to dobutamine during minimally hyperthermic conditions mimics previously published data acquired during normothermic conditions. For the carotid artery, the relative area response was nearly identical (-20% at 38 °C vs. -19% at 37 °C, respectively). At the suprarenal location, the relative area response was larger during hyperthermic conditions (-24% vs. -16%, at 38 and 37 °C, respectively). For the infrarenal and iliac locations, the relative area response was smaller (infrarenal: -7% at 38 °C vs. -14% at 37 °C; iliac: -6% at 38 °C vs. -12% at 37 °C). Dobutamine-induced decreases in average cross-sectional area of the core arteries during normothermic conditions are consistent with redistribution of blood to the skin/periphery due to dobutamine’s vasodilatory effects [17,18]. Conversely, cross-sectional area of the core arteries increases with increasing temperature, paralleling hyperthermia-induced vasodilation known to occur in the skin/periphery [14,15]. Comparing these recently published results with data presented here, one can begin to estimate the seemingly opposing factors of changes in core temperature and dobutamine administration on core arteries. For example, Crouch et al. quantified an ~4%, 1%, and 6% increase in area for the carotid artery, infrarenal aorta, and femoral artery, respectively, when core temperature is increased from 37 to 38 °C [15]. Here, we show a ~20%, 7%, and 5% decrease in area for the same vessels, respectively, when dobutamine is applied at 38 °C. This implies that the vasodilatory effects of dobutamine on downstream vasculature outweigh the local effects of

temperature. This balance becomes less evident in the more superficial vessels (i.e. the femoral artery), which could be related to fewer vessels downstream to be dilated by dobutamine and/or the fact that these vessels, themselves, play a larger role in heat exchange with the environment.

Dobutamine administration during hypothermia resulted in smaller or no decreases in area for the carotid, suprarenal, and infrarenal aorta compared to hyperthermic conditions. Crouch et al. also demonstrated that the cross-sectional area of some core arteries decreases due to decreases in temperature, paralleling hypothermia-induced vasoconstriction known to occur in the skin/periphery [15]. For example, while there was a 7% increase for the carotid artery at 35 °C compared to 37 °C, conversely, the areas of the infrarenal aorta and femoral artery decreased by 11% and 72%, respectively. Here, we show a 5% increase in area at the carotid, no change at the infrarenal aorta, and a 13% increase in the femoral artery when dobutamine is applied at 35 °C. This suggests that reductions in area of the core arteries due to hypothermia are mitigated by the application of dobutamine. Similarly, Oung et al. showed an increase in vasodilation from dobutamine during hypothermic conditions compared to normothermic conditions [19]. Focusing on the femoral artery, the difference between a large reduction in area due to hypothermia, to minimize heat loss to the environment [14,29,30],and an enlargement when dobutamine [18] is applied during hypothermia would be hypothesized to cause further decreases in core temperature due to increased heat exchange with the environment. However, these structural changes are not necessarily indicative of blood flow changes. In addition to blood pressure measurements, laser Doppler imaging and phase contrast MRI could be used to determine whether changes in subcutaneous perfusion and blood flow velocity and volume, respectively, are accompanying geometric alterations.

Circumferential cyclic strain is a calculation of vessel deformation across the cardiac cycle [31]. The magnitude of strain in the healthy, adult, infrarenal aorta at rest has been shown to be invariant across species [32] and reductions in strain can accompany the onset of pathology [33–35]. Consistent with previous work [15], baseline strain was qualitatively larger during hypothermic conditions compared to hyperthermic conditions. Like normothermia, maximum cyclic strain increased with dobutamine during both hypothermic and hyperthermic conditions, reaching significance for some core arteries. Notably, the elastic arteries (carotid artery, aorta, and iliac artery), which act to dampen the pulsatility of flow from the heart through expansion and elastic recoil [36–38], had qualitatively greater increases in maximum cyclic strain (1.5-6 fold larger) compared to the only muscular artery studied in this work (femoral artery).

Dobutamine is a pharmacological agent frequently included in the multi-therapeutic treatment for cardiogenic and septic shock. The primary mechanism of a racemic mixture of dobutamine is direct stimulation of β1-adrenergic receptors in the heart to increase cardiac contractility and output. However, one enantiomer is a β2-agonist and α1-antagonist while the other is an α1-agonist, which often leads to vasodilation [11]. Conversely, temperature elicits a full body autonomic response to maintain core body temperature. With increasing core temperature, regional changes in cerebral blood flow [39–41], increased cardiac output [29,42], and decreased total peripheral resistance due to vasodilation [29,30] have been observed. The adenosine A1 receptors which are involved in regulation of body temperature, heart rate and locomotion activity [43] are likely interacting with the adrenergic receptors [44] causing a varied vascular response during the hypo- and hyper- thermic conditions as well as differences across locations. Previous in vitro studies using isoproterenol, a β-adrenoreceptor specific agonist, show a vasodilatory effect in the core vessels; however, studies on isolated vessels are unable to

account for blood flow redistribution due to changes in downstream resistance resulting from vasodilation [45]. Chruscinski et al. did show that the distribution of β1 and β2 receptors varied by location, and this could partially explain the location-dependent response seen in this study [45]. In future studies, the non-invasive methods established in this work can be combined with more specific reagents to determine the contribution of receptors and control mechanisms for both thermoregulation and β-adrenergic stimulation.

Limitations

We did not have a saline control in this study; however, previous studies have shown that the administration of saline does not induce a large response in the heart [46] or the vasculature [17] as compared to dobutamine. Regarding potential effects of isoflurane on vasculature, Crouch et al. showed minimal changes in vasculature or heart rate after a two-hour anesthesia exposure [15]. Dobutamine response also varies between mice and humans, particularly in the heart, with human studies showing stroke volume changes [11] whereas these changes are not seen in the mouse [24]. Human studies would be necessary to determine if dobutamine response in the vasculature is consistent across species.

5.6 Conclusion

This study provides quantitative insight into cardiovascular responses to two clinically relevant stressors, administration of dobutamine and variation of core temperature, while illustrating an innovative non-invasive approach. To our knowledge, these data are the first to empirically quantify the spatially and temporally resolved response of core vasculature to dobutamine at hypo- and hyper-thermic conditions in vivo from head-to-toe. The study was performed in healthy male mice and not a specific disease model. However, stressing the cardiovascular system can reveal deficits that otherwise remain undetectable at rest. Therefore,

these initial data for healthy animals subjected to two cardiac stressors can be used to compare future measurements from disease models, such as cardiac failure or sepsis, to quantify early deficits, thereby helping to improve our understanding of how changes in core temperature interact with a clinical standard of treatment. Our data show that the response in core vasculature depends on anatomical location and varies for hypothermic and hyperthermic conditions. The results presented here also provide foundational data (geometry of the vessels) to begin coupling empirical values of the physiological response to temperature and dobutamine with computational fluid dynamics modeling to better understand how the cardiovascular system responds to stress. A better understanding of how the cardiovascular system responds to these two stressors, independently and combined, could provide motivation for further clinical studies on the effects of temperature and adrenergic stress on core vasculature.

5.7 References

[1] van der Zee J. Heating the patient: a promising approach? Ann. Oncol. Off. J. Eur. Soc. Med. Oncol. 2002;13:1173–1184.

[2] Tucker R, Rauch L, Harley YR, et al. Impaired exercise performance in the heat is associated with an anticipatory reduction in skeletal muscle recruitment. Pflugers Arch. - Eur. J. Physiol. 2004;448:422–430.

[3] Stewart IB, Rojek AM, Hunt AP. Heat Strain During Explosive Ordnance Disposal. Mil. Med. 2011;176:959–963.

[4] Polderman KH. Application of therapeutic hypothermia in the intensive care unit. Intensive Care Med. 2004;30:757–769.

[5] Centers for Disease Control and Prevention U. Hypothermia-related deaths--United States, 1999-2002 and 2005. MMWR Morb. Mortal. Wkly. Rep. 2006;55:282–284.

[6] Schortgen F. Fever in sepsis. Minerva Anestesiol. 2012;78:1254–1264.

[7] Schmidt-Schweda S, Ohler A, Post H, et al. Moderate hypothermia for severe cardiogenic shock (COOL Shock Study I & II). Resuscitation. 2013;84:319–325.

[8] Mauro VF, Mauro LS. Use of intermittent dobutamine infusion in congestive heart failure. Drug Intell. Clin. Pharm. 1986;20:919–924.

[9] Abram S, Arruda-Olson AM, Scott CG, et al. Typical blood pressure response during dobutamine stress echocardiography of patients without known cardiovascular disease who have normal stress echocardiograms. Eur. Hear. J. – Cardiovasc. Imaging. 2016;17:557–563.

[10] Brink HL, Dickerson JA, Stephens JA, et al. Comparison of the Safety of Adenosine and Regadenoson in Patients Undergoing Outpatient Cardiac Stress Testing. Pharmacother. J. Hum. Pharmacol. Drug Ther. 2015;35:1117–1123.

[11] Ruffolo RR. Review: The Pharmacology of Dobutamine. Am. J. Med. Sci. 1987;294:244–248.

[12] Wissler EH. Pennes' 1948 paper revisited. J. Appl. Physiol. 1998;85:35–41.

[13] Bhowmik A, Singh R, Repaka R, et al. Conventional and newly developed bioheat transport models in vascularized tissues: A review. J. Therm. Biol. 2013;38:107–125.

[14] Crouch AC, Manders AB, Cao AA, et al. Cross-sectional area of the murine aorta linearly increases with increasing core body temperature. Int. J. Hyperth. 2018;34:1121–1133.

[15] Crouch AC, Scheven UM, Greve JM. Cross-sectional areas of deep/core veins are smaller at lower core body temperatures. Physiol. Rep. 2018;6:e13839.

[16] Palmer OR, Chiu CB, Cao A, et al. In vivo characterization of the murine venous system before and during dobutamine stimulation: implications for preclinical models of venous disease. Ann. Anat. - Anat. Anzeiger. 2017;214:43–52.

[17] Castle PE, Scheven U., Crouch AC, et al. Anatomical location, sex, and age influence murine arterial circumferential cyclic strain before and during dobutamine infusion. J. Magn. Reson. Imaging. 2018;Accepted.

[18] Shitara T, Wajima Z, Ogawa R. Dobutamine Infusion Modifies Thermoregulation During General Anesthesia. Anesth. Analg. 1996;83:1154–1159.

[19] Oung CM, English M, Chiu RC-J, et al. Effects of hypothermia on hemodynamic responses to dopamine and dobutamine. J. Trauma. 1992;33:671–678.

[20] FLURKEY K, MCURRER J, HARRISON D. Mouse Models in Aging Research. Mouse Biomed. Res. Elsevier; 2007. p. 637–672.

[21] Constantinides C, Mean R, Janssen BJ. Effects of isoflurane anesthesia on the cardiovascular function of the C57BL/6 mouse. ILAR J. 2011;52:e21-31.

[22] Teng D, Hornberger TA. Optimal Temperature for Hypothermia Intervention in Mouse Model of Skeletal Muscle Ischemia Reperfusion Injury. Cell. Mol. Bioeng. 2011;4:717–723.

[23] Duhan V, Joshi N, Nagarajan P, et al. Protocol for long duration whole body hyperthermia in mice. J. Vis. Exp. 2012;e3801.

[24] Wiesmann F, Ruff J, Engelhardt S, et al. Dobutamine-Stress Magnetic Resonance Microimaging in Mice : Acute Changes of Cardiac Geometry and Function in Normal and Failing Murine Hearts. Circ. Res. 2001;88:563–569.

[25] Ahonen J, Aranko K, Iivanainen A, et al. Pharmacokinetic-Pharmacodynamic Relationship of Dobutamine and Heart Rate, Stroke Volume and Cardiac Output in Healthy Volunteers. Clin. Drug Investig. 2008;28:121–127.

[26] Minson CT, Wladkowski SL, Cardell AF, et al. Age alters the cardiovascular response to direct passive heating. J. Appl. Physiol. 1998;84:1323–1332.

[27] Gershon M. The Second Brain : The Scientific Basis of Gut Instinct and a Groundbreaking New Understanding of Nervous Disorders of the Stomach and Intestines. New York: HarperCollins; 1998.

[28] Carabotti M, Scirocco A, Maselli MA, et al. The gut-brain axis: interactions between enteric microbiota, central and enteric nervous systems. Ann. Gastroenterol. 2015;28:203–209.

[29] Crandall CG. Heat stress and baroreflex regulation of blood pressure. Med. Sci. Sports Exerc. 2008;40:2063–2070.

[30] Kuhn LA, Turner JK. Alterations in Pulmonary and Peripheral Vascular Resistance in Immersion Hypothermia. Circ. Res. 1959;7:366–374.

[31] Humphrey JD, O'Rourke SL. An introduction to biomechanics : solids and fluids, analysis and design. Springer-Verlag; 2004.

[32] Greve JM, Williams SP, Bernstein LJ, et al. Reactive hyperemia and BOLD MRI demonstrate that VEGF inhibition, age, and atherosclerosis adversely affect functional recovery in a murine model of peripheral artery disease. J. Magn. Reson. Imaging. 2008;28:996–1004.

[33] Phillips EH, Di Achille P, Bersi MR, et al. Multi-Modality Imaging Enables Detailed Hemodynamic Simulations in Dissecting Aneurysms in Mice. IEEE Trans. Med. Imaging. 2017;36:1297–1305.

[34] Phillips EH, Yrineo AA, Schroeder HD, et al. Morphological and Biomechanical Differences in the Elastase and AngII apoE(-/-) Rodent Models of Abdominal Aortic Aneurysms. Biomed Res. Int. 2015;2015:413189.

[35] Goergen CJ, Azuma J, Barr KN, et al. Influences of Aortic Motion and Curvature on Vessel Expansion in Murine Experimental Aneurysms. Arterioscler. Thromb. Vasc. Biol. 2011;31:270–279.

[36] Shadwick RE. Mechanical design in arteries. J. Exp. Biol. 1999;202.

[37] Quinn U, Tomlinson LA, Cockcroft JR. Arterial stiffness. JRSM Cardiovasc. Dis. 2012;1:1–8.

[38] Humphrey JD, Na S. Elastodynamics and arterial wall stress. Ann. Biomed. Eng. 2002;30:509–523.

[39] Nybo L, Møller K, Volianitis S, et al. Effects of hyperthermia on cerebral blood flow and metabolism during prolonged exercise in humans. J. Appl. Physiol. 2002;93:58–64.

[40] Bain AR, Nybo L, Ainslie PN. Cerebral Vascular Control and Metabolism in Heat Stress. Compr. Physiol. Hoboken, NJ, USA: John Wiley & Sons, Inc.; 2015. p. 1345–1380.

[41] Qian S, Jiang Q, Liu K, et al. Effects of short-term environmental hyperthermia on patterns of cerebral blood flow. Physiol. Behav. 2014;128:99–107.

[42] Siddiqui A. Effects of Vasodilation and Arterial Resistance on Cardiac Output. J. Clin. Exp. Cardiolog. 2011;02.

[43] Yang J-N, Tiselius C, Daré E, et al. Sex differences in mouse heart rate and body temperature and in their regulation by adenosine alpha1 receptors. Acta Physiol. 2007;190:63–75.

[44] Schimmel RJ, Elliott ME, Dehmel VC. Interactions between adenosine and alpha 1-adrenergic agonists in regulation of respiration in hamster brown adipocytes. Mol. Pharmacol. 1987;32:26–33.

[45] Chruscinski A, Brede ME, Meinel L, et al. Differential distribution of beta-adrenergic receptor subtypes in blood vessels of knockout mice lacking beta(1)- or beta(2)-adrenergic receptors. Mol. Pharmacol. 2001;60:955–962.

[46] Puhl S-L, Weeks KL, Ranieri A, et al. Assessing structural and functional responses of murine hearts to acute and sustained β-adrenergic stimulation in vivo. J. Pharmacol. Toxicol. Methods. 2016;79:60–71.

Chapter 6
Conclusion and Future Work

6.1 Conclusions

This thesis focused on the development of a novel and physiologically accurate approach to studying thermoregulation by quantifying structural and functional changes in the CV system occurring in the core. Overall, we hypothesized that a relationship between vessel size/deformation, blood flow, and temperature exists in the core, and these changes should be incorporated into modeling. We began by optimizing MR parameters to study the core arteries as described in section 2.3. Because the arterial blood is the input in the bioheat equation (Equation 4), we began with the core arteries. Due to challenges associated with making measurements from the core, there was a lack of empirical information regarding how arteries change with changing core temperature and their role in thermoregulation. Although researchers have begun to study this response in the leg, and we have expanded this to the whole body. To our knowledge, Chapter 2 is the first work to quantify and compare temperature-induced changes in core arteries of the head, torso, and periphery of murine models. These data provide a broad view of physiological alterations of the murine arterial system due to increases in core temperature, from head-to-toe. Our most important finding that the cross-sectional area of the infrarenal aorta increases significantly with increasing core temperature is biologically significant due to the potential impact these changes could have on conductive and convective processes involved in thermoregulation. This work provides further evidence of the effects of sex and age on CV responses and emphasizes the necessity to properly control an animal's temperature and report it in publications.

Given the surprising result that the core arteries do change with temperature, we sought to quantify the venous response and to quantify the functional data in the neck and periphery. Chapter 3 describes and compares the structural and functional arterial and venous response. The MR parameters for the arterial and venous locations were optimized by two members of the Greve lab: Paige Castle (arteries) and Olivia Palmer (veins). As described in 3.6, the veins are an important part of the cardiovascular system's role in thermoregulation. Our data show that changes in the IVC, despite its depth, must also be considered. Our most important finding that the cross-sectional area of the core veins, particularly the IVC, is significantly smaller at lower temperatures is biologically significant due to the potential impact these changes could have on conductive and convective processes involved in thermoregulation.

The changes quantified in Chapter 3 motivated further studies of the core vasculatures' response to temperature, including blood velocity and volumetric flow. Chapter 4 describes the blood distribution, quantifying blood velocity and flow across sex and age, with increases in core body temperature. In collaboration with previous Greve lab members (Amos Cao) and research scientist (Ulrich Scheven), pulse sequences were implemented for PCMRI (including parameter optimization for individual vessels developed by myself) and an in-house Matlab code developed to quantify velocity and volumetric flow. Our most important finding was to distinguish contributions from changes in area and blood velocity which could lead to more accurate bioheat modeling. In aged animals compared to adult animals, flow increases were driven primarily by velocity changes. These changes in blood velocity are also likely causing changes in wall shear stress which is an important metric in cardiovascular disease progression.

The previous three chapters (Chapters 2, 3, and 4) focus on the basic and fundamental understanding of the effects of temperature on the cardiovascular system. Chapter 5 describes a collaboration study with Paige Castle combining two cardiovascular stressors: thermal stress and dobutamine. To our knowledge, these data were the first to empirically quantify the spatially and temporally resolved response of core vasculature to dobutamine at hypo- and hyper-thermic conditions in vivo from head-to-toe. These initial data for healthy animals subjected to two cardiac stressors can be used to compare future measurements from disease models, such as cardiac failure or sepsis, to quantify early deficits, thereby helping to improve our understanding of how changes in core temperature interact with a clinical standard of treatment.

Overall, this thesis provides a novel and physiologically accurate approach to studying thermoregulation by incorporating structural and functional changes in the CV system occurring in the core. This thesis focused on using murine models to study the effect of temperature on core vasculature. Future work is required to fully understand the CV system's role in thermoregulation, but our work has provided motivation to study the core vasculature and incorporate these previously unknown changes into modeling.

6.2 Future Work

As described in section 1.1, temperature matters, and the scope of thermoregulation studies and the effect of temperature on the body is seemingly limitless and largely unexplored in the biomedical sciences. This section focuses on a small sample of futures directions for this work.

Extreme temperature's effect on core vasculature

One future direction for this type of work is extreme temperature. Homeotherms, an organism that maintains its body temperature, will often prioritize thermoregulation at extreme

temperatures (e.g. maintaining body temperature through metabolic heat generation during starvation or sweating despite dehydration levels or even decreased blood pressure leading to heat syncope) [1]. While the temperatures in this thesis were physiologically relevant and not pathological [2,3], future work in both extremes with methods derived in this thesis would further elucidate the role of the cardiovascular system in thermoregulation. Two studies would be conducted for the two extremes: a 'cool' study with core body temperatures below 35°C and a heat stress study with core body temperature over 40.5 °C. After this baseline data is quantified, additional stressors could be added including dobutamine, exercise, starvation, or dehydration.

Thermoregulatory disorders and illnesses

Thermoregulatory disorders and illnesses pose a threat to maintaining homeostasis [4]. In this thesis, we used healthy murine models; however, the same methods could be applied to genetically modified animals to understand if the deficiencies in thermoregulation affect the CV system [5]. Thermoregulation dysfunctions are also seen as symptoms of other physiological states and diseases such as hot flashes and cold sweats in menopausal women [6]. In the future, human studies with subjects who have thermoregulation dysfunction could be conducted using non-invasive MRI to quantify how the CV system is responding during these dysfunctions.

Experimental measurements of the temperature variation from the core, in artery-vein pairs, to muscle to skin in rat intraperitoneal cavity

Although this thesis has focused on the convective term of the bioheat equation [7], for the past three years, I have been working with Dr. Jose Diaz on a project focused on the conductive term. The preliminary work was presented at the World Congress of Biomechanics in July 2018 in Dublin, Ireland. We are currently working with Connie Lee and Dr. Kevin Pipe in

the Mechanical Engineering Department at the University of Michigan to continue this project and expand it to brain cooling.

Human studies

As discussed in section 1.5, murine studies have limitations including the animal's ability to thermoregulate (sweat glands only in the paws and a hairless tail). However, with this thesis, we have provided support for future human studies on the changes of core vasculature with temperature. Using MRI and external temperature control, similar studies could be conducted in humans providing motivation to alter current bioheat modeling.

6.3 References

[1] Parsons KC. Human thermal environments: the effects of hot, moderate, and cold environments on human health, comfort, and performance. 3rd ed. CRC Press/Taylor & Francis; 1993.

[2] Teng D, Hornberger TA. Optimal Temperature for Hypothermia Intervention in Mouse Model of Skeletal Muscle Ischemia Reperfusion Injury. Cell. Mol. Bioeng. 2011;4:717–723.

[3] Duhan V, Joshi N, Nagarajan P, et al. Protocol for long duration whole body hyperthermia in mice. J. Vis. Exp. 2012;e3801.

[4] Cheshire WP. Thermoregulatory disorders and illness related to heat and cold stress. Auton. Neurosci. 2016;196:91–104.

[5] Leon LR. The use of gene knockout mice in thermoregulation studies. J. Therm. Biol. 2005;30:273–288.

[6] Deecher DC. Physiology of thermoregulatory dysfunction and current approaches to the treatment of vasomotor symptoms. Expert Opin. Investig. Drugs. 2005;14:435–448.

[7] Pennes HH. Analysis of tissue and arterial blood temperatures in the resting human forearm. J. Appl. Physiol. 1948;1:93–121